

# **Cosmic Structure:**

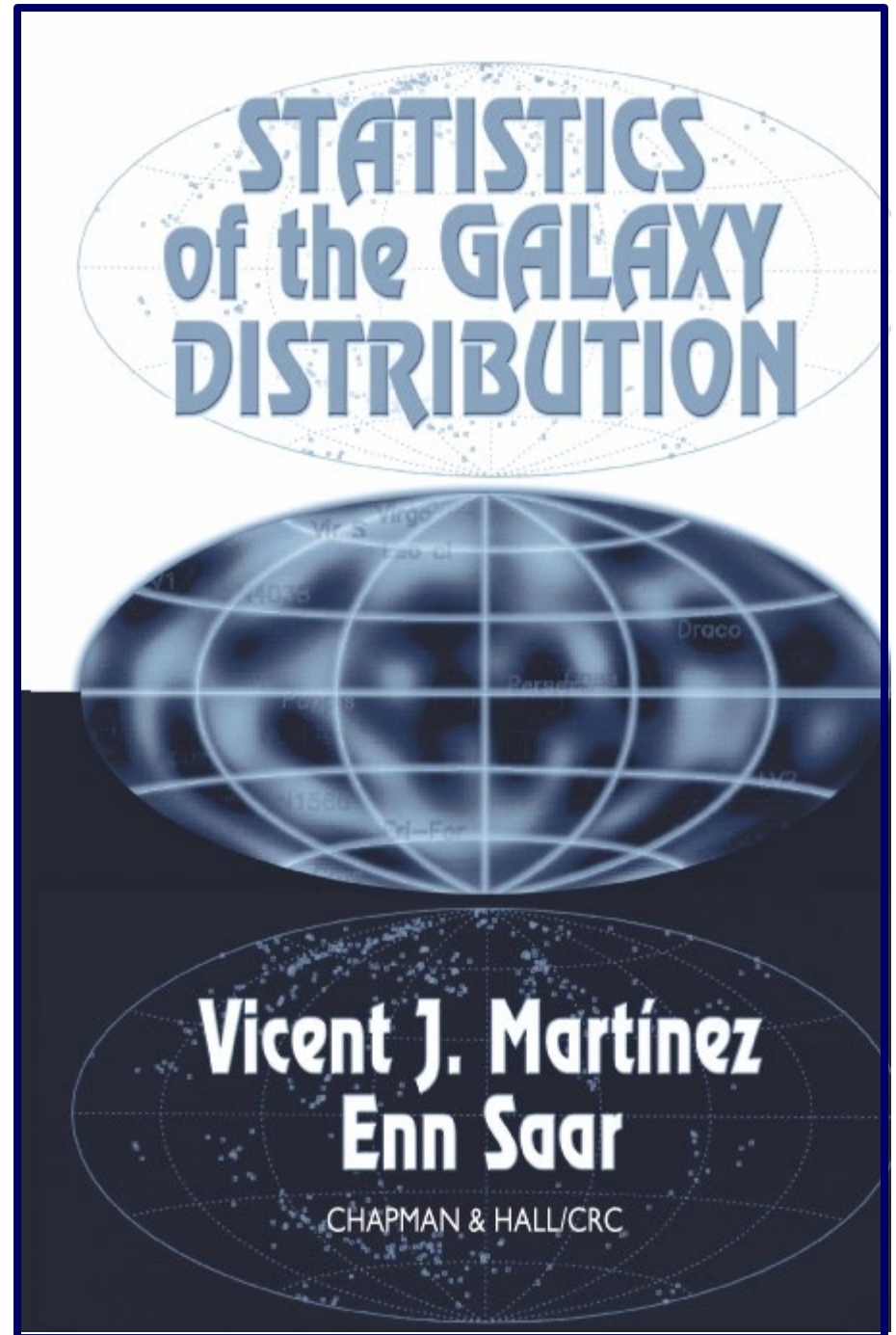
## **Lecture 10**

# **Measures of Cosmic Structure**

Rien van de Weijgaert,  
Cosmic Structure Formation, Oct. 2018

If Standard to  
Reference:....

Martinez & Saar



# Ergodic Theorem

# Statistical Cosmological Principle

Cosmological Principle:

Universe is Isotropic and Homogeneous

Homogeneous & Isotropic Random Field  $\psi(\vec{x})$  :

Homogenous  $p[\psi(\vec{x} + \vec{a})] = p[\psi(\vec{x})]$

Isotropic  $p[\psi(\vec{x} - \vec{y})] = p[\psi(|\vec{x} - \vec{y}|)]$

Within Universe one particular realization  $\psi(\vec{x})$  :

Observations: only spatial distribution in that one particular  $\psi(\vec{x})$

Theory:  $p[\psi(x)]$

# Ergodic Theorem

Ensemble Averages



Spatial Averages  
over one realization  
of random field

- Basis for statistical analysis cosmological large scale structure
- In statistical mechanics Ergodic Hypothesis usually refers to time evolution of system, in cosmological applications to spatial distribution at one fixed time

# Ergodic Theorem

Validity Ergodic Theorem:

- Proven for Gaussian random fields with continuous power spectrum
- Requirement:

spatial correlations decay sufficiently rapidly with separation

such that

many statistically independent volumes in one realization



All information present in complete distribution function  $p[\psi(\vec{x})]$  available from single sample  $\psi(\vec{x})$  over all space

# Fair Sample Hypothesis

- Statistical Cosmological Principle

+

- Weak cosmological principle  
(small fluctuations initially and today over Hubble scale)

+

- Ergodic Hypothesis

fair sample hypothesis  
(Peebles 1980)

Discrete e.g. Continuous



# Discrete & Continuous Distributions

- How to relate discrete and continuous distributions:
- Define number density  $n(\vec{x})$  for a point process:

$$n(\vec{x}) = \bar{n}[1 + \delta(\vec{x})] = \sum_i \delta_D(\vec{x} - \vec{x}_i)$$

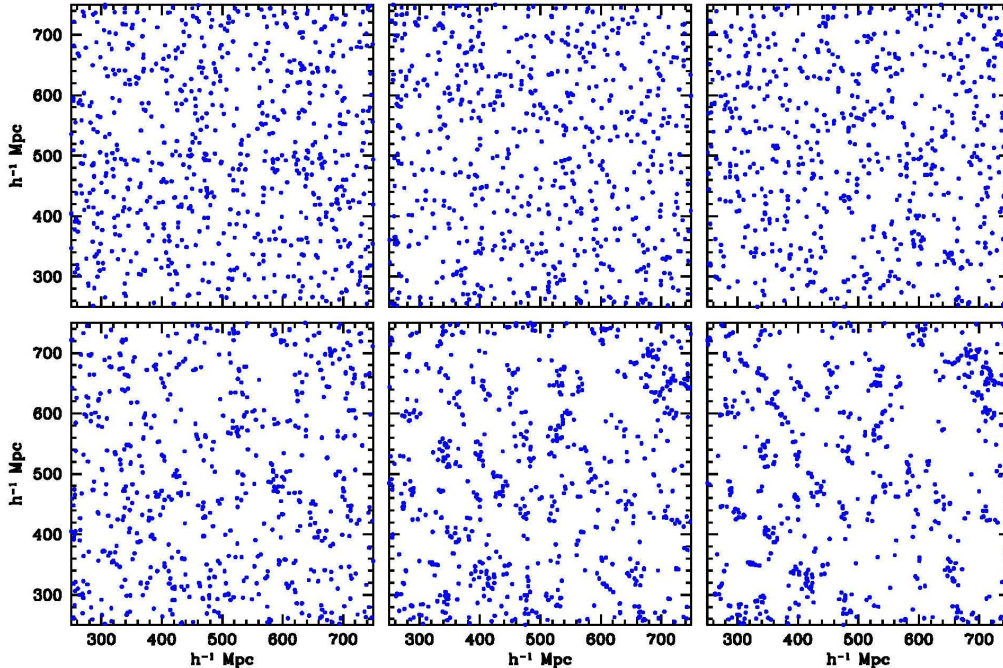
$$\delta_D(\vec{x})$$

Dirac Delta function

$$\left\langle \sum_i \delta_D(\vec{x} - \vec{x}_i) \right\rangle = \bar{n} \quad \text{ensemble average}$$

# Correlation Functions

# Correlation Functions



Joint probability that  
in each one of

the two infinitesimal volumes  
 $dV_1$  &  $dV_2$ ,

at distance  $r$ ,

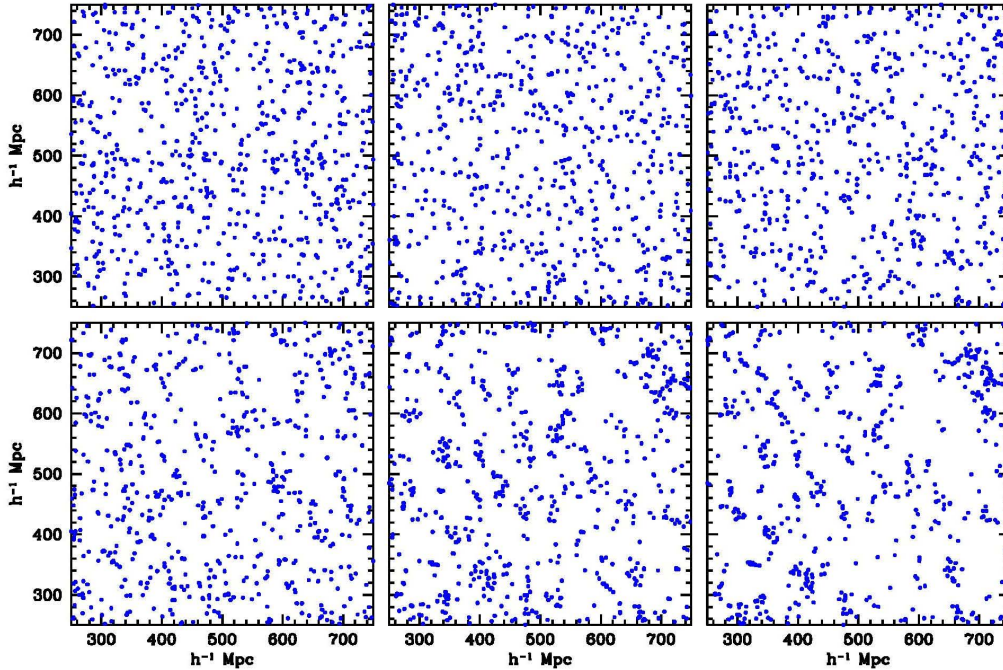
lies a galaxy

Infinitesimal Definition Two-Point Correlation Function:

$$dP(r) = \bar{n}^2 (1 + \xi(r)) dV_1 dV_2$$

mean density

# Correlation Functions



In case of  
Homogeneous & Isotropic  
point process

then  $\xi(\vec{r})$

only dependent on

$$|\vec{r}| = r$$

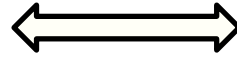
Infinitesimal Definition Two-Point Correlation Function:

$$dP(r) = \bar{n}^2 (1 + \xi(r)) dV_1 dV_2$$

mean density

# Correlation Functions

Discrete



Continuous

## Two-point correlation function

$$dP(\vec{x}_1, \vec{x}_2) = \bar{n}^2 dV_1 dV_2 [1 + \xi(r_{12})]$$

$$r_{12} = |\vec{x}_1 - \vec{x}_2|$$

$$\langle \delta(\vec{x}) \rangle = 0$$

## Autocorrelation function

$$\xi(r_{12}) = \langle \delta(\vec{x}_1) \delta(\vec{x}_2) \rangle$$

probability for 2 points in  
 $dV_1$  and  $dV_2$

# Correlation Functions

- Gaussian (primordial and large-scale) density field:

Autocorrelation function  $\xi(r)$  Fourier transform power spectrum  $P(k)$

$$\xi(\mathbf{r}) = \xi(|\mathbf{r}|) = \int \frac{d\mathbf{k}}{(2\pi)^3} P_f(k) e^{-i\mathbf{k}\cdot\mathbf{r}}$$

Autocorrelation function completely specifies statistical properties of field

- First order measure of deviations from uniformity
- Nonlinear objects (halos):  
 $\xi(r)$  measure of density profile
- Large Scales:  
related to dynamics of structure formation via e.g.  
cosmic virial theorem

# Correlation Functions: related measures

Other measures related to  $\xi(r)$  :

- Second-order intensity  $\lambda_2(r) = \bar{n}^{-2} \xi(r) + 1$
- Pair correlation function  $g(r) = 1 + \xi(r)$
- Conditional density  $\Gamma(r) = \bar{n}(1 + \xi(r))$

# Correlation Functions: related measures

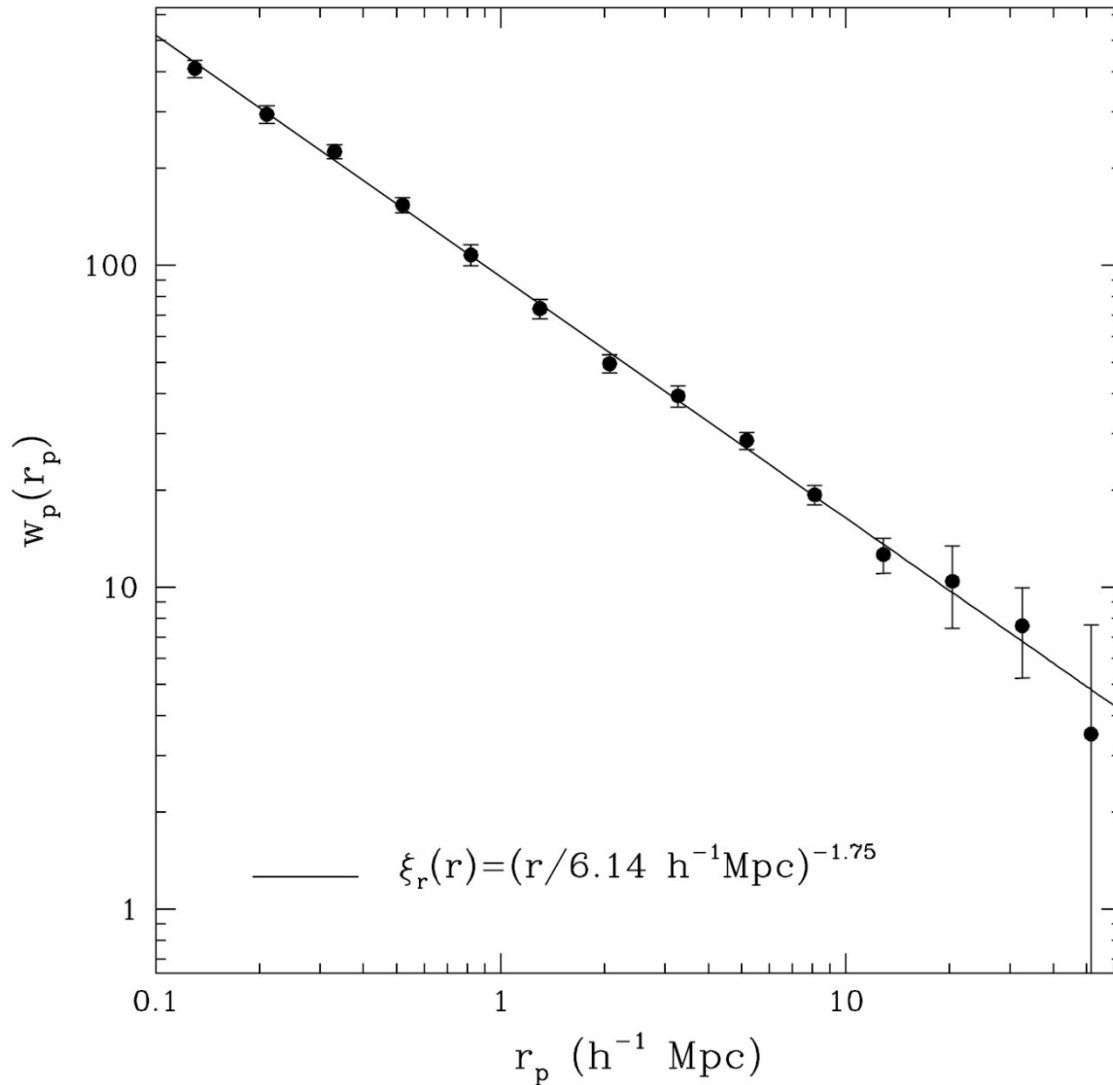
$$J_3(r) \equiv \int_0^\infty \xi(y) y^2 dy$$

Volume averaged correlation function  $\bar{\xi}(r)$

$$\bar{\xi}(r) = \frac{3}{4\pi r^3} \int_0^r 4\pi \xi(x) x^2 dx = \frac{3J_3(r)}{r^3}$$



# Power-law Correlations



$$\xi(r) = \left( \frac{r}{r_0} \right)^{-\gamma}$$

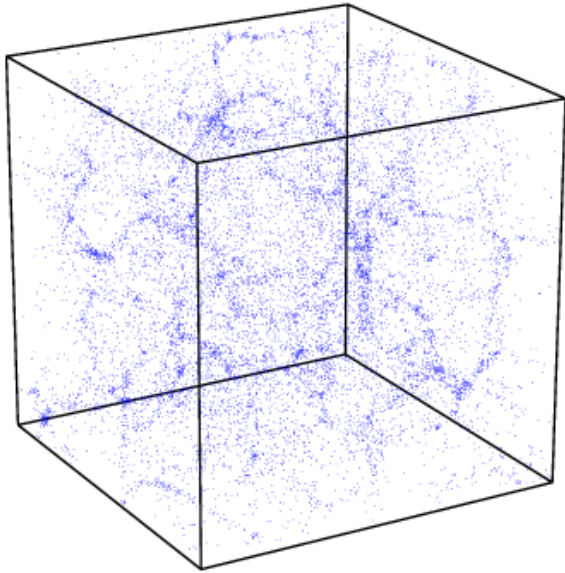
$$\gamma \approx 1.8$$

$$r_0 \approx 5 h^{-1} \text{ Mpc}$$

Totsuji & Kihara 1969

Peebles 1975, 1980, ...

# Correlation Functions

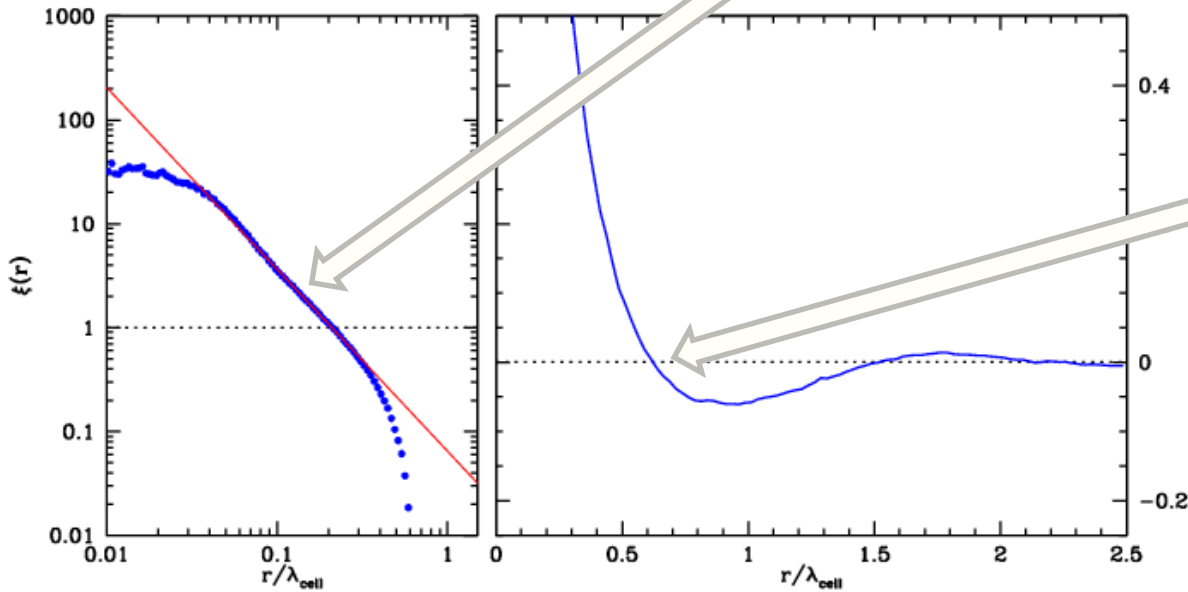


$$\xi_{cc}(r) = \left(\frac{r_0}{r}\right)^\gamma$$
$$\xi(r_0) = 1.$$

Clustering length/  
"Correlation" length

Coherence length

$$\xi(r_a) = 0$$



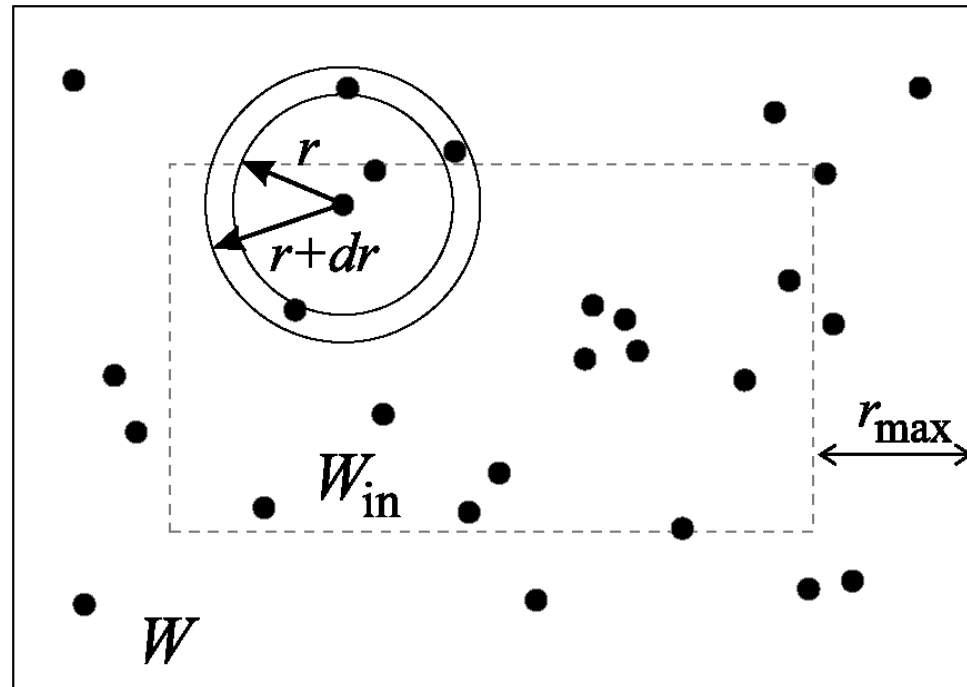
# Correlation Function Estimators

# Minimal Estimator

$$\hat{\xi}_{\min}(r) = \frac{V(W)}{NN_{in}} \sum_{i=1}^{N_{in}} \frac{n_i(r)}{V_{sh}} - 1$$

For galaxies close to the boundary the number of neighbours is Underestimated. One way to overcome this problem is to consider as centers for counting neighbours only galaxies lying within an inner window  $W_{in}$

$V_{sh}$  is the volume of the shell of width  $dr$



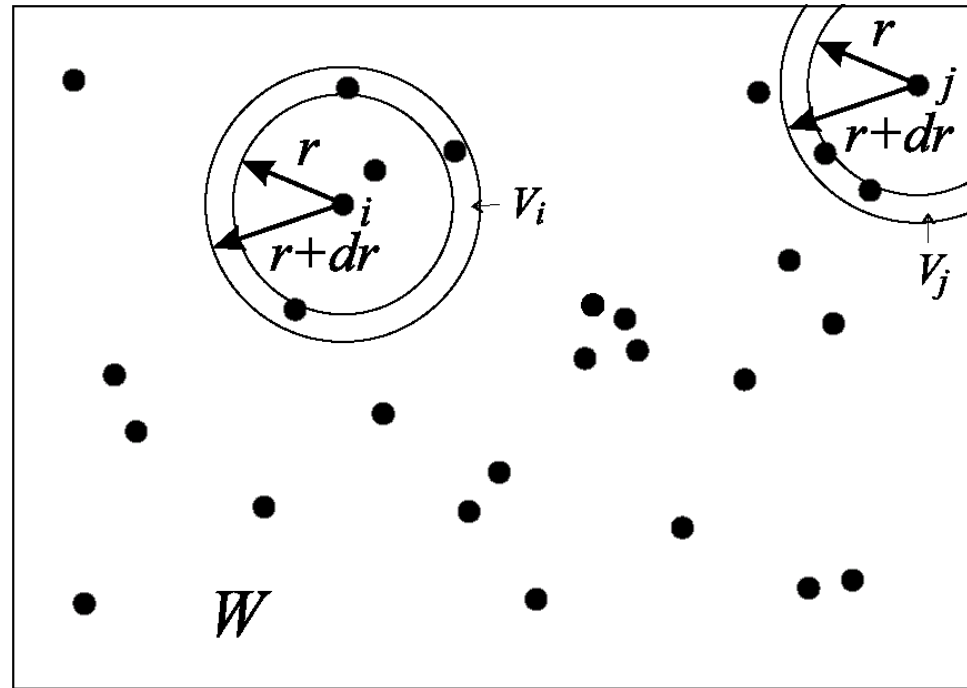
# Edge-Corrected Estimator

$$\hat{\xi}_{edge}(r) = \frac{V(W)}{N^2} \sum_{i=1}^{N_{in}} \frac{n_i(r)}{V_i} - 1$$

$N_i(r)$ : number of neighbours at distance in the interval  $[r, r+dr]$  from galaxy  $i$

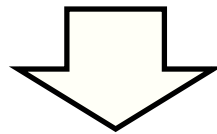
$V_i$ : volume of the intersection of the shell with  $W$

$W$ : when  $W$  a cube, an analytic expression for  $V_i$  can be found in Baddely et al. (1993).



# Estimators Redshift Surveys

- In redshift surveys, galaxies are not sampled uniformly over the survey volume
- Depth selection:  
in magnitude-limited surveys, the sampling density decreases as function of distance
- Survey Geometry  
boundaries of survey often nontrivially defined:
  - slice surveys
  - non-uniform sky coverage
  - etc.



Clustering in survey compared with sample of Poisson distributed points, following the same sampling behaviour in depth and survey geometry

Difference in clustering between  
data sample (D) and Poisson sample (R)  
genuine clustering

# Estimators Redshift Surveys

Clustering in survey compared with sample of Poisson distributed points, following the same sampling behaviour in depth and survey geometry

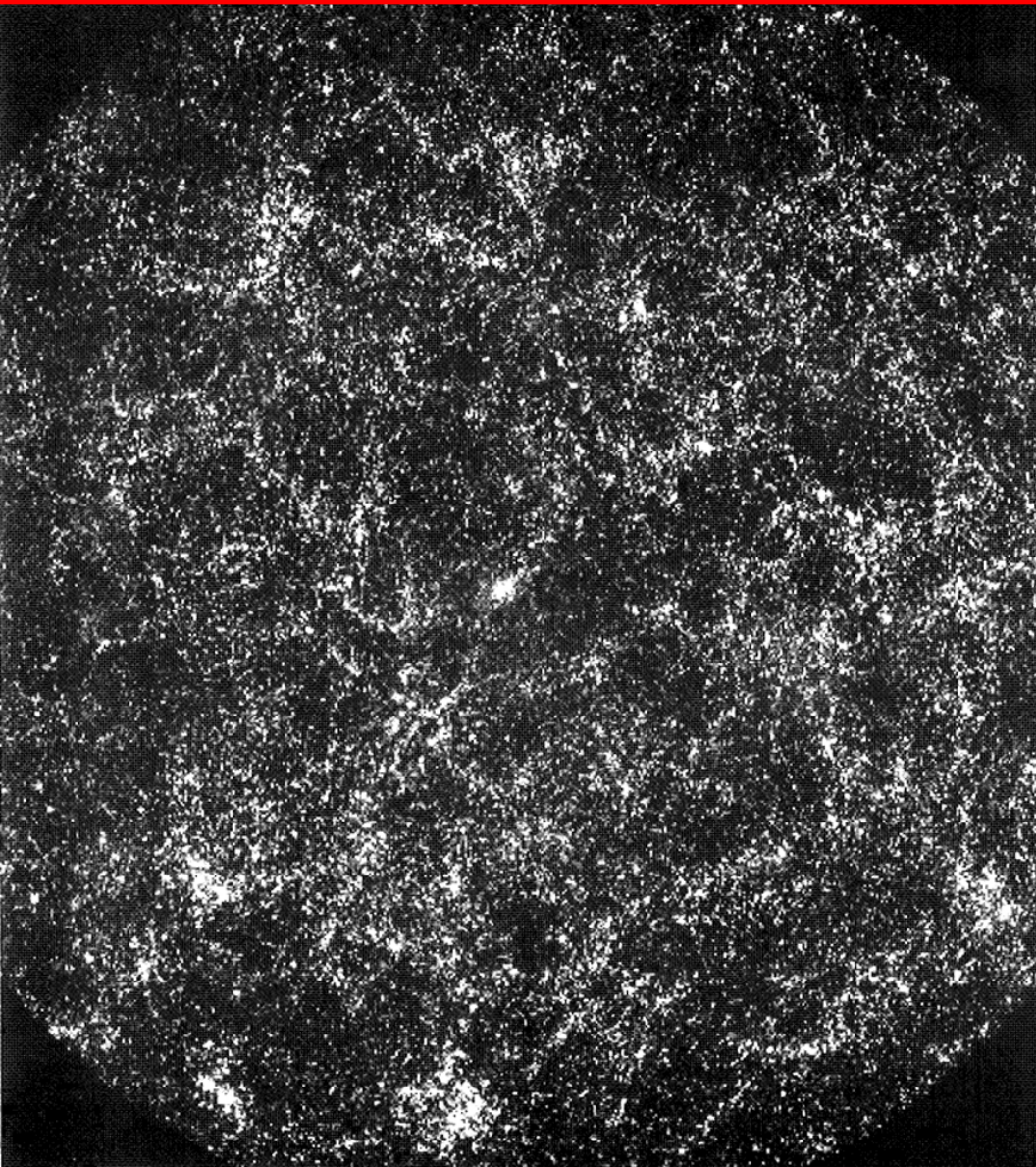
Difference in clustering between  
data sample (D) and Poisson sample (R)  
genuine clustering

- $\xi_{DP}(r) = \frac{n_R}{n_D} \frac{\langle DD \rangle}{\langle DR \rangle} - 1$  Davis-Peebles (1983)
- $\xi_{Ham}(r) = \frac{\langle DD \rangle \langle RR \rangle}{\langle DR \rangle^2} - 1$  Hamilton (1993)
- $\xi_{LS}(r) = 1 + \left( \frac{n_R}{n_D} \right)^2 \frac{\langle DD \rangle}{\langle RR \rangle} - 2 \frac{n_R}{n_D} \frac{\langle DR \rangle}{\langle RR \rangle}$  Landy-Szalay (1993)

# Angular Two-point Correlation Function



# Angular Correlation Function



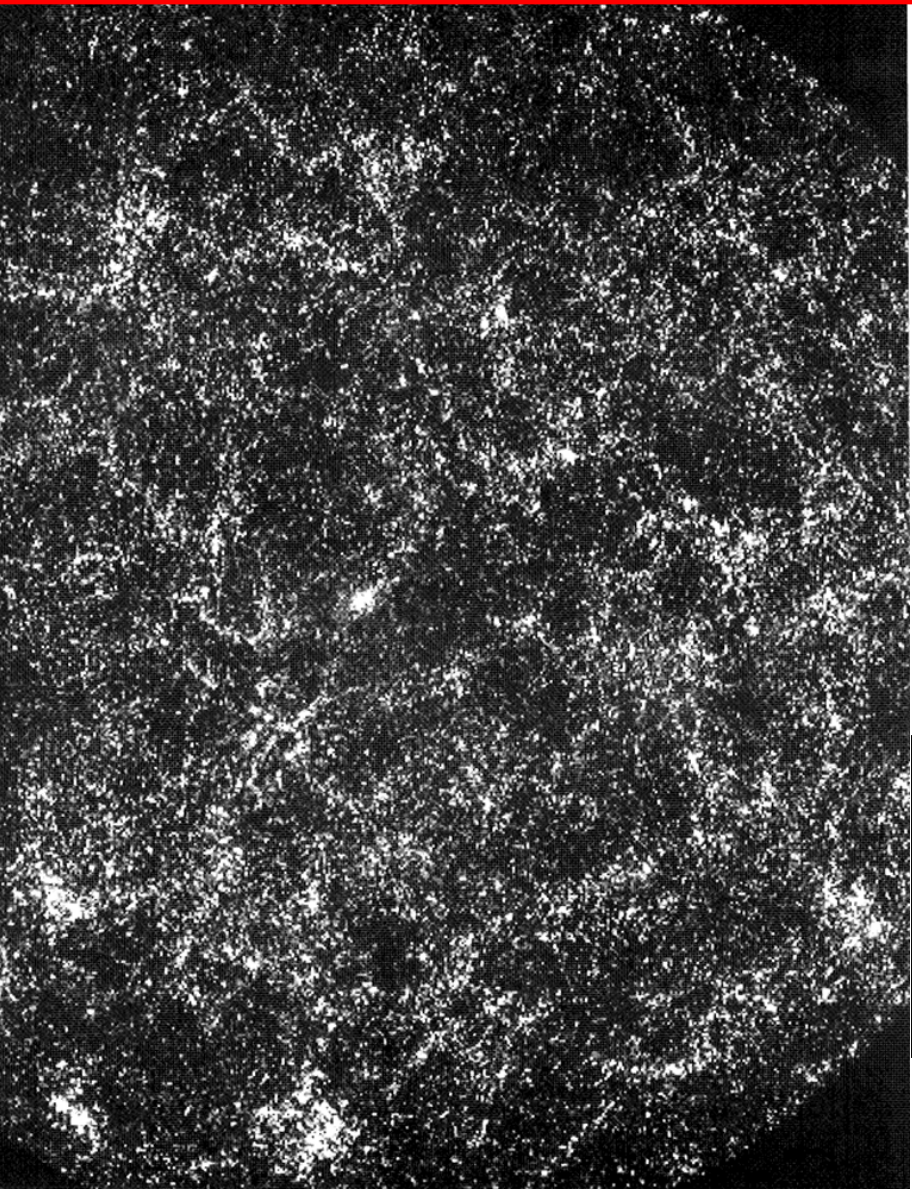
Galaxy sky distribution:

- Galaxies clustered, a projected expression of the true 3-D clustering
- Probability to find a galaxy near another galaxy higher than average (Poisson) probability
- Quantitatively expressed by 2-pt correlation function  $w(\theta)$ :

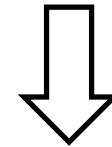
$$dP(\theta) = \bar{n}^2 \{1 + w(\theta)\} d\Omega_1 d\Omega_2$$

Excess probability of finding 2 gal's at angular distance  $\theta$

# Angular & Spatial Clustering



$$dP(\theta) = \bar{n}^2 \{1 + w(\theta)\} d\Omega_1 d\Omega_2$$



Two-point angular correlation function is the “projection” of  $\xi(r)$

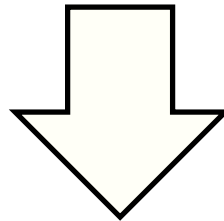
Limber's Equation:

$$w(\theta) = \frac{\iint p(\vec{x}_1) p(\vec{x}_2) x_1^2 x_2^2 dx_1 dx_2 \xi(|\vec{x}_1 - \vec{x}_2|)}{\left[ \int_0^\infty x^2 p(x) dx \right]^2}$$

$p(x)$ : survey selection function

# Limber Equation

$$w(\theta) = \frac{\iint p(\vec{x}_1) p(\vec{x}_2) x_1^2 x_2^2 dx_1 dx_2 \xi(|\vec{x}_1 - \vec{x}_2|)}{\left[ \int_0^\infty x^2 p(x) dx \right]^2}$$



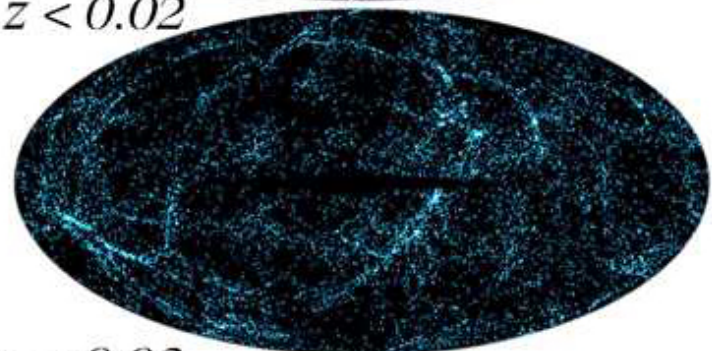
$$\xi(r) = \left( \frac{r_0}{r} \right)^\gamma \longleftrightarrow w(\theta) = A \left( \frac{1}{\theta} \right)^{\gamma-1}$$



$z < 0.01$



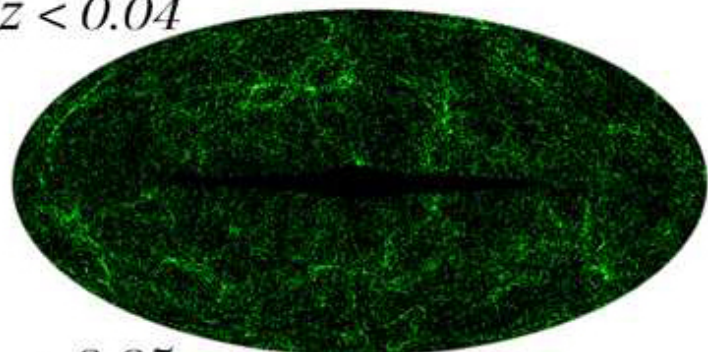
$0.01 < z < 0.02$



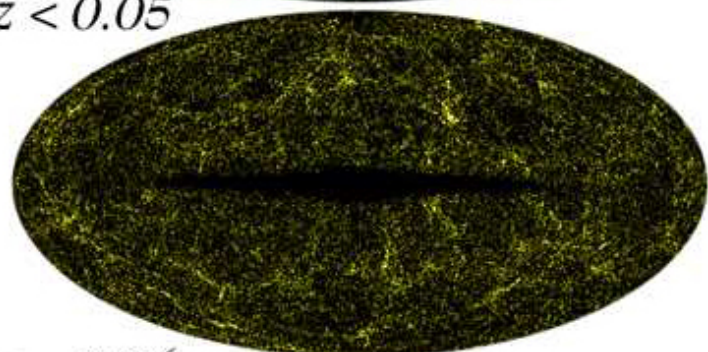
$0.02 < z < 0.03$



$0.03 < z < 0.04$



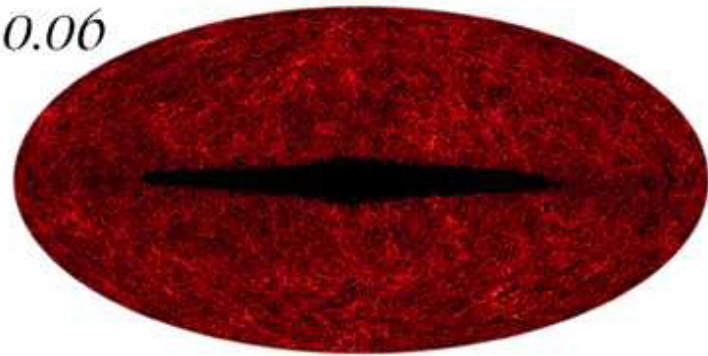
$0.04 < z < 0.05$



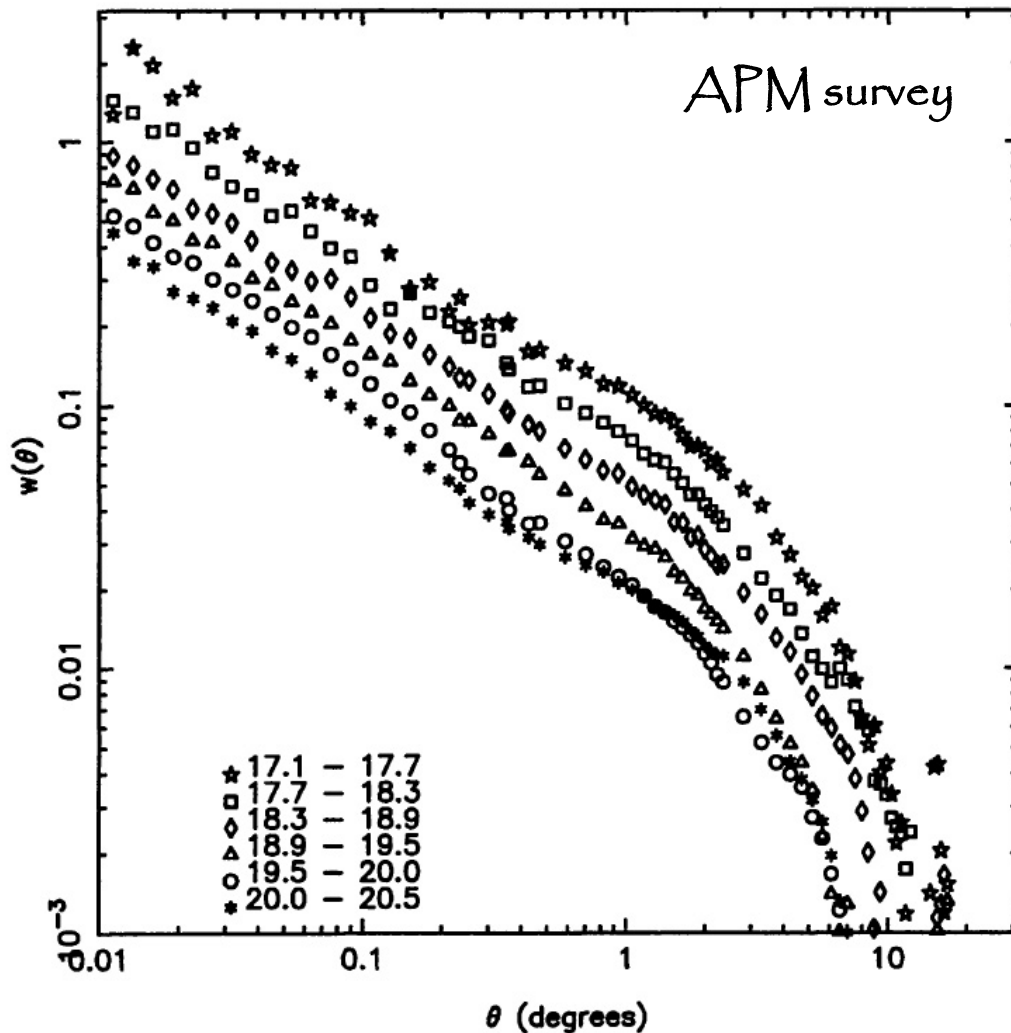
$0.05 < z < 0.06$



$z > 0.06$



# Angular Clustering Scaling



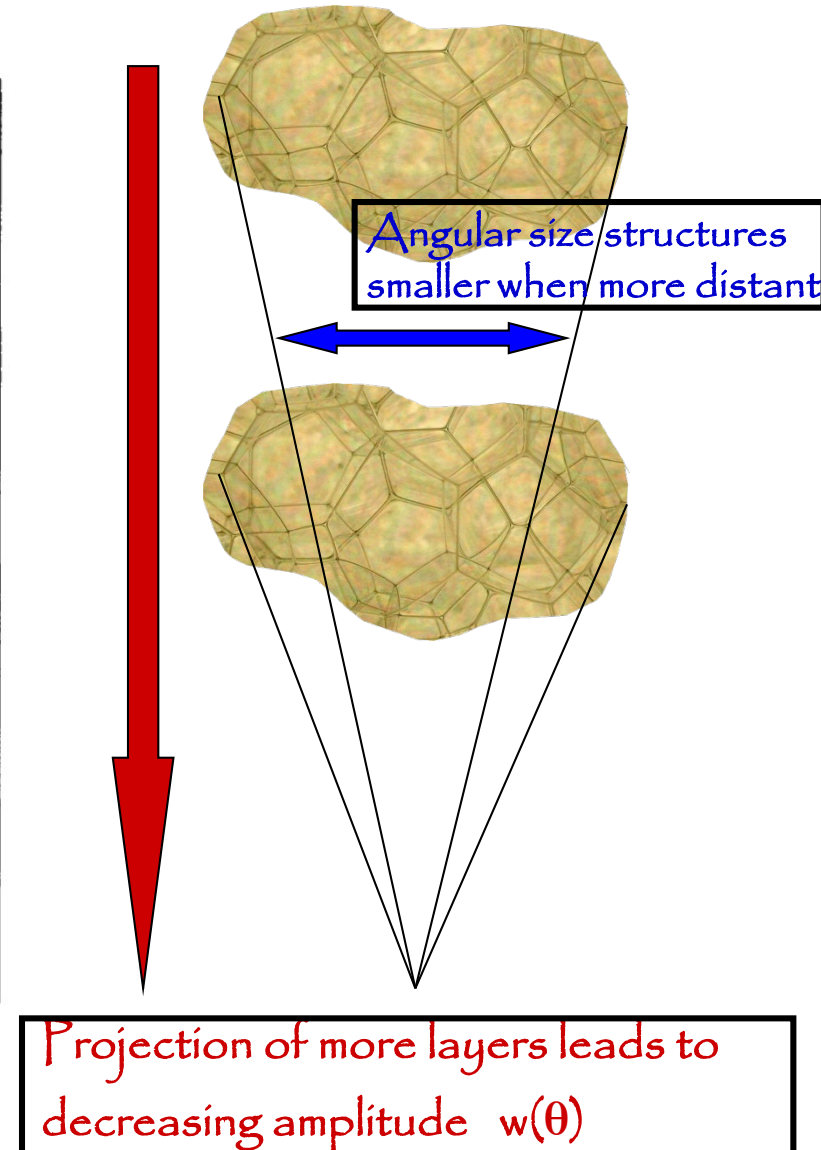
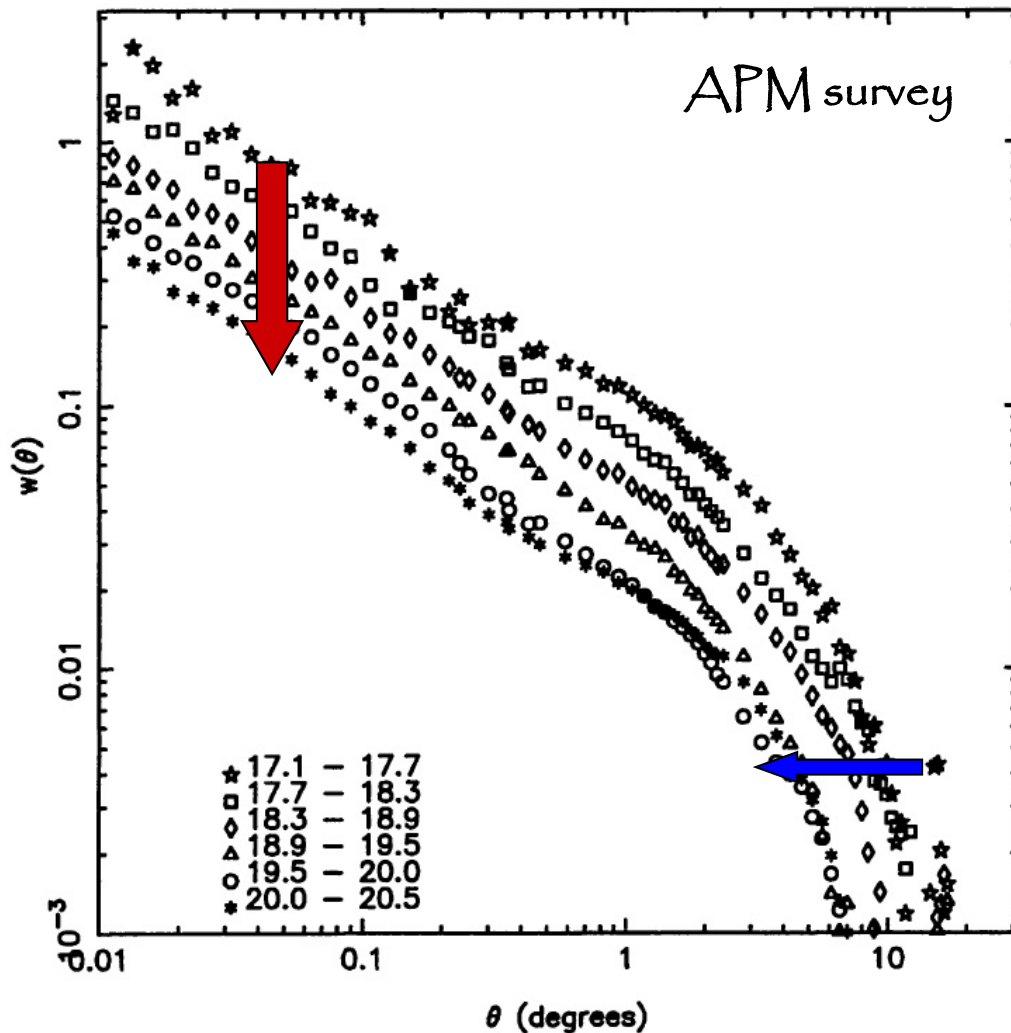
Two-point correlation function:

- small angles: power-law

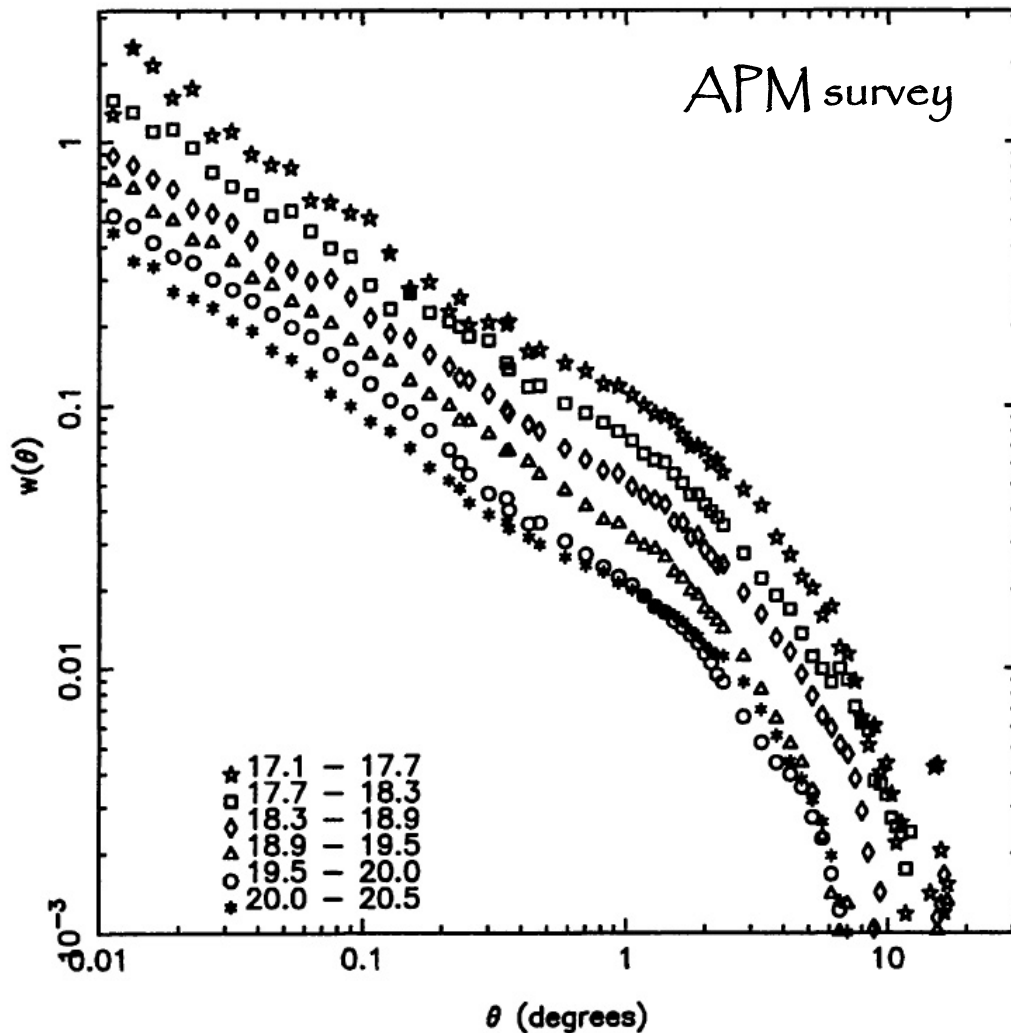
$$w(\theta) = \left( \frac{\theta_0}{\theta} \right)^\gamma$$
$$\gamma \approx 0.8$$

- large angles  $\longrightarrow$  ○  
ie. to homogeneity

# Angular Clustering Scaling



# Angular Clustering Scaling

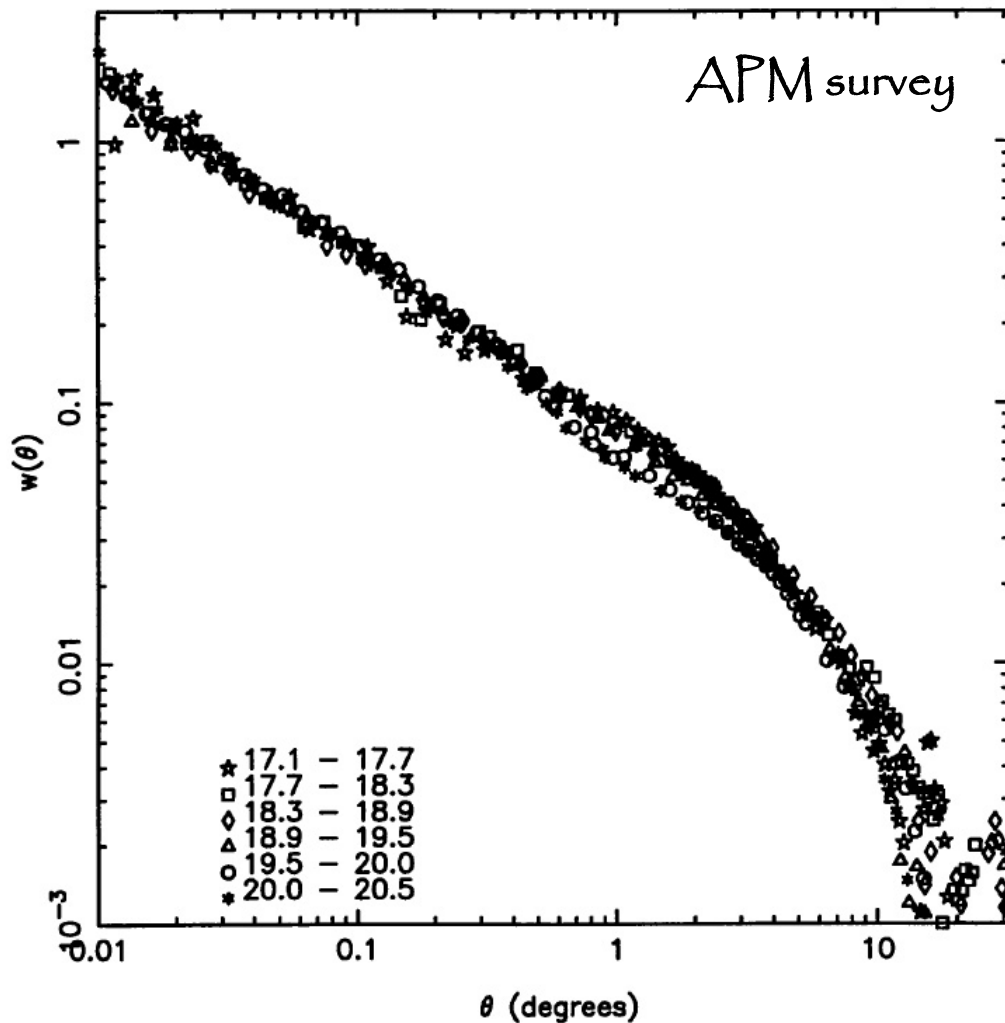


Angular size structures  
smaller when more distant

Projection of  
more layers  
leads to  
decreasing  
amplitude  $w(\theta)$

$$w(\theta, D_*) = \frac{1}{D_*} w(\theta D_*)$$

# Angular Clustering Scaling



Angular size structures  
smaller when more distant

Projection of  
more layers  
leads to  
decreasing  
amplitude  $w(\theta)$

$$w(\theta, D_*) = \frac{1}{D_*} w(\theta D_*)$$

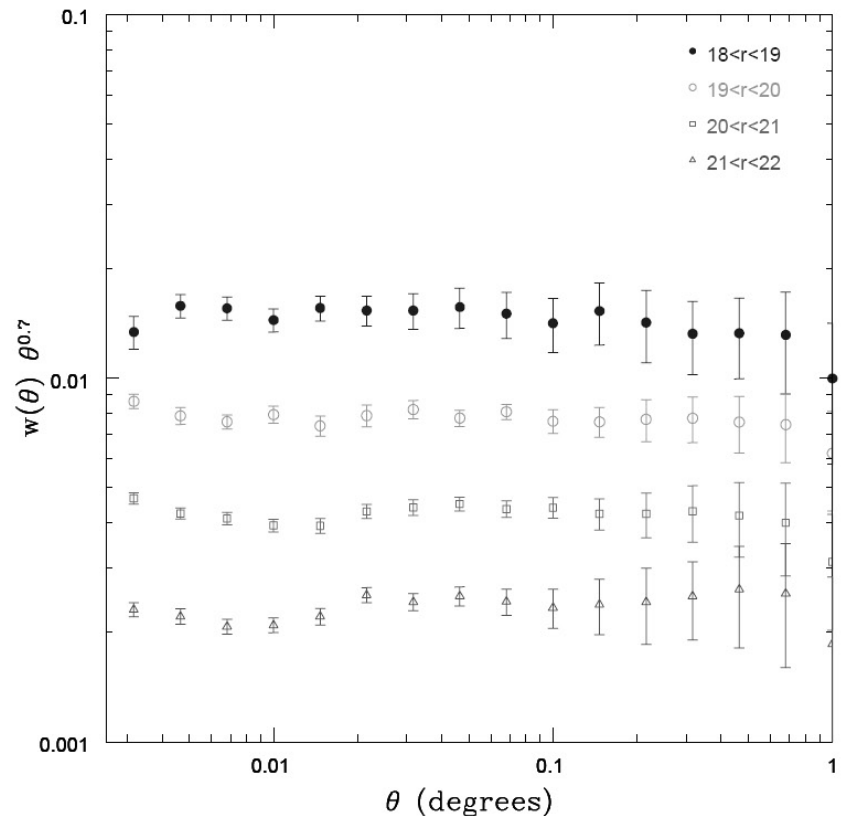
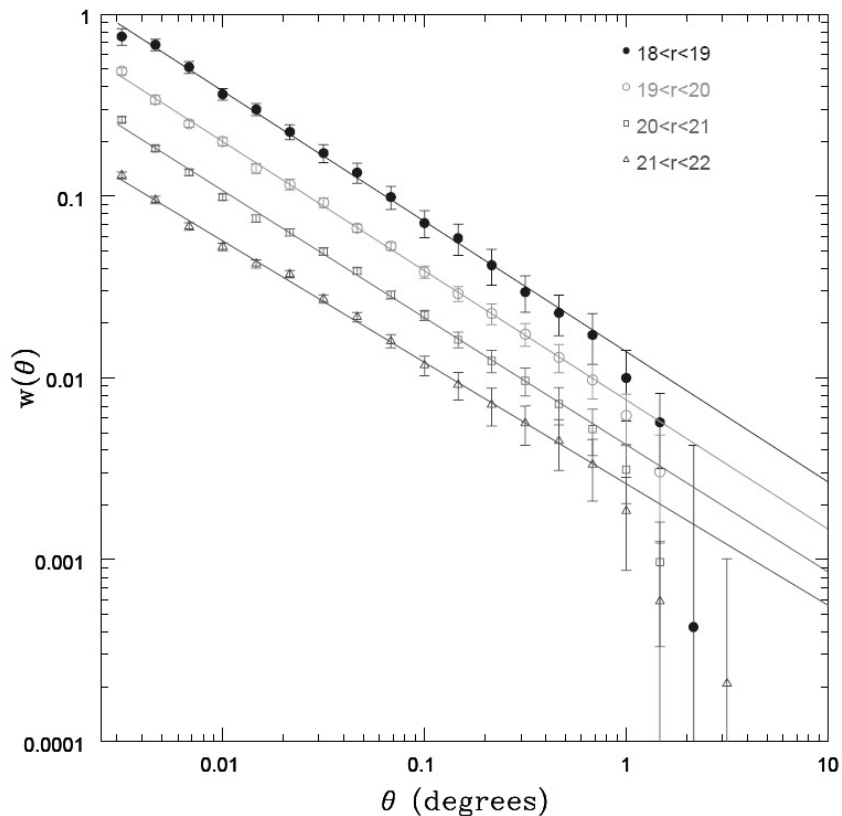


# Angular Clustering Scaling

The angular scaling of  $w(\theta)$  is found back to even fainter magnitudes in the

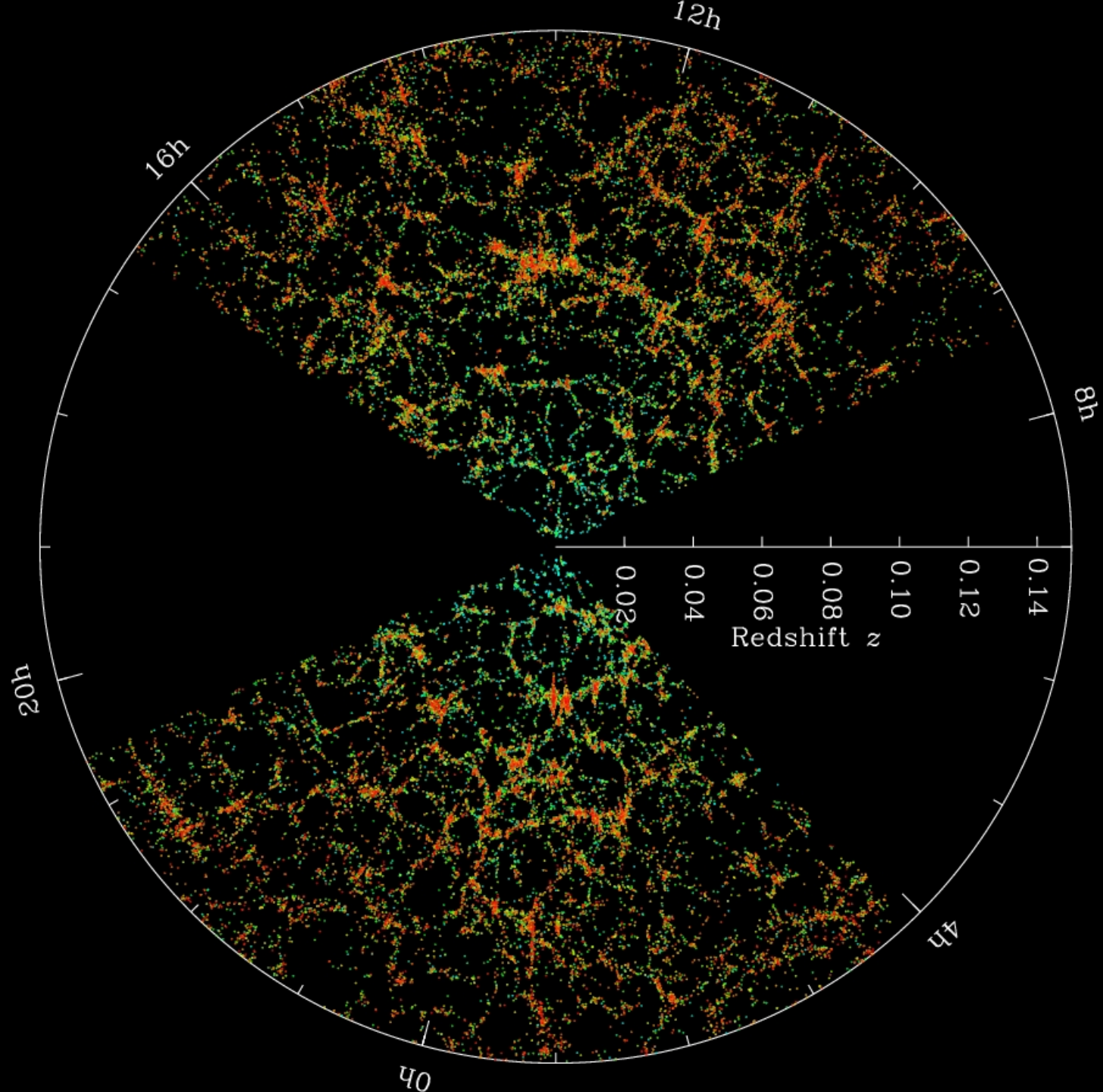
*SDSS* survey ( $m=22$ )

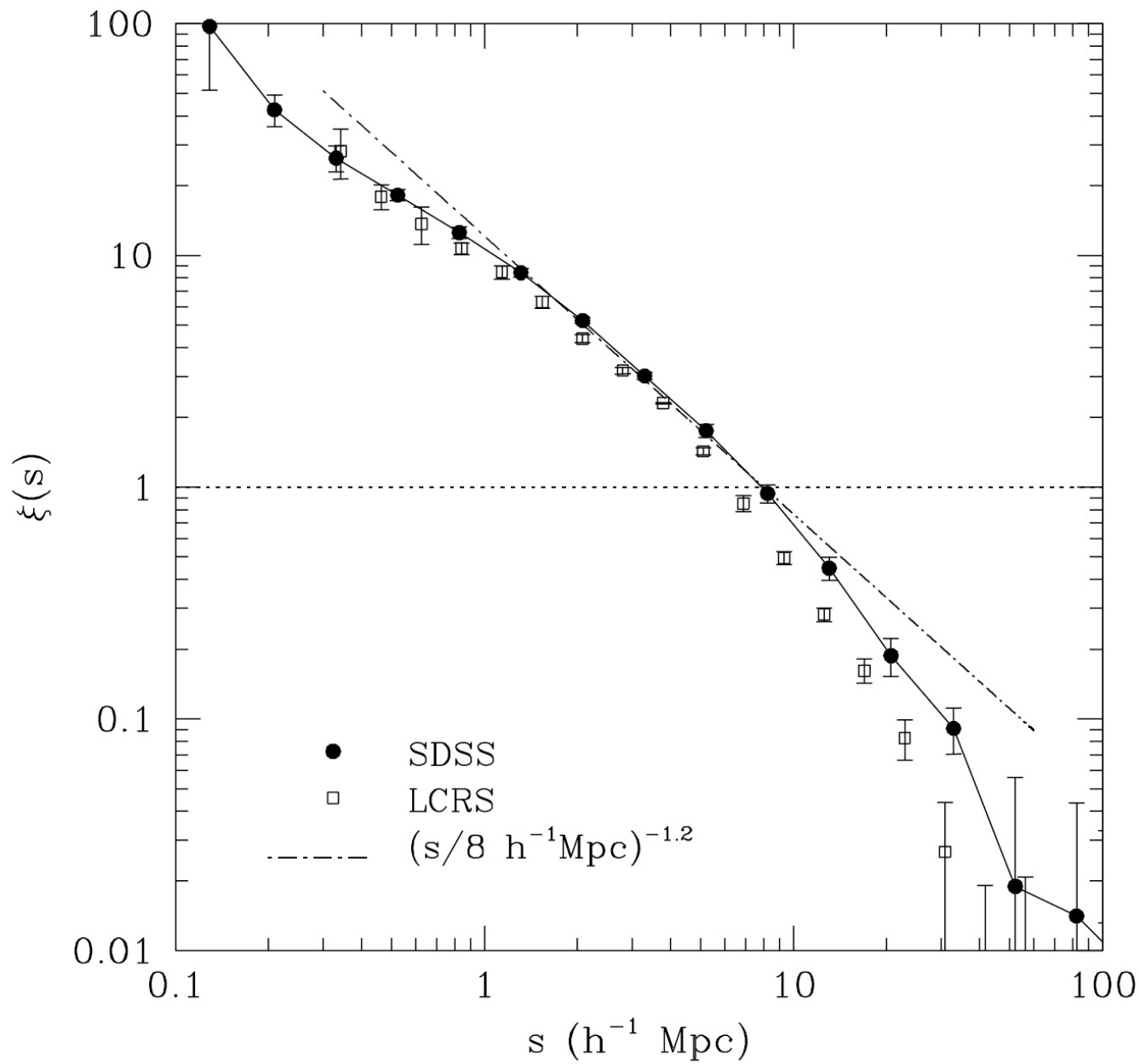
Clear evidence that there are no significant large structures on scales  $> 100\text{-}200$  Mpc



Correlation Functions:

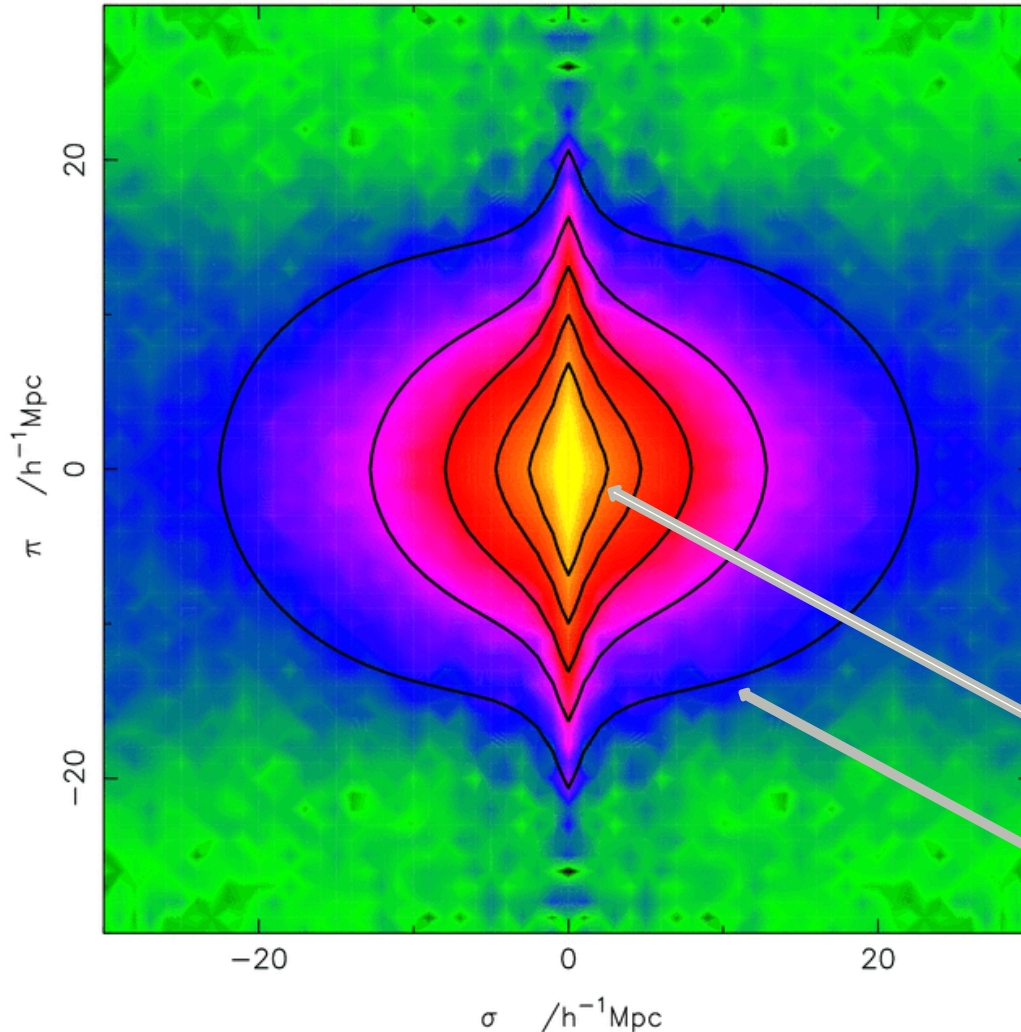
Redshift Space





# sky-redshift space

## 2-pt correlation function $\xi(\sigma, \pi)$



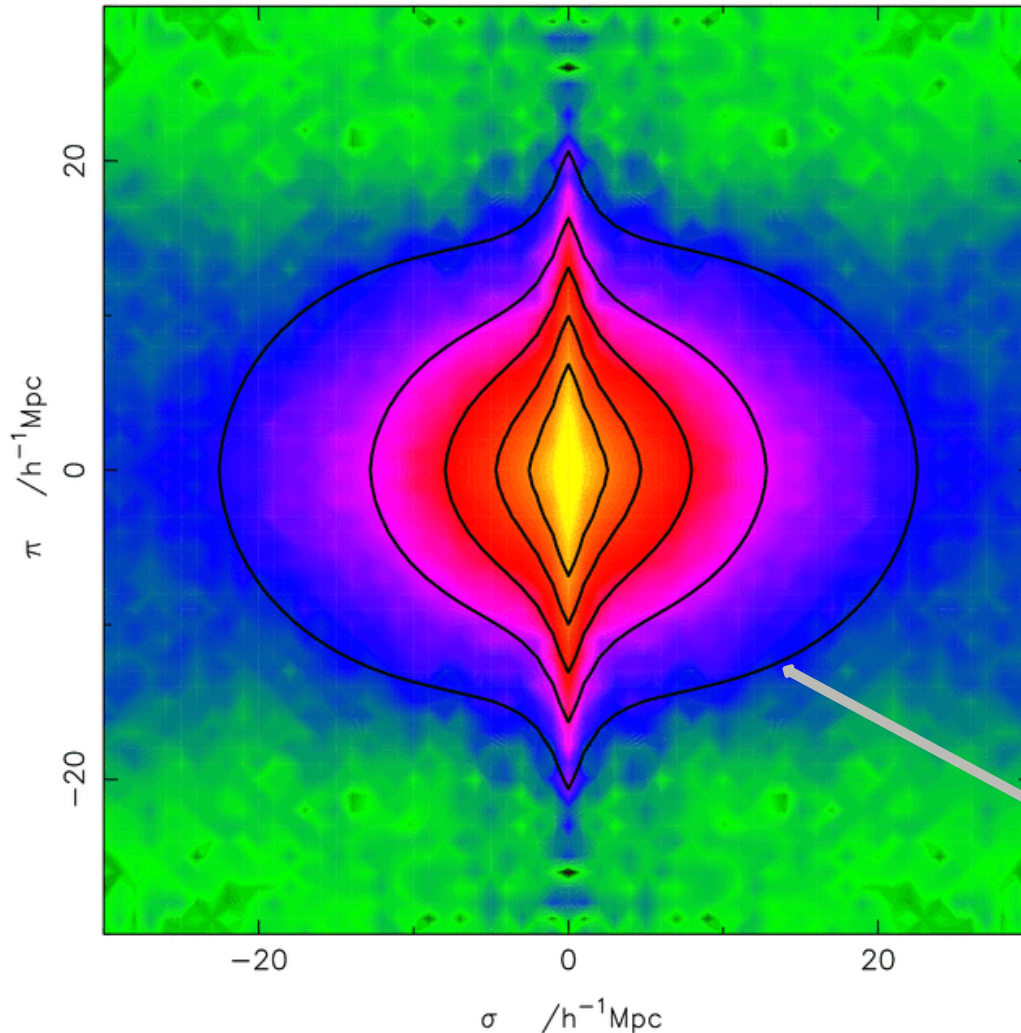
Correlation function determined  
in sky-redshift space:

$$\xi(\sigma, \pi)$$

sky position:  $\sigma = (\alpha, \delta)$   
redshift coordinate:  $\pi = cz$

Close distances:  
distortion due to non-linear  
Finger of God  
Large distances:  
distortions due to large-scale  
flows

# Redshift Space Distortions Correlation Function



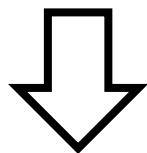
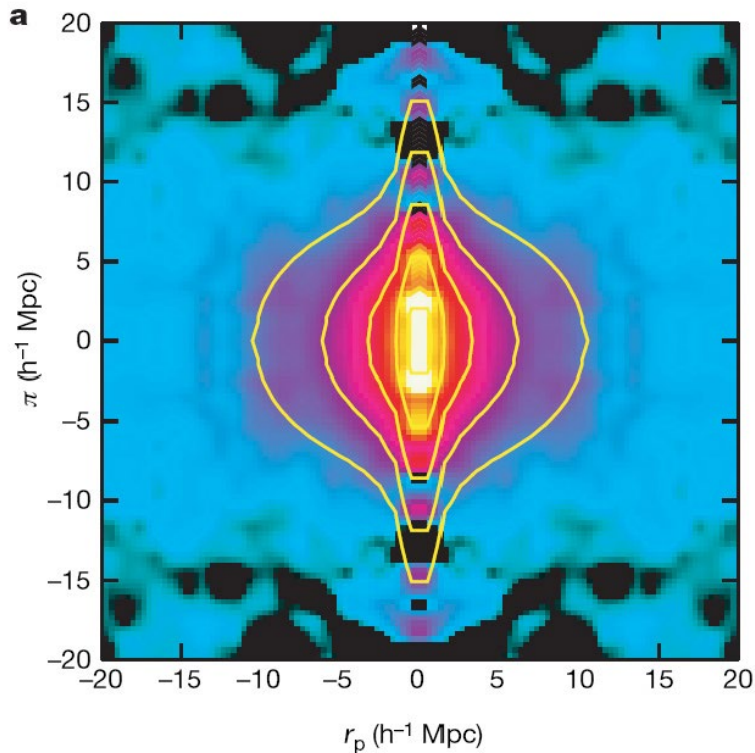
On average,  $\xi_s(s)$  gets amplified  
wrt.  $\xi_r(r)$

Linear perturbation theory  
(Kaiser 1987):

$$\xi_s(s) = \left(1 + \frac{2}{3}\Omega^{0.6} + \frac{1}{5}\Omega^{1.2}\right)\xi_r(s)$$

Large distances:  
distortions due to large-scale  
flows

# Evolution Growth Rate

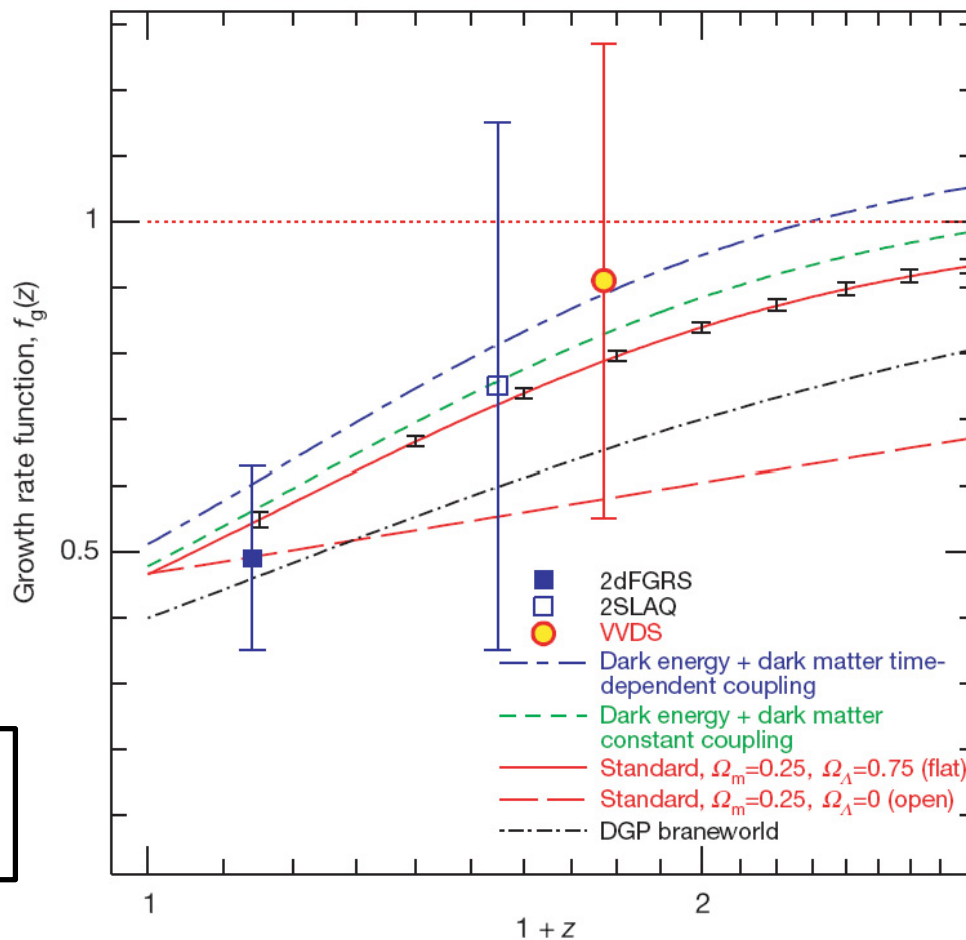


$$f(\Omega_m, \Omega_\Lambda) = \frac{a}{D} \frac{dD}{da} \approx \Omega_m^{0.55}$$

Peebles growth rate factor

Linder 2008

Guzzo et al. 2008



Measurement

Spatial 2pt-Correlation Function



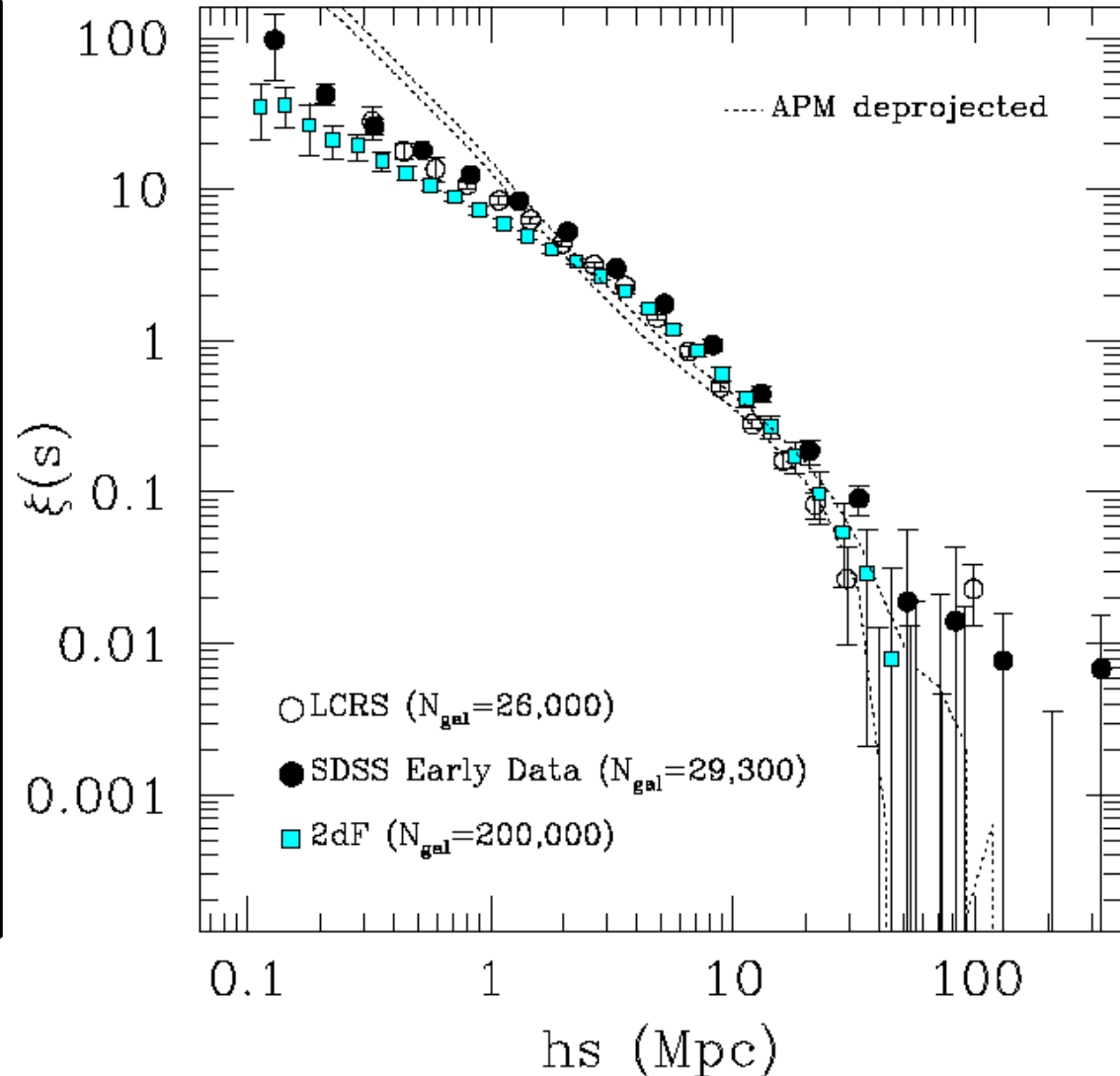
# Deprojected Spatial Correlations

2pt correlation function  
not an ideal power-law:

Halo Model:

Two-point correlation function  
combination of

- 1) small-scale correlations,  
due to galaxies inside  
one dark matter halo
- 2) large scale correlations  
between dark matter halos

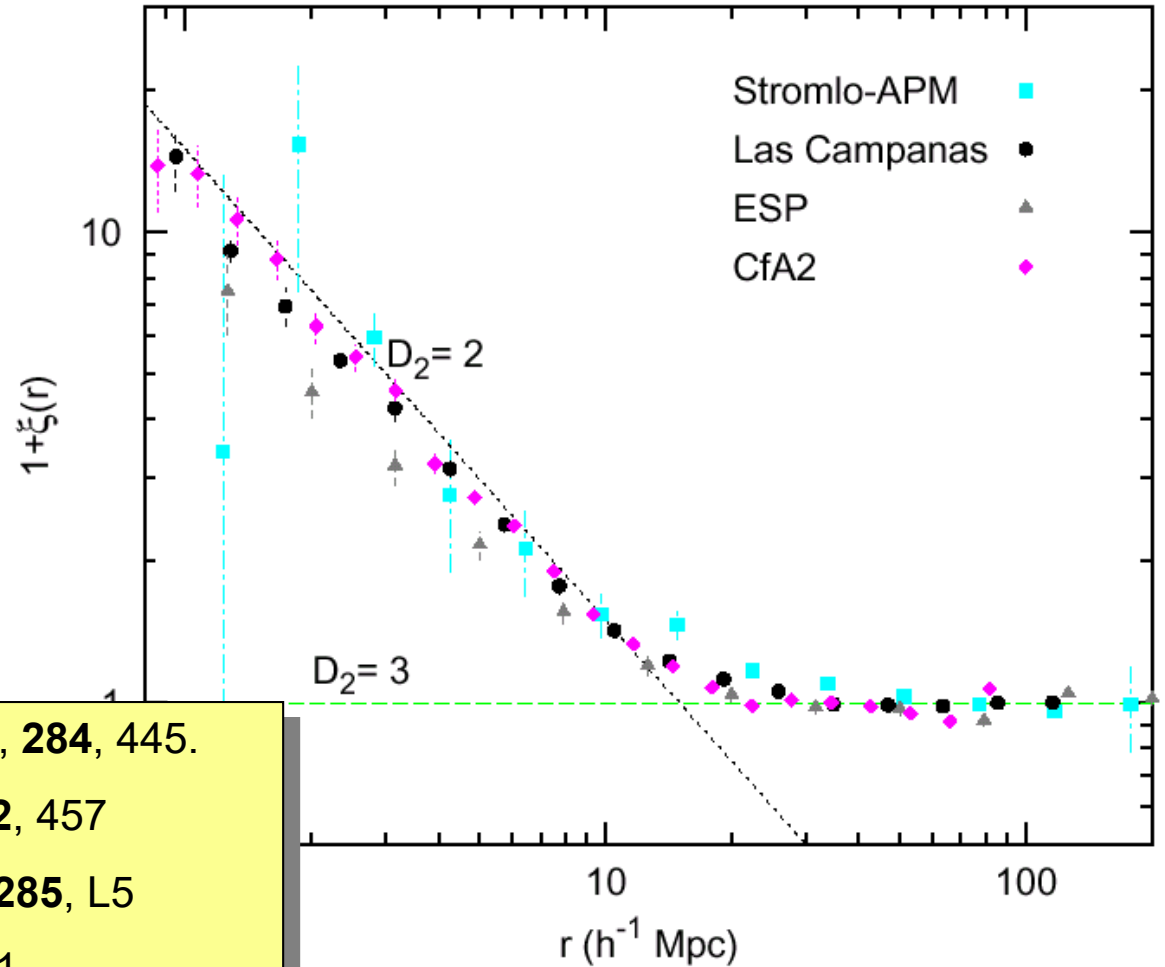


# Convergence to Homogeneity

The correlation function  
 $g(r)=1+\xi(r)$

Stromlo-APM, Las Campanas  
CfA2, ESP redshift surveys.

The fractal behavior at small  
scales disappears at larger  
distances, providing evidence  
for a gradual transition to  
homogeneity.

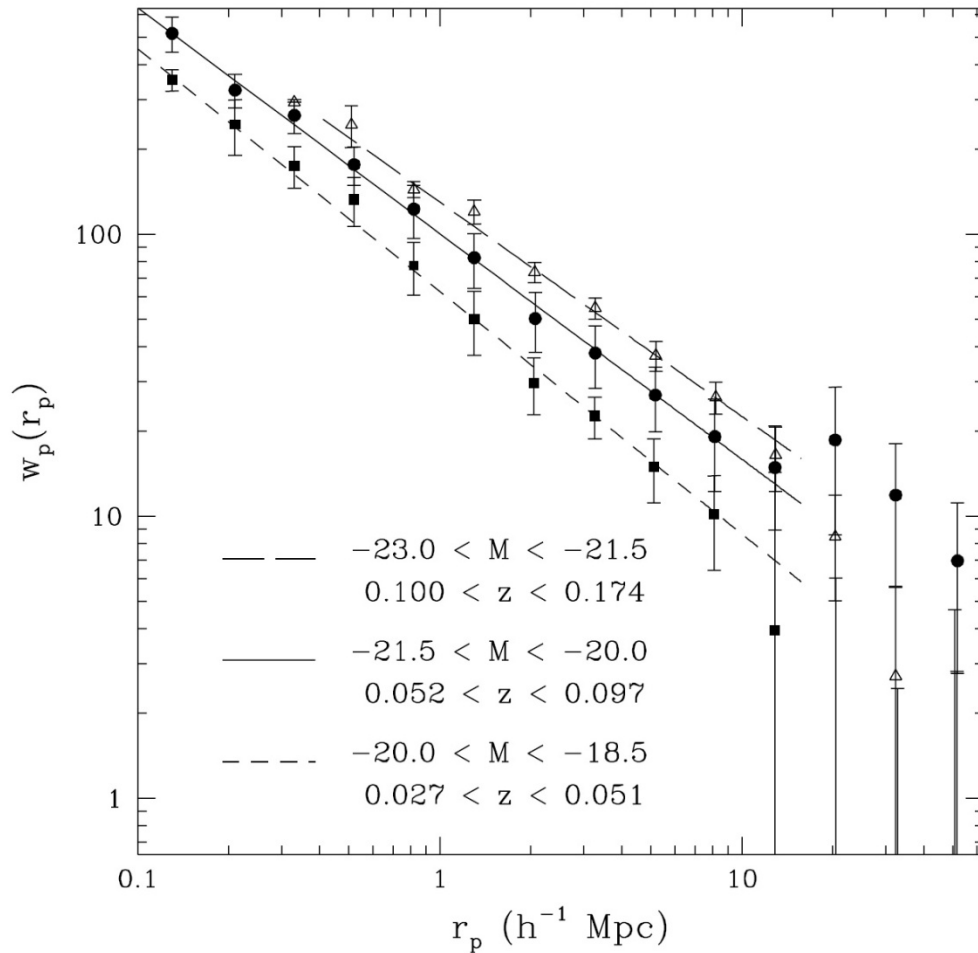


Plot from Martínez, 1999, *Science*, **284**, 445.

- (1) Loveday *et al.*, 1995, *ApJ*, **442**, 457
- (2) Tucker *et al.*, 1997, *MNRAS*, **285**, L5
- (3) Guzzo *et al.*, 2000, *AA*, **355**, 1

# Luminosity Dependence Correlation Functions

# Galaxy Luminosity Dependence



SDSS

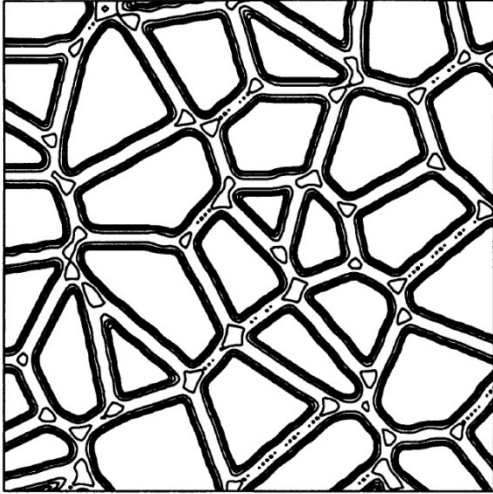
correlation function

for galaxies in different  
luminosity bins

# Spatial Structure & Correlation Functions

# Structural Insensitivity

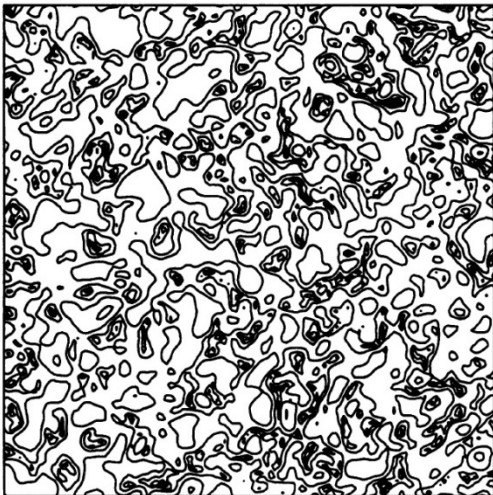
Voronoi foam,  $R=1.6$ , smoothed original



2-pt correlation function is highly insensitive to the geometry & morphology of weblike patterns:

compare 2 distributions with same  $\bar{\rho}(r)$ , cq.  $P(k)$ , but totally different phase distribution

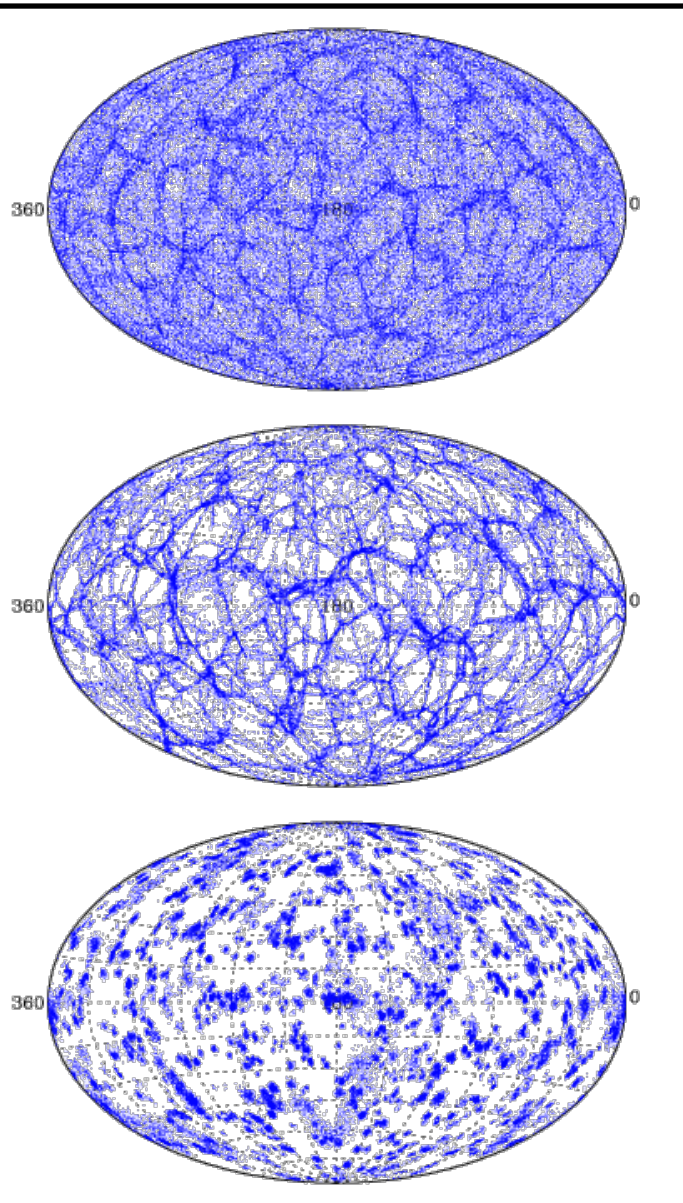
Voronoi foam,  $R=1.6$ , random phases



In practice, some sensitivity in terms of distinction Field, Filamentary, Wall-like and Cluster-dominated distributions:

because of different fractal dimensions

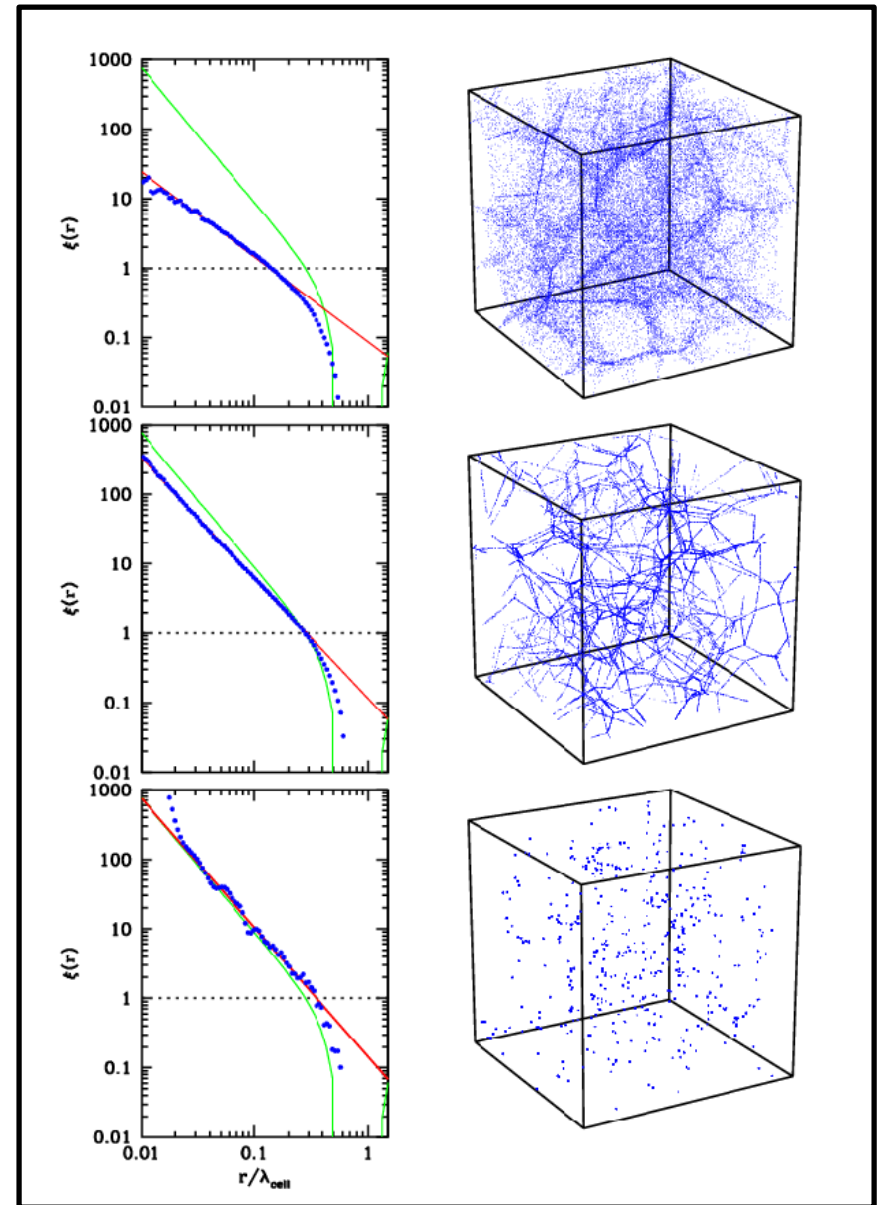
# Structural Sensitivity



Wall-  
dominated

Filamentary

Cluster-like

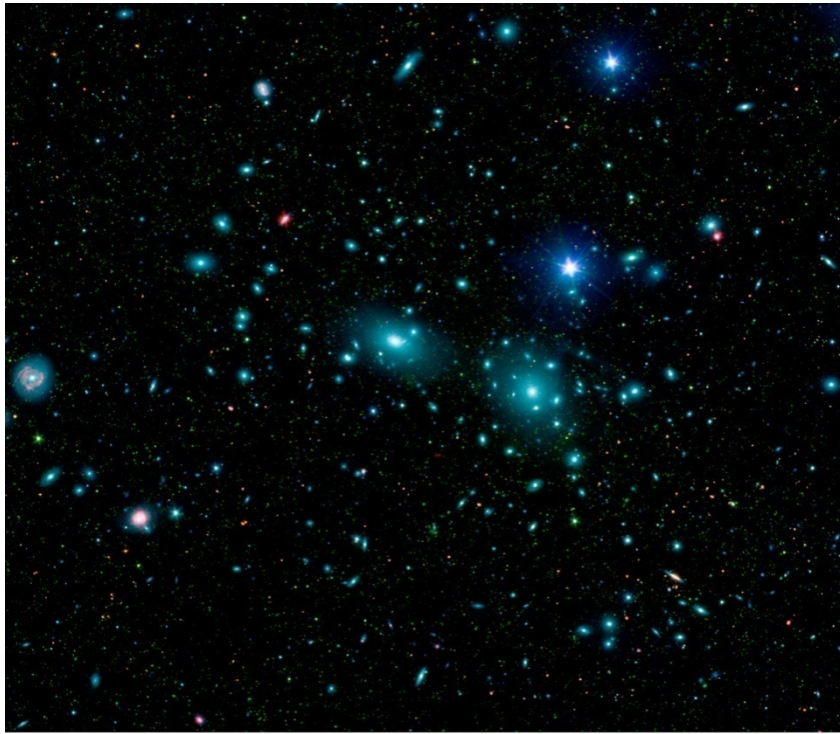


Cluster

Correlation Functions



# Clusters of Galaxies



Coma Cluster

Perseus Cluster

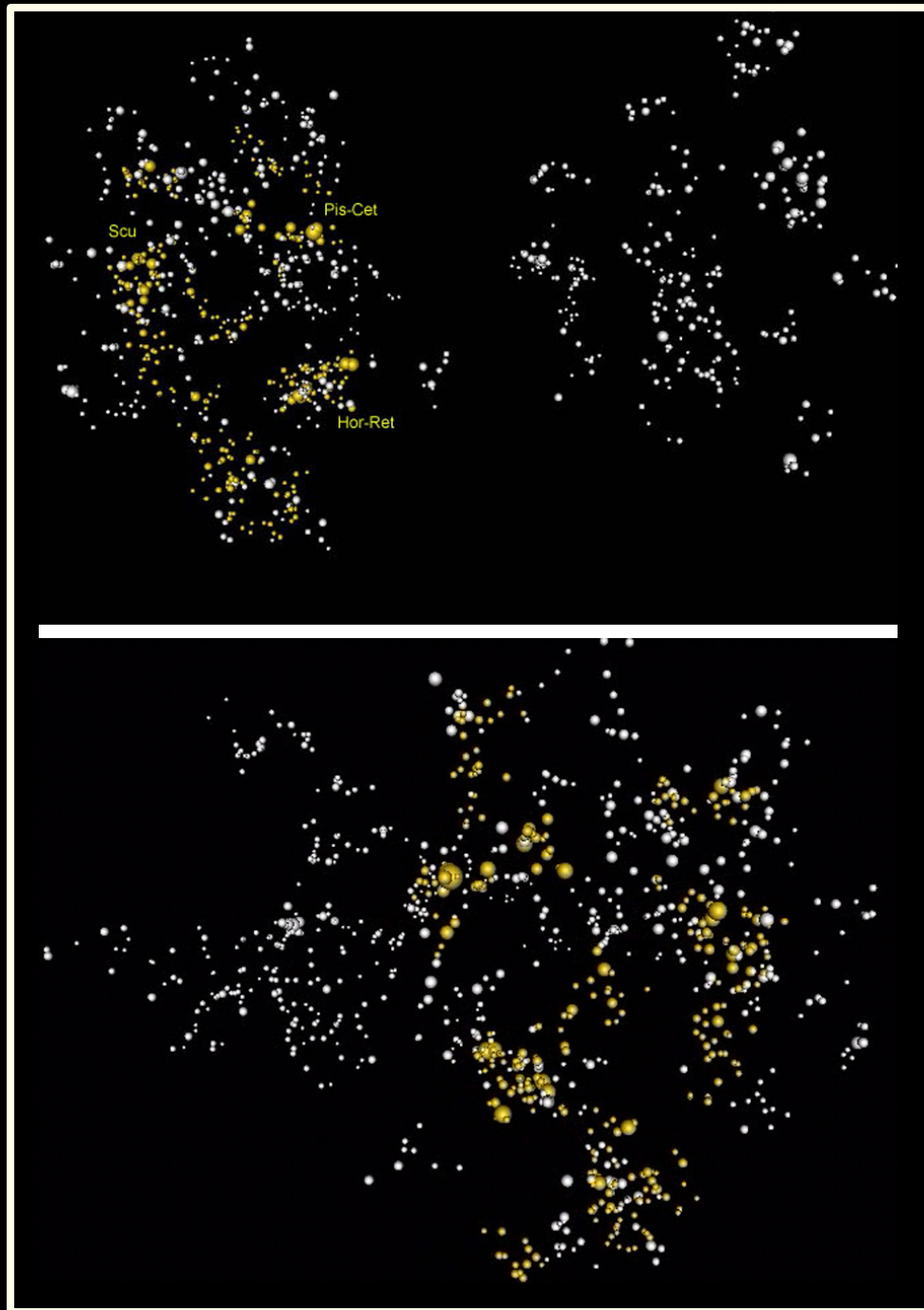


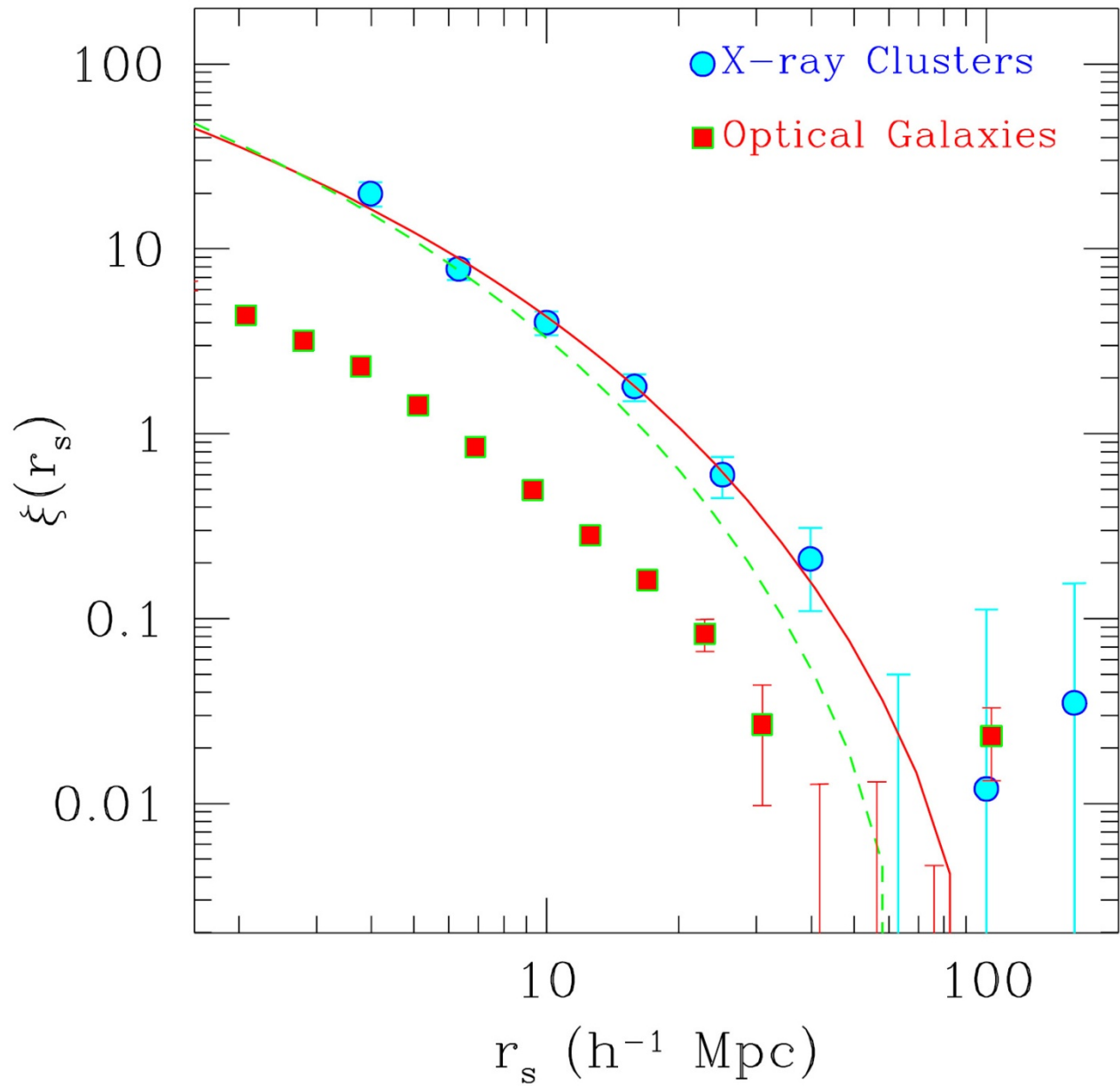
# Clustering of Clusters

Clusters cluster much more strongly than galaxies:

- clustering defines superclusters !
- also power-law 2-pt correlation fct.
- same power law slope  $\approx 1.8$
- much higher correlation length  $r_0$  :

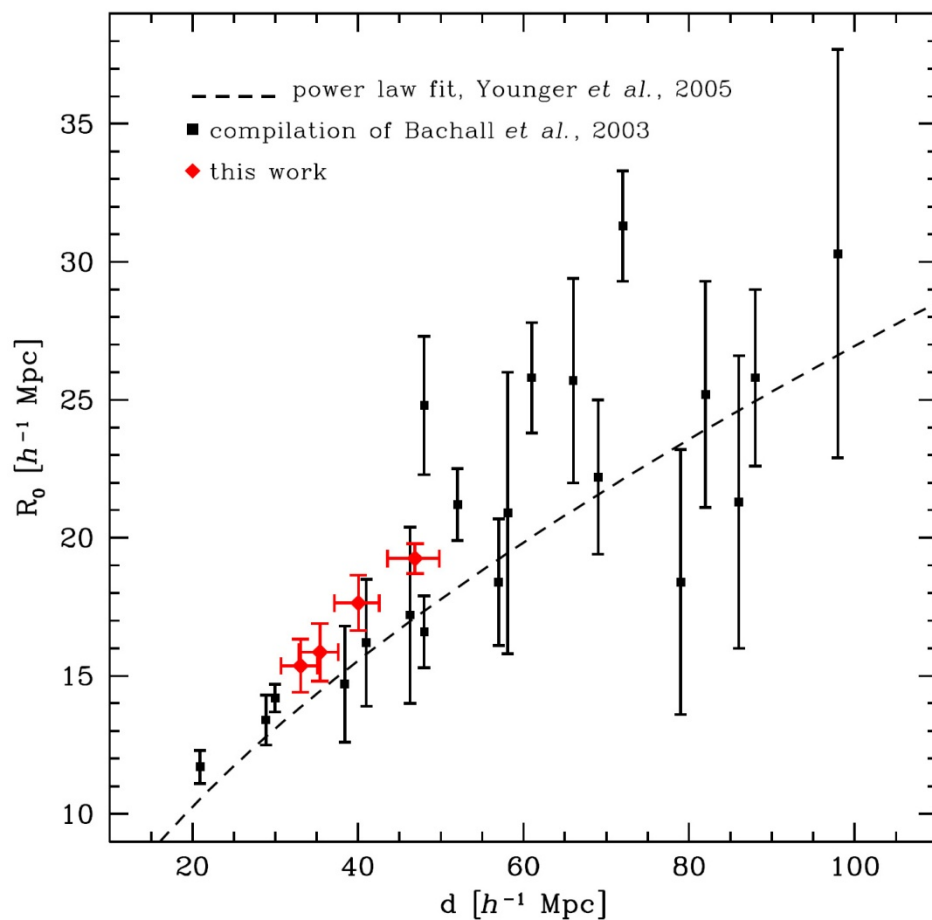
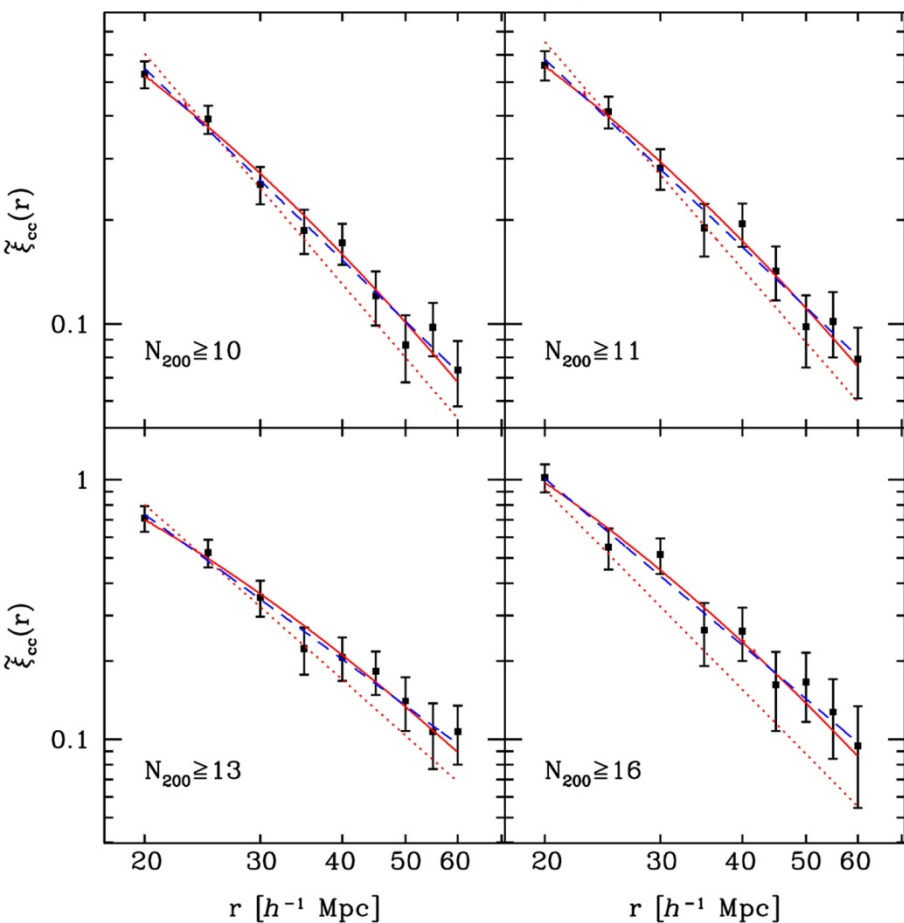
$$r_0 \sim 15-25 h^{-1} \text{ Mpc}$$





# Richness-Dependent Cluster Correlations

More massive clusters are systematically more strongly clustered than lower mass ones.



# Richness-Dependent Cluster Correlations

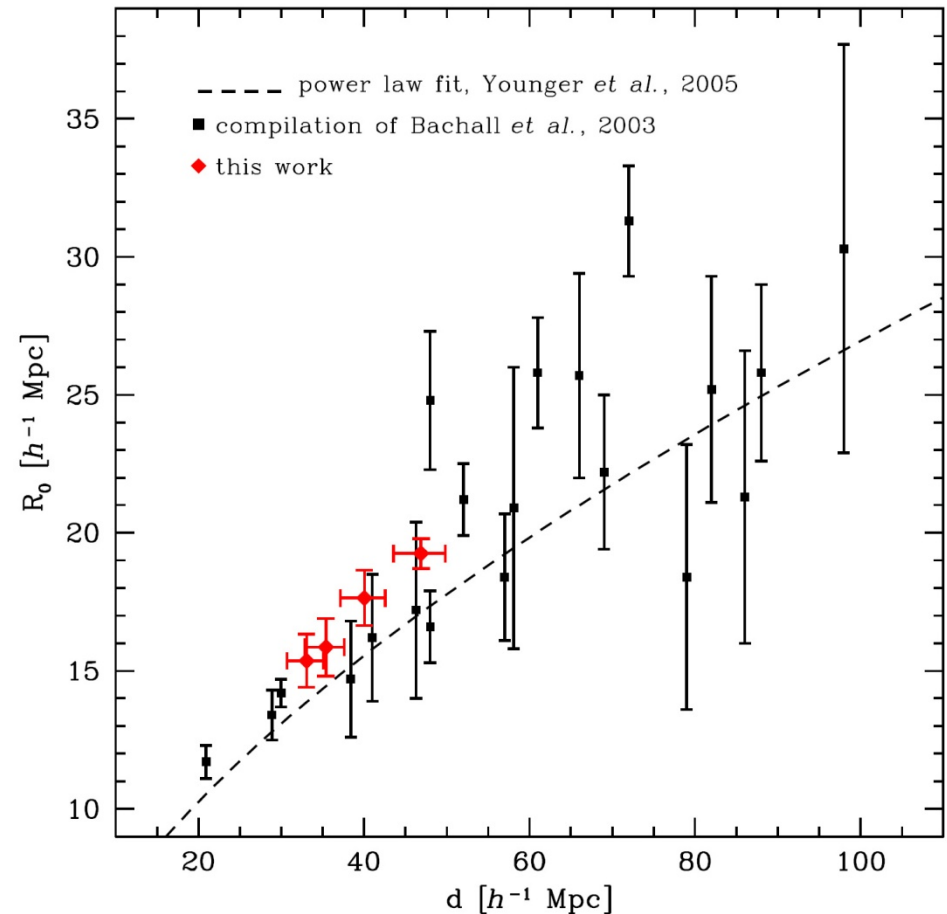
More massive clusters are more systematically more strongly clustered than lower mass ones:

simple model:

Szalay & Schramm 1985

$$\xi_{cc}(r) = \beta \left( \frac{L(r)}{r} \right)^\gamma$$

$$L(R) = n^{-1/3}$$



Higher Order

Correlation Functions:

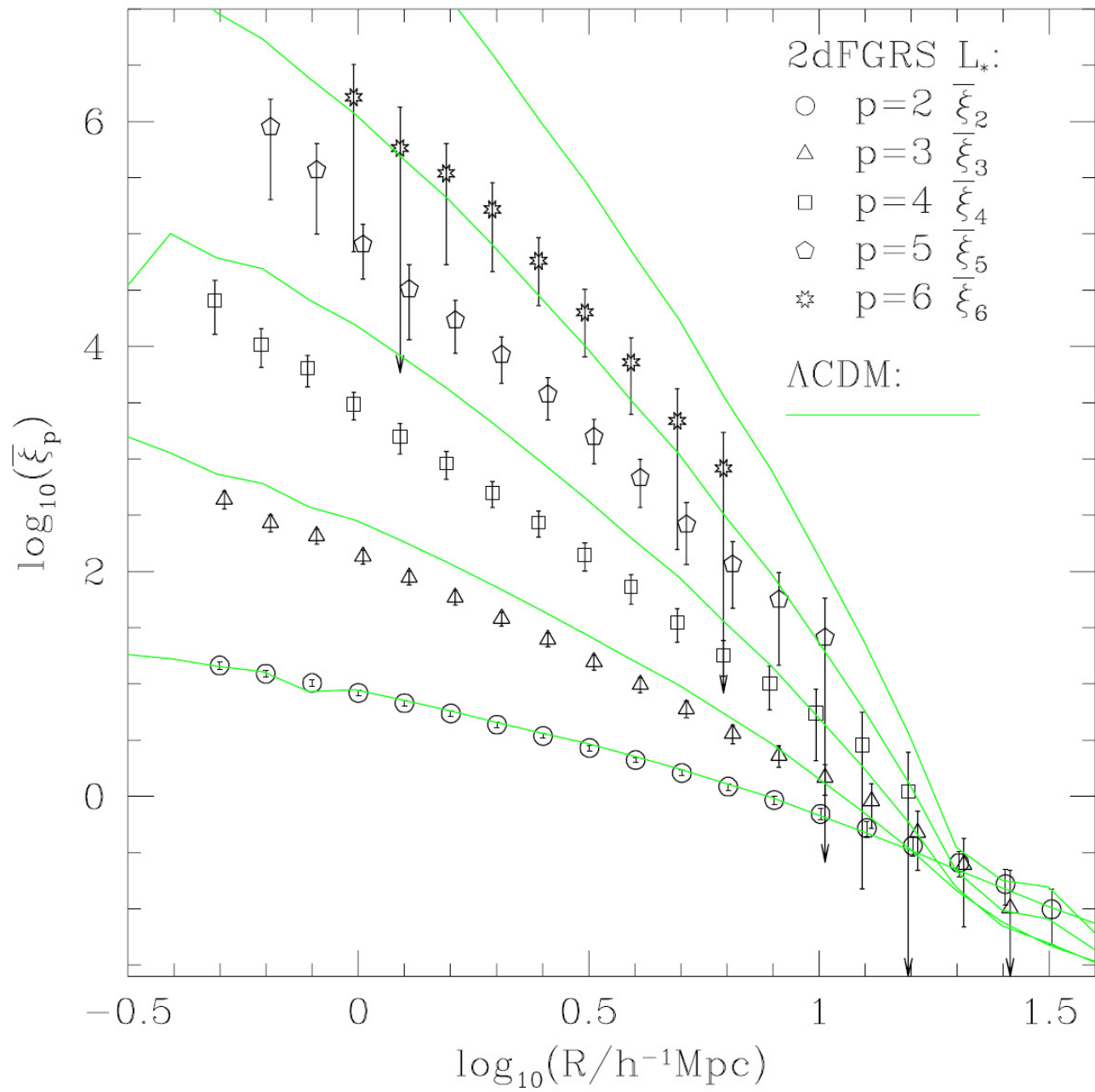
# N-point correlation functions

- N-point correlation function

$$\xi^{(n)}(\vec{x}_1, \vec{x}_2, \dots, \vec{x}_n)$$

- Probability function of finding an n-tuplet of galaxies in n specified volumes  $dV_1, dV_2, \dots, dV_n$

$$dP(\vec{x}_1, \vec{x}_2, \dots, \vec{x}_n) = \bar{n}^n [1 + \xi^{(n)}] dV_1 dV_2 \dots dV_n$$



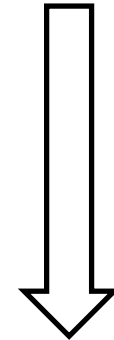


# 3-point correlation functions

3-point correlation function

$$dP(\vec{x}_1, \vec{x}_2, \vec{x}_3) = \bar{n}^{-3} [1 + \xi^{(3)}] dV_1 dV_2 dV_3$$

$$[1 + \xi^{(3)}] = \left\langle \prod_i (1 + \delta_i) \right\rangle$$



$$[1 + \xi^{(3)}] = 1 + \xi(r_{12}) + \xi(r_{13}) + \xi(r_{23}) + \zeta(\vec{r}_1, \vec{r}_2, \vec{r}_3)$$

# 3-point correlation functions

3-point correlation function

$$[1 + \xi^{(3)}] = 1 + \xi(r_{12}) + \xi(r_{13}) + \xi(r_{23}) + \zeta(\vec{r}_1, \vec{r}_2, \vec{r}_3)$$

reduced 3-point correlation function

$$\zeta(\vec{r}_1, \vec{r}_2, \vec{r}_3) = \langle \delta_1 \delta_2 \delta_3 \rangle$$

excess correlation over that described by the 2-pt contributions

- $\neq 0$ : non-Gaussian density field
- Hierarchical ansatz (Groth & Peebles 1977)

$$\zeta(\vec{r}_1, \vec{r}_2, \vec{r}_3) = Q(\xi_{12}\xi_{23} + \xi_{23}\xi_{31} + \xi_{31}\xi_{12})$$

# Power Spectrum

# Power Spectrum

- Directly measuring clustering in Fourier space:
  - More intuitive physically:  
separating processes on different scales
  - Theoretical model predictions are made in terms of power spectrum
  - Amplitudes for different wavenumbers are statistically orthogonal

# Power Spectrum $P(k)$

$$\delta(\mathbf{x}) = \int \frac{d\mathbf{k}}{(2\pi)^3} \hat{\delta}(\mathbf{k}) e^{-i\mathbf{k}\cdot\mathbf{x}}$$

$$\begin{aligned} (2\pi)^3 P(k_1) \delta_D(\mathbf{k}_1 - \mathbf{k}_2) &\equiv \langle \hat{f}(\mathbf{k}_1) \hat{f}^*(\mathbf{k}_2) \rangle \\ &\Updownarrow \\ P(k) &\propto \langle \hat{f}(\mathbf{k}) \hat{f}^*(\mathbf{k}) \rangle \end{aligned}$$

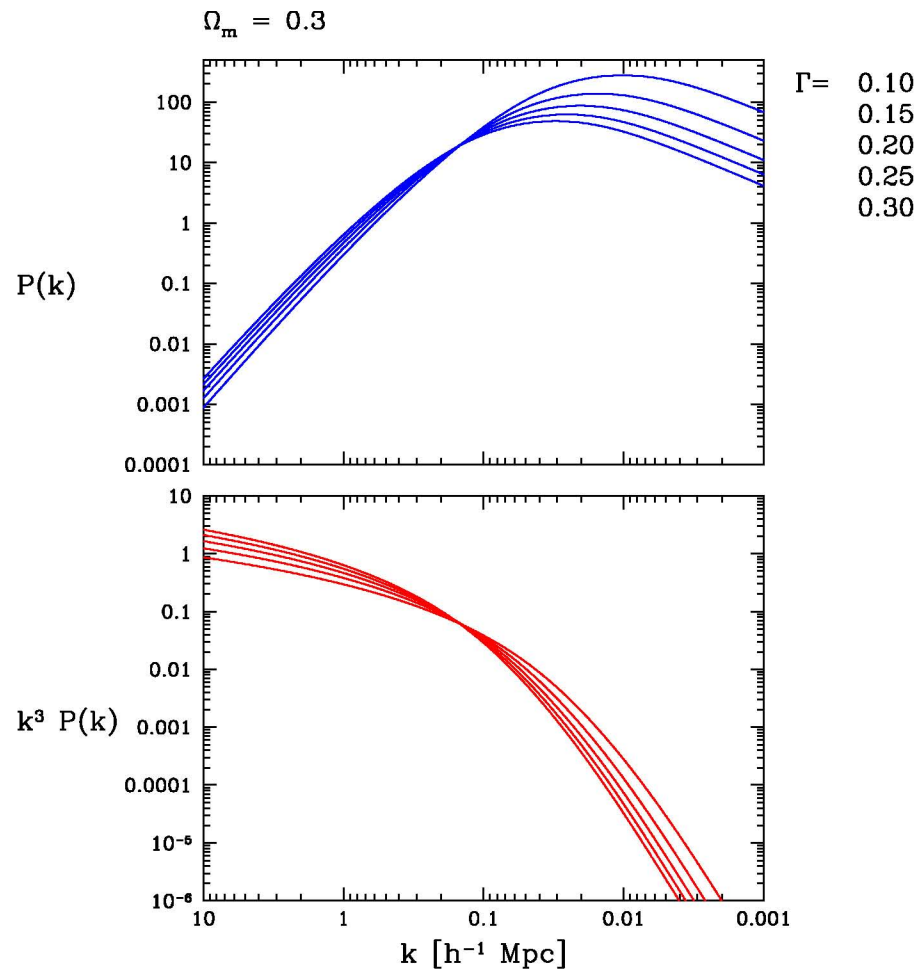
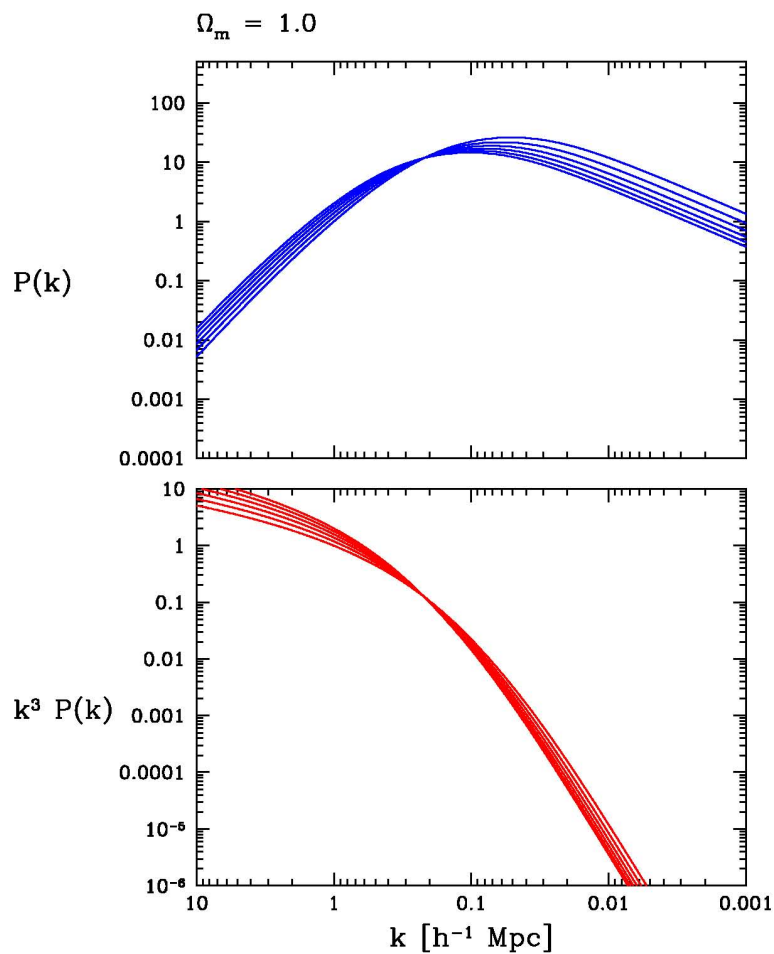
# CDM Power Spectrum $P(k)$

$$P_{\text{CDM}}(k) \propto \frac{k^n}{[1 + 3.89q + (16.1q)^2 + (5.46q)^3 + (6.71q)^4]^{1/2}} \times \frac{[\ln(1 + 2.34q)]^2}{(2.34q)^2}$$

$$q = k/\Gamma$$

$$\Gamma = \Omega_{m,\circ} h \exp\left\{-\Omega_b - \frac{\Omega_b}{\Omega_{m,\circ}}\right\}$$

# Power Spectrum $P(k)$



# Power Spectrum - Correlation Function

$$P(k) = \int d^3 r \xi(\vec{r}) e^{i\vec{k}\cdot\vec{r}}$$

$$\xi(\vec{r}) = \int \frac{d^3 k}{(2\pi)^3} P(k) e^{-i\vec{k}\cdot\vec{r}}$$

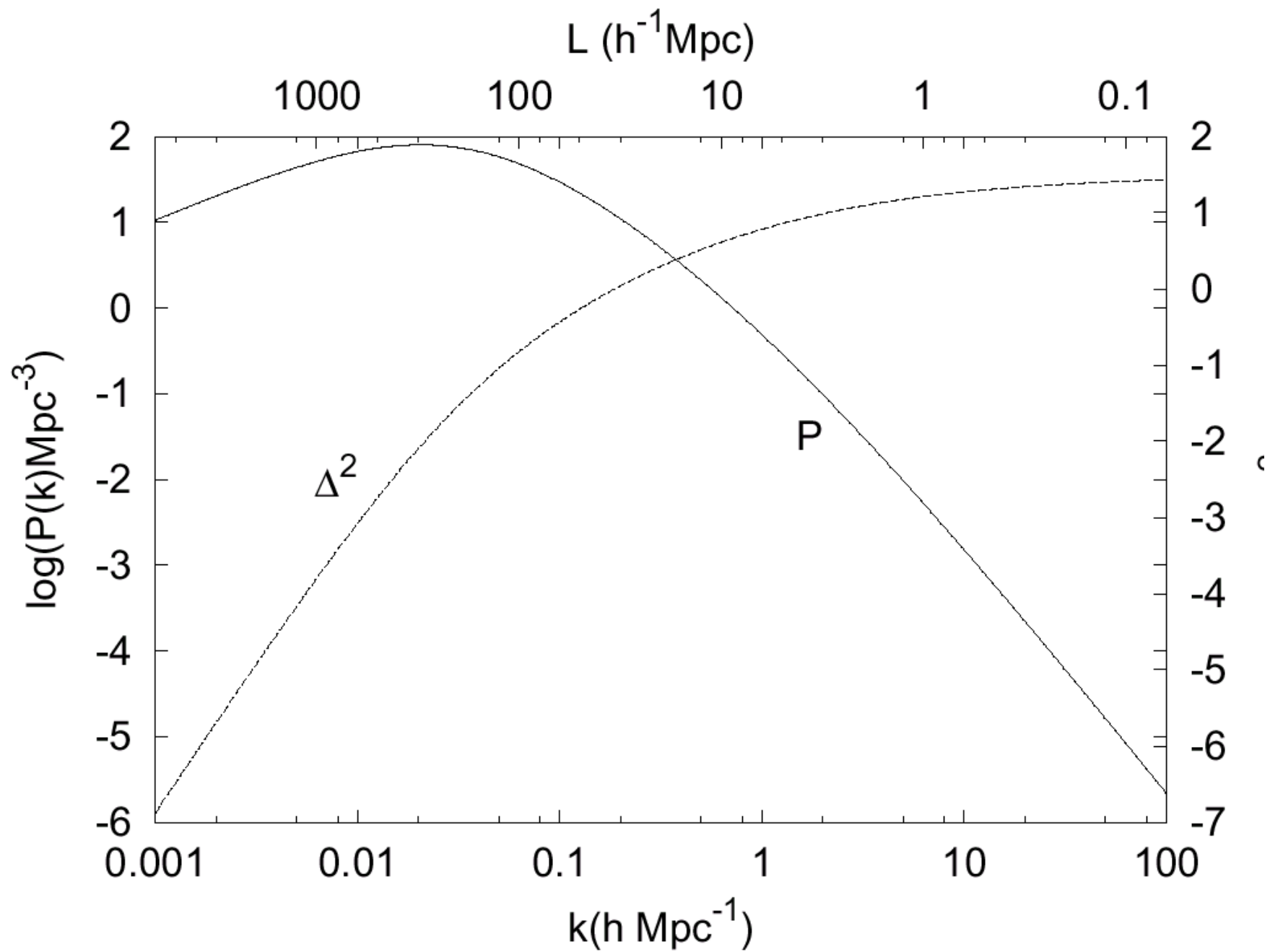
Isotropy:

$$\xi(r) = 4\pi \int_0^\infty \frac{k^2 dk}{(2\pi)^3} P(k) \frac{\sin(kr)}{kr}$$

Delta-power

$$\Delta^2(k) = \frac{1}{2\pi^2} P(k) k^2$$





# Power Spectrum Estimators

Estimators of  $P(k)$

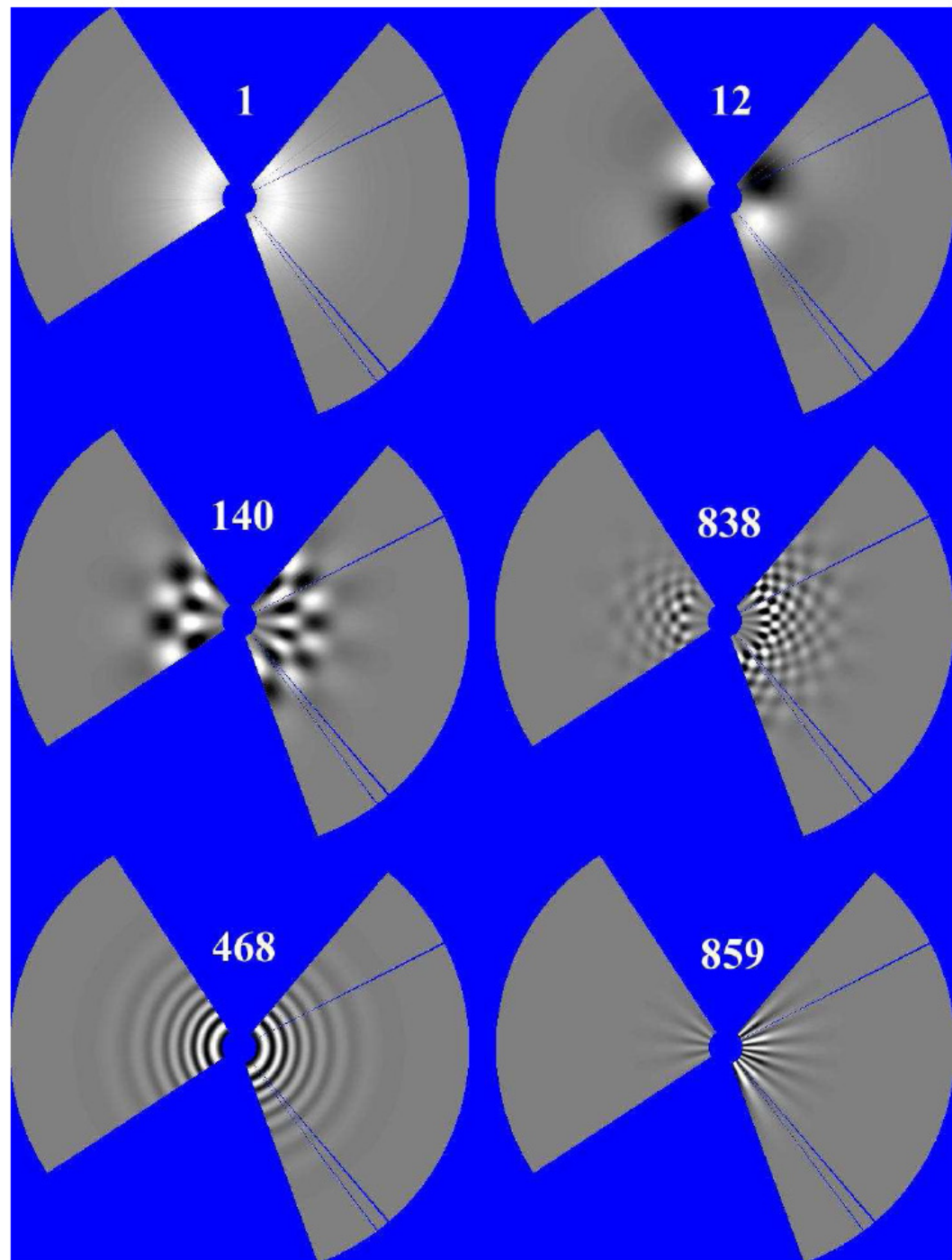
- Direct estimator
- Pixelization and maximum likelihood
- Karhunen-Loève (signal-to-noise) transform
- Quadratic compression
- Bayesian
- Multiresolution decomposition

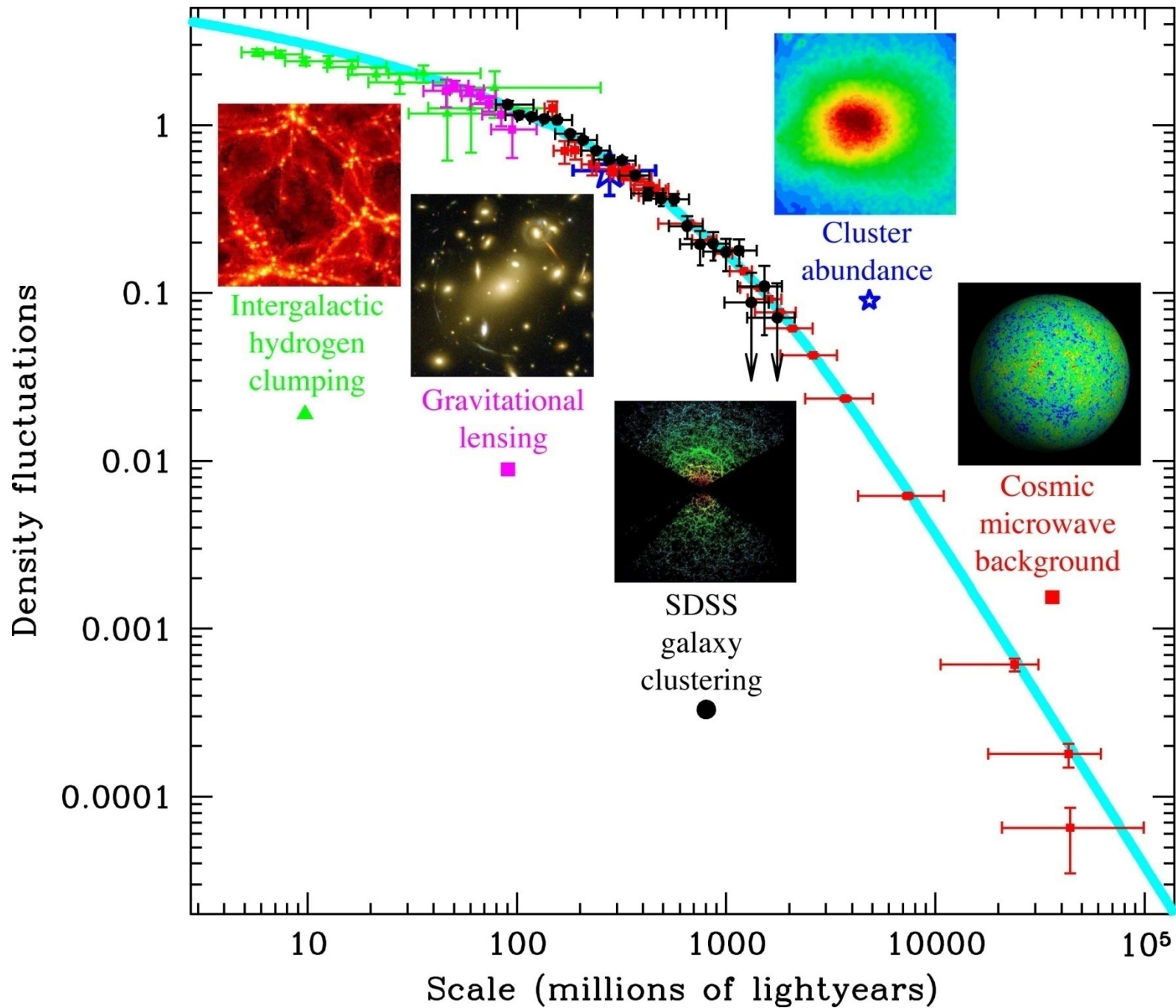
Tegmark, Hamilton, Strauss, Vogeley, and Szalay, (1998),  
Measuring the galaxy power spectrum with future redshift  
surveys, ApJ, **499**, 555

# Karhunen- Loeve

Decomposition in series of  
orthogonal  
signal-noise eigenfunctions

Vogelely & Szalay 1995





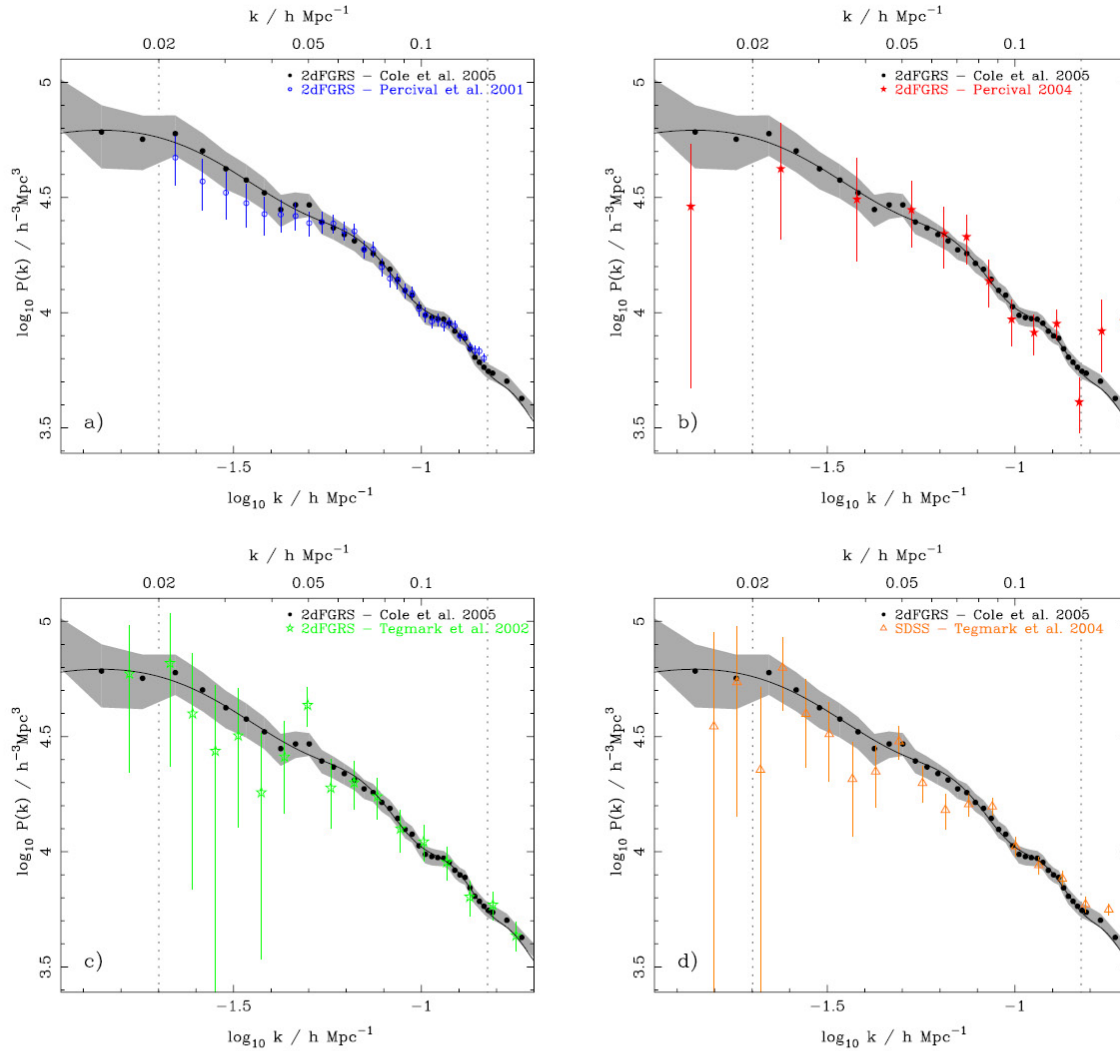
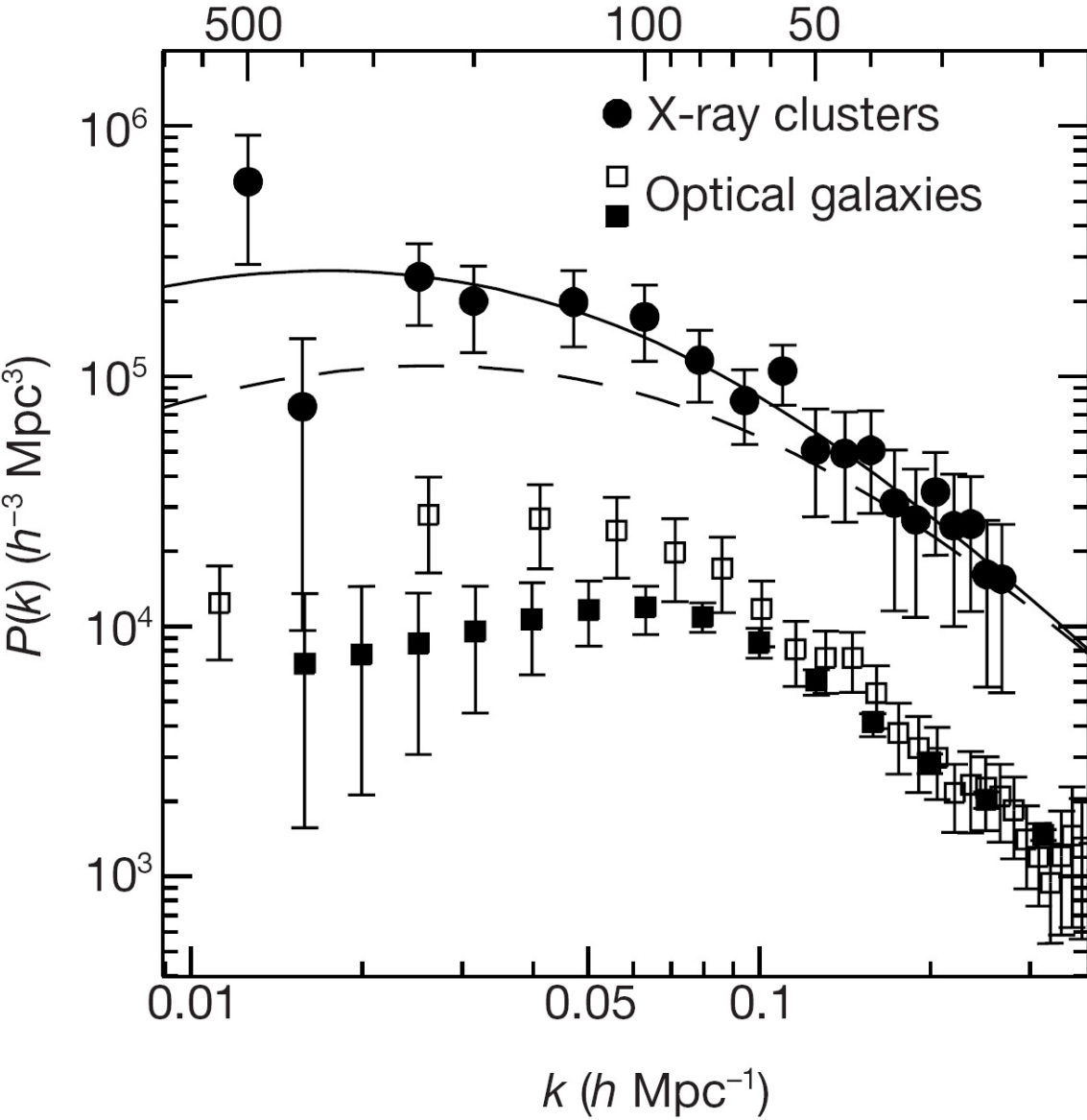


**Figure 16.** The redshift-space power spectrum calculated in this paper (solid circles with  $1\sigma$  errors shown by the shaded region) compared with other measurements of the 2dFGRS power-spectrum shape by (a) Percival et al. (2001), (b) Percival (2005), and (c) Tegmark et al. (2002). For the data with window functions, the effect of the window has been approximately corrected by multiplying by the net effect of a model power spectrum with  $\Omega_m h = 0.168$ ,  $\Omega_b/\Omega_m = 0.0$ ,  $h = 0.72$  &  $n_s = 1$ . A zero-baryon model was chosen in order to avoid adding features into the power spectrum. All of the data are renormalized to match the new measurements. Panel (d) shows the uncorrelated SDSS real-space  $P(k)$  estimate of Tegmark et al. (2004), calculated using their ‘modelling method’ with no FOG compression (their Table 3). These data have been corrected for the SDSS window as described above for the 2dFGRS data. The solid line shows a model linear power spectrum with  $\Omega_m h = 0.168$ ,  $\Omega_b/\Omega_m = 0.17$ ,  $h = 0.72$ ,  $n_s = 1$  and normalization matched to the 2dFGRS power spectrum.

Spatial wavelength ( $h^{-1}$  Mpc)



Topological Analysis  
of the Cosmic Web

# Cosmic Structure Analysis

To assess the

key aspects of the

nonlinear cosmic matter and galaxy distribution:

- multiscale character
- weblike network
- volume dominance voids



hierarchical structure formation  
anisotropic collapse  
asymmetry overdense vs. underdense

Many statistical measures:

clustering measures (correlation functions)  
density distribution functions

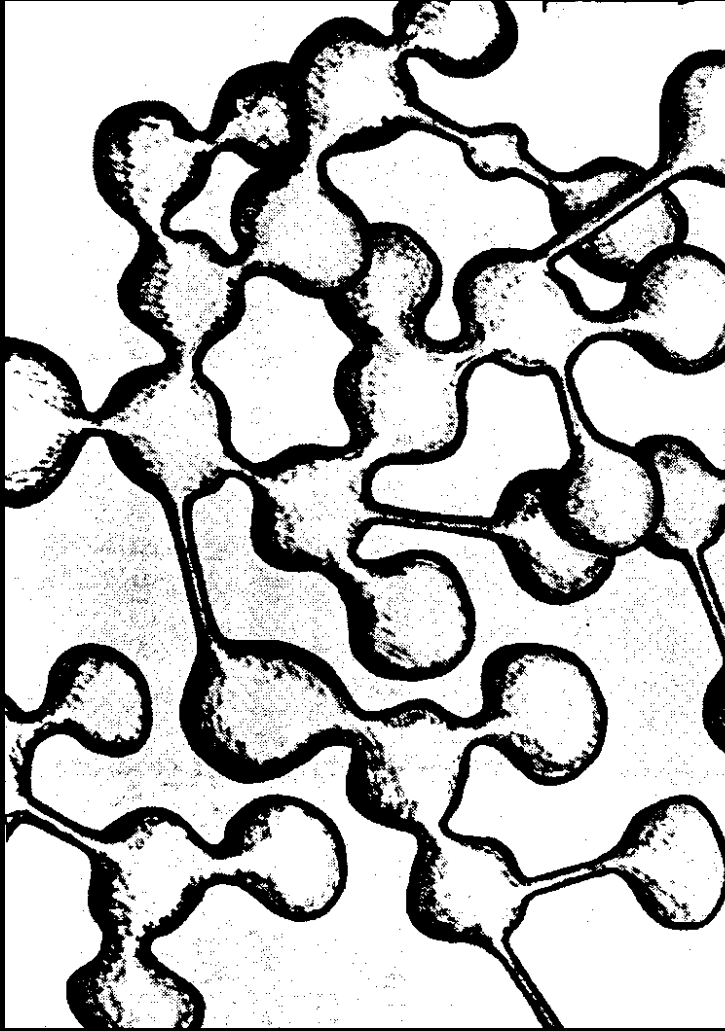
Topological Characteristic of network:

genus statistics

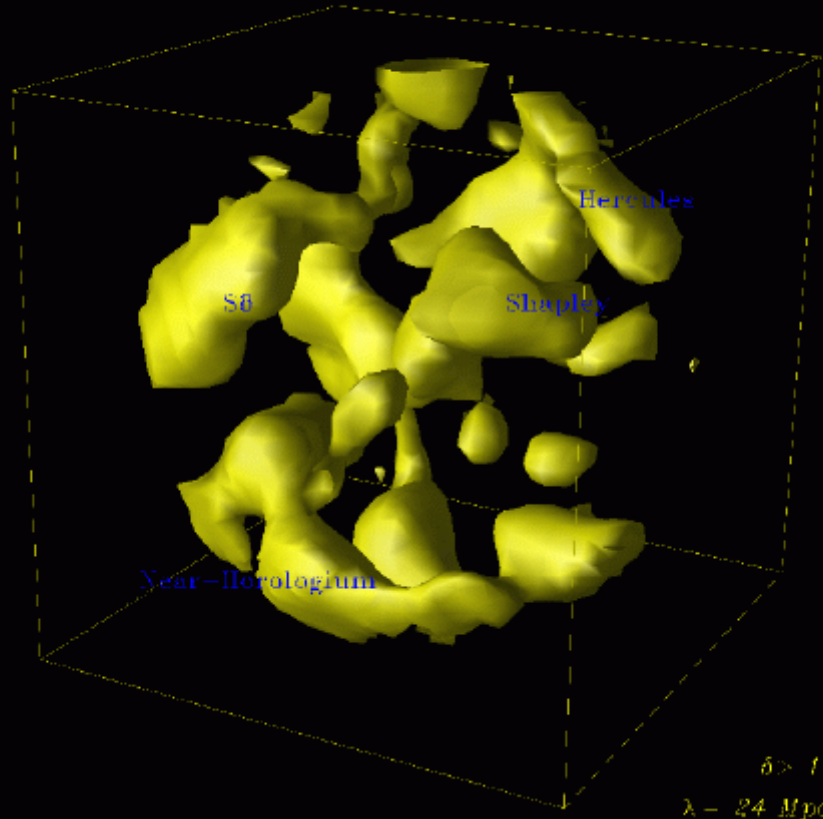
Geometric Characteristics:

Minkowski functionals





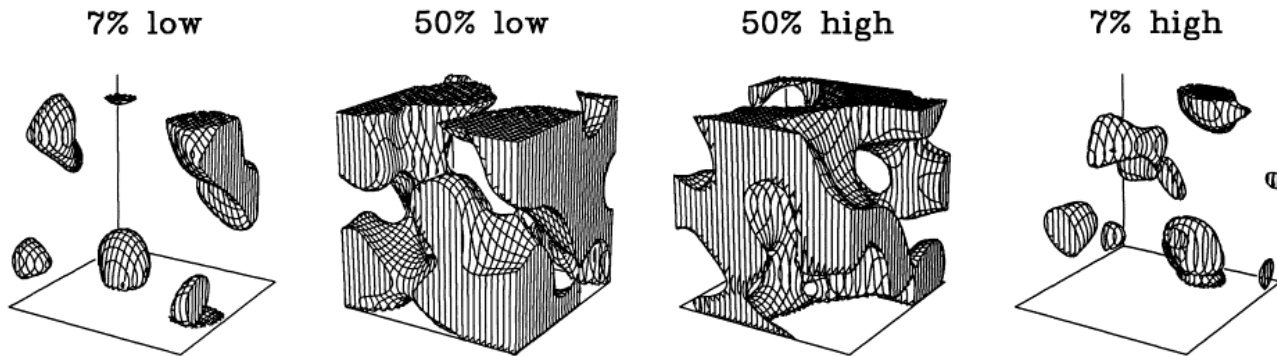
*PSCz density field < 160 Mpc/h.*



# Why is the topology study useful?

## 1. Direct intuitive meanings

- characterize the LSS as a quantitative measure with a physical interpretation attached



## 2. Easy to measure

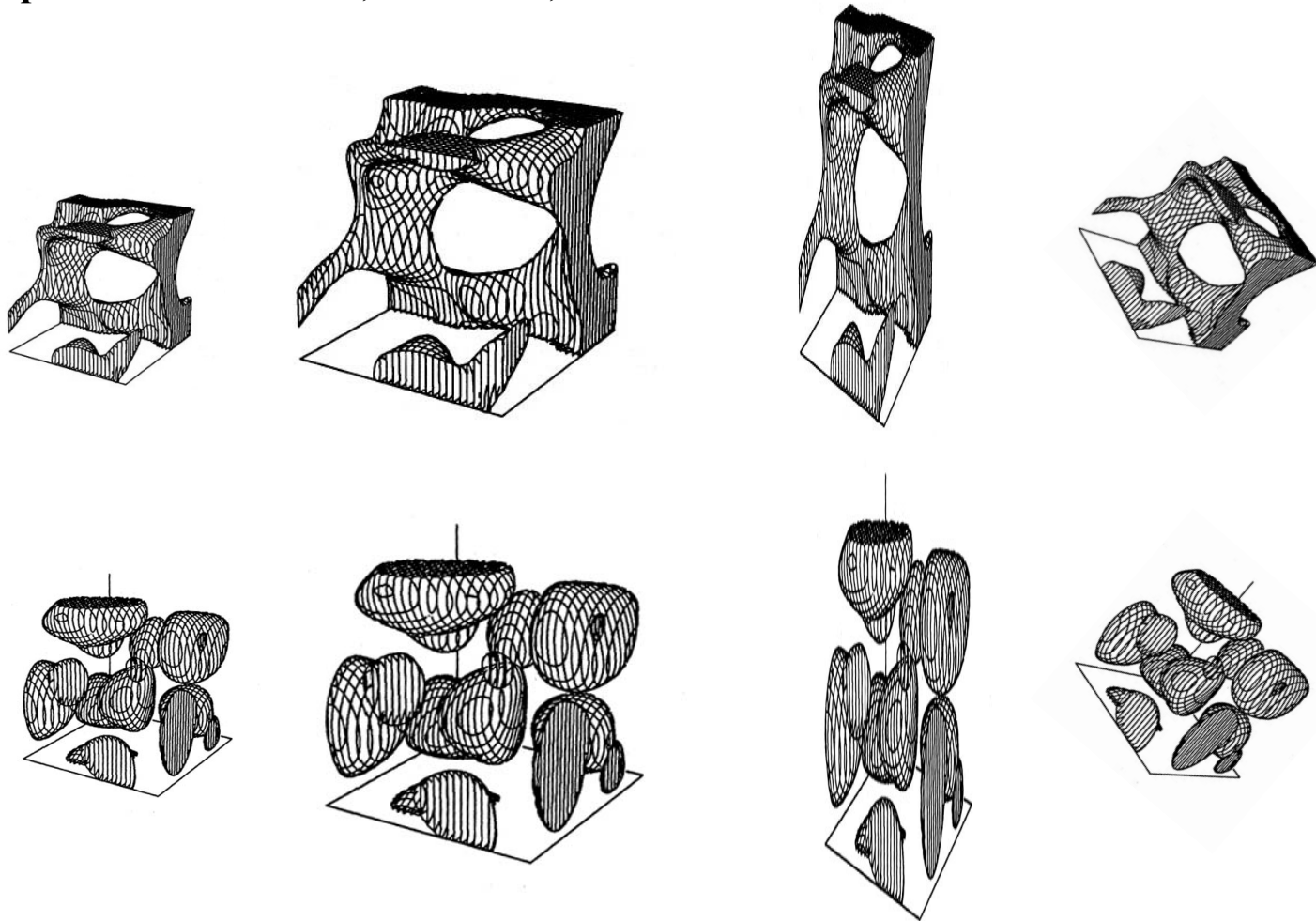
- global genus topology from integration of local curvature:

According to the Gauss-Bonnet theorem the integrated Gaussian curvature of a surface is related with its topological genus by

$$C = \int K dA = 4\pi(1 - G)$$

# Intrinsic topology

does not change by trivial change in the shape of structure  
or by trivial coordinate transformation, which result in monotonic  
expansion/contraction, distortion, rotation ...



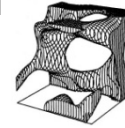
## II. Introductory theory of topology statistics

### Measures of intrinsic topology - **Minkowski Functionals**

#### 3D

1. 3d genus (Euler characteristic)
2. mean curvature
3. contour surface area
4. volume fraction

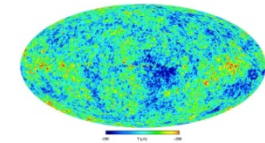
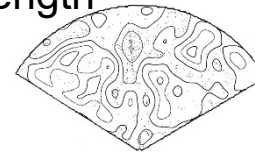
→ 3d galaxy redshift survey data, 3d HI map



#### 2D

1. 2d genus (Euler characteristic)
2. contour length
3. area fraction

→ CMB temp./polarization, 2d galaxy surveys



#### 1D

1. level crossings
2. length fraction

→ Ly $\alpha$  clouds, deep HI surveys, pencil beam galaxy surveys

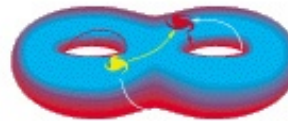
### II. Introductory theory of topology statistics

1. Measures of intrinsic topology
2. Definitions of MFs
3. Gaussian formulae

Topological definition of the genus,  $G = -V_3$

**Genus = # of holes in iso-density contour surfaces - # of isolated regions**

**[ex.  $G(\text{sphere}) = -1$ ,  $G(\text{torus}) = 0$ ,  $G(\text{two tori}) = +1$  ]**



: 2 holes – 1 body = +1

The topological genus is related with the integrated Gaussian curvature of a surface by (Gauss-Bonnet theorem )

$$C = \int K dA = 4\pi(1 - G)$$

# Gauss – Bonnet Theorem

For a surface with  $c$  components, the genus  $G$  specifies  $G$  handles on surface, and is related to the Euler characteristic  $\chi(M)$  via:

$$G = c - \frac{1}{2} \chi(\partial M)$$

where, according to the Gauss-Bonnet theorem, the Euler-Poincare characteristic is given by the surface integral over the Gaussian curvature

$$\chi(\partial M) = \frac{1}{2\pi} \oint \left( \frac{1}{R_1 R_2} \right) dS$$

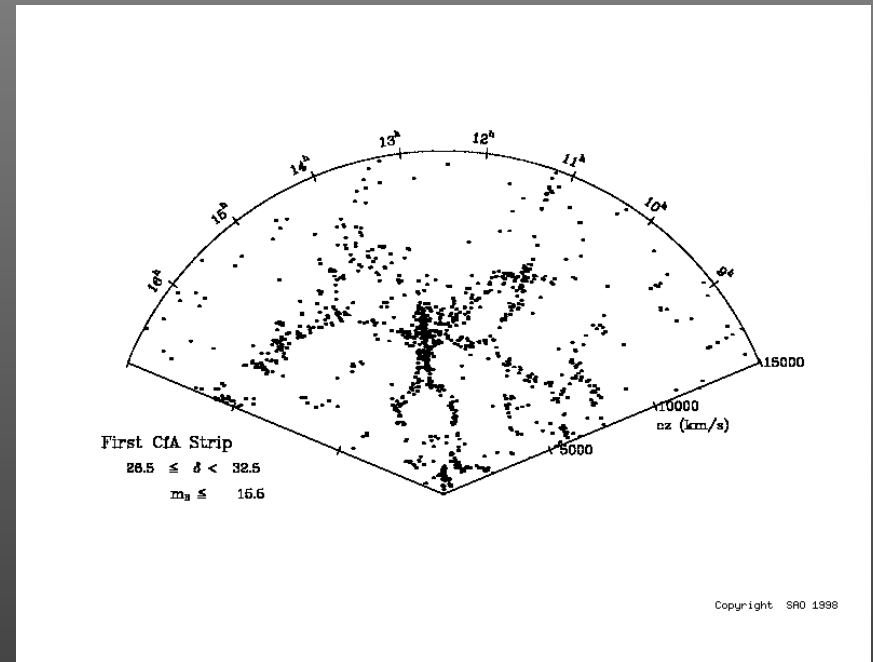
# The usefulness of Euler

The mean value of  $\chi$  can be calculated analytically for Gaussian random fields (test of GRF hypothesis?)

In 3D the mean level is characterised by  $g > 0$  (a sponge)

In 2D the mean level has  $\chi = 0$ .

There is no 2D equivalent of a sponge!



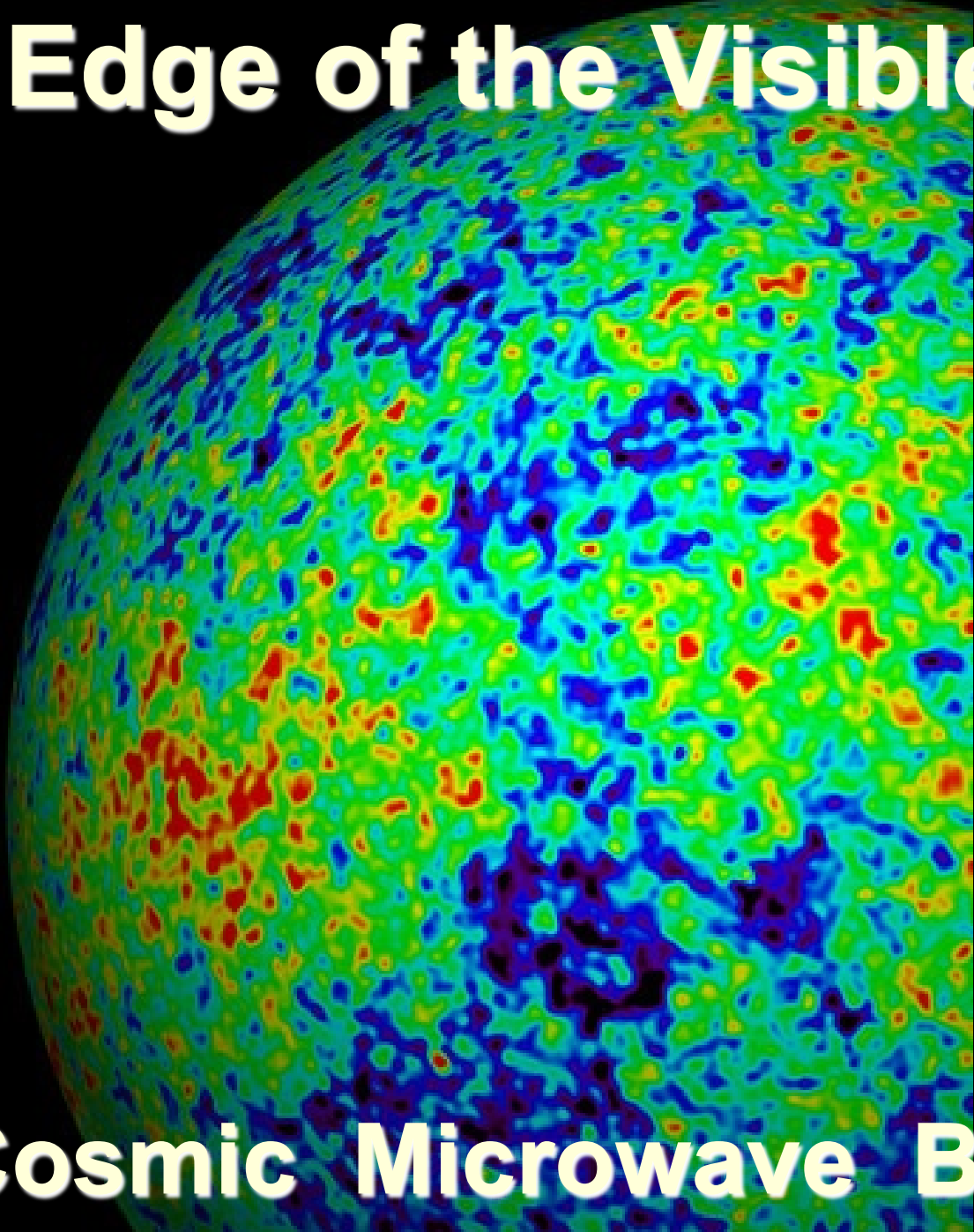
**Topology**

**of the**

**Primordial Gaussian Field**



# Edge of the Visible Universe



**Earliest View  
of our Cosmos:**

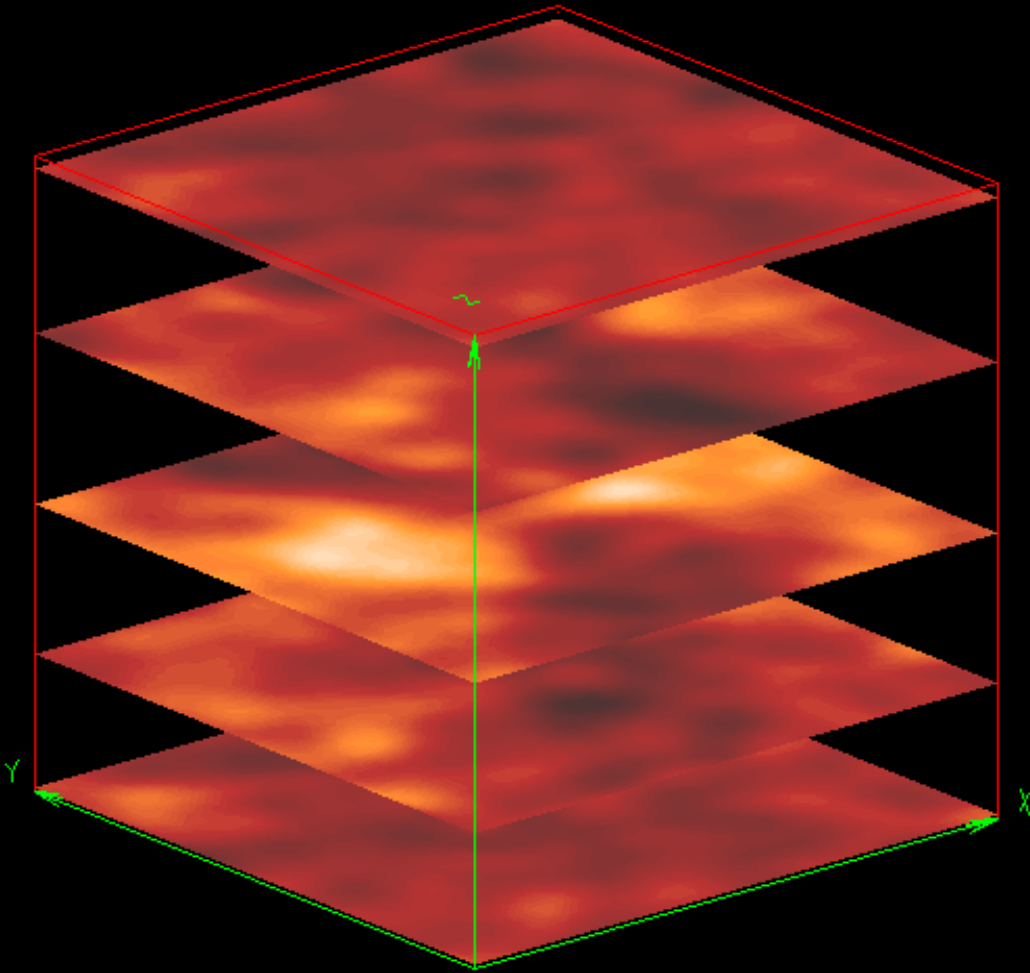
**the Universe  
379,000 years  
after the Big Bang**

**Perfect  
Gaussian Field**

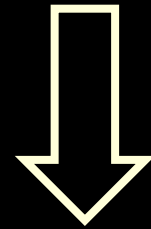
**Origin: Inflation,  
 $t = 10^{-36}$  sec**

# Cosmic Microwave Background

# Primordial Gaussian Field



$$P_N = \frac{\exp\left[-\frac{1}{2} \sum_{i=1}^N \sum_{j=1}^N f_i (M^{-1})_{ij} f_j\right]}{\left[(2\pi)^N (\det M)\right]^{1/2}} \prod_{k=1}^N df_k$$



$$P_N \propto \exp\left[-\sum_i \frac{|\hat{f}(\vec{k}_i)|^2}{2P(k_i)}\right] \propto \prod_i \exp\left[-\frac{|\hat{f}(\vec{k}_i)|^2}{2P(k_i)}\right]$$

$$f(\vec{x}) = \int \frac{d\vec{k}}{(2\pi)^3} \hat{f}(\vec{k}) e^{-i\vec{k}\cdot\vec{x}}$$

$$\hat{f}(\vec{k}) = \hat{f}_r(\vec{k}) + i \hat{f}_i(\vec{k}) = |\hat{f}(\vec{k})| e^{i\theta(\vec{k})}$$

$$P_1(|\hat{f}(\vec{k})|) d|\hat{f}(\vec{k})| = \exp\left[-\frac{|\hat{f}(\vec{k})|^2}{2P(k)}\right] \frac{|\hat{f}(\vec{k})| d|\hat{f}(\vec{k})|}{P(k)}$$

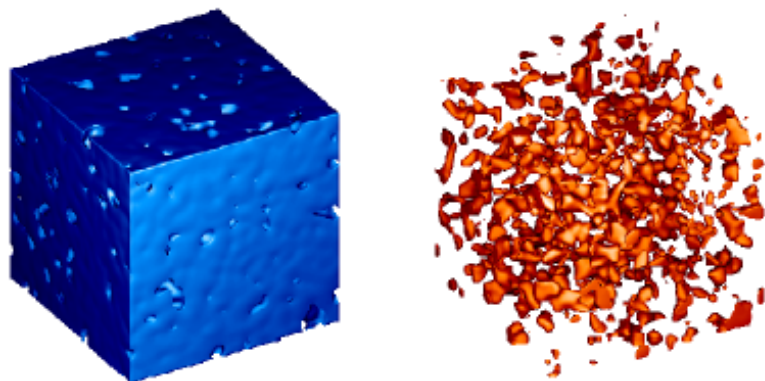
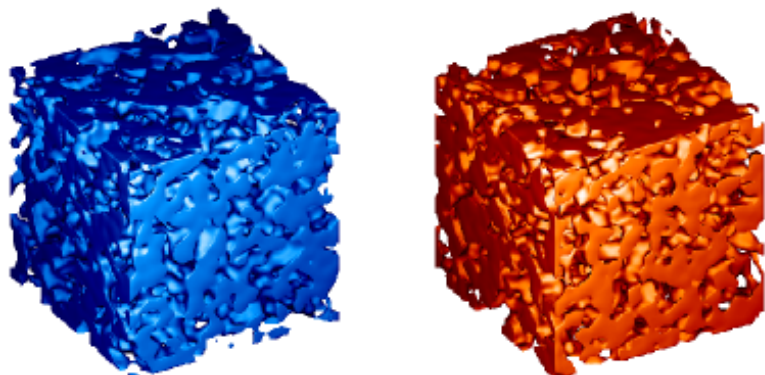
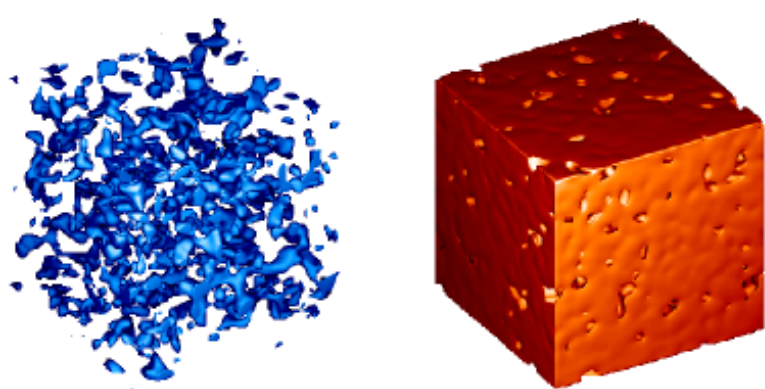


FIG. 1.— Spatial distribution of the low- (left column) and high density (right column) regions for a realization of a Gaussian random field, with comparatively little smoothing. The upper pair shows the 7% low, 93% high density regions, the middle pair stands for 50%–50%, and the lower pair shows the 93% low-density, 7% high-density case.

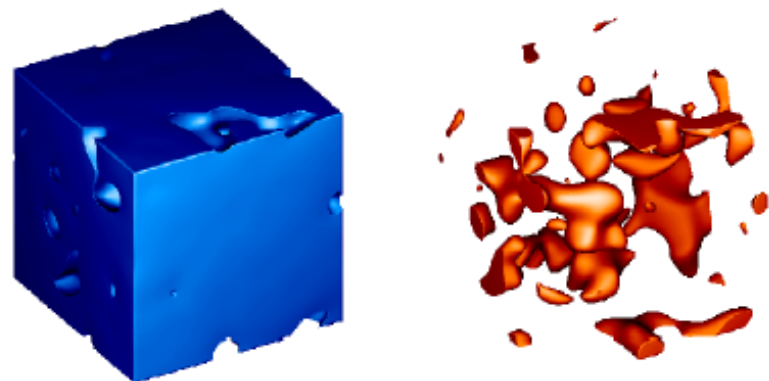
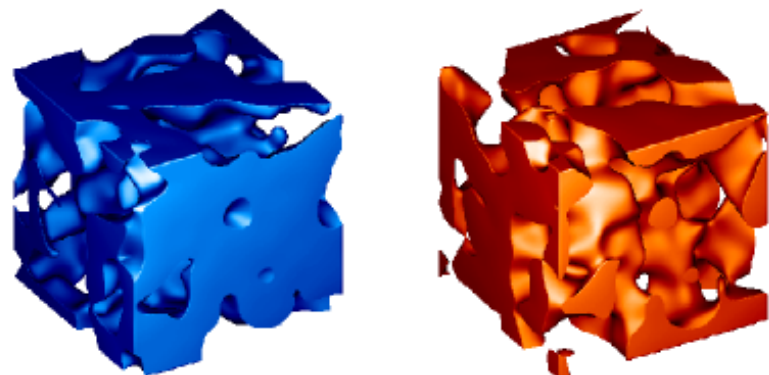
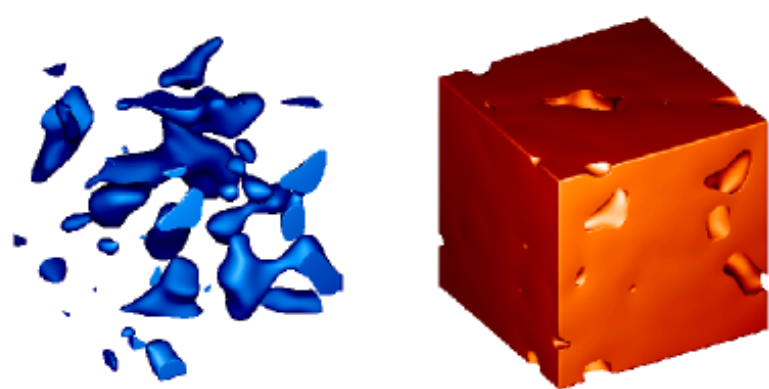
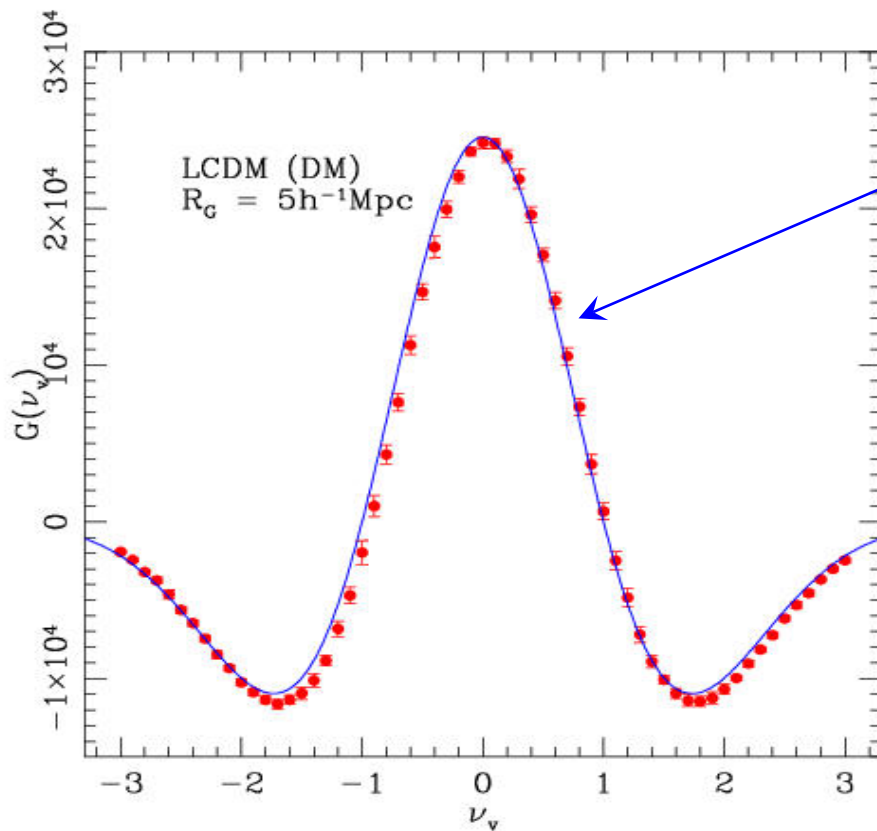


FIG. 2.— Spatial distribution of the low- (left column) and high density (right column) regions for a realization of a Gaussian random field, with heavy smoothing. The upper pair shows the 7% low, 93% high density regions, the middle pair stands for 50%–50%, and the lower pair shows the 93% low-density, 7% high-density case.

# Gaussian Random Fields: Genus

Genus Gaussian Field, the “cosmological” way :

$$g = G - c$$

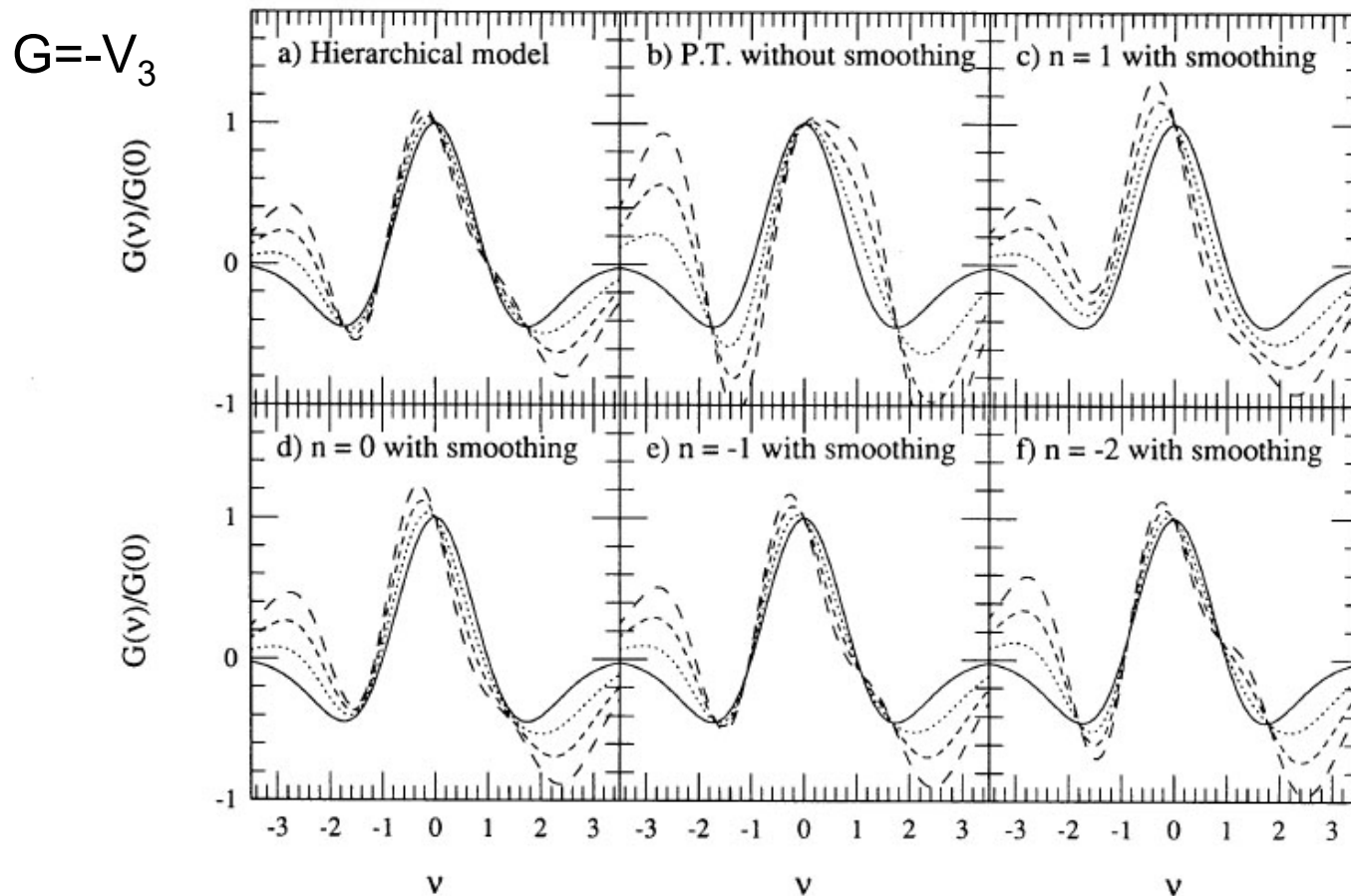


$$g(v) = -\frac{1}{8\pi^2} \left( \frac{\langle k^2 \rangle}{3} \right)^{3/2} (1-v^2) e^{-v^2/2}$$

$$g(v) = -\beta_0(v) + \beta_1(v) - \beta_2(v)$$

**Topology**  
**of**  
**non-Gaussian Fields**

Analytic formulae for the genus in weakly nonlinear regime due to gravitational evolution are known too (Matsubara 1994). So the non-Gaussianity due to non-linear gravitational evolution can be separated, and the primordial topology can be better explored.



Moore et al. (1992): The topology of the QDOT IRAS redshift survey

The amplitude of the genus curves on large (21Mpc/h) scales is inconsistent with the predictions of a constant-bias SCDM model, and the shape of the best-fit PS from genus analysis is  $n=-1$

\* IRAS QDOT: 2163 redshifts out to  $z=0.07$ , randomly sampled at a rate of 1/6 from IRAS PSC ( $f_{60\mu m} > 0.6\text{Jy}$ ),  $|b| > 10$

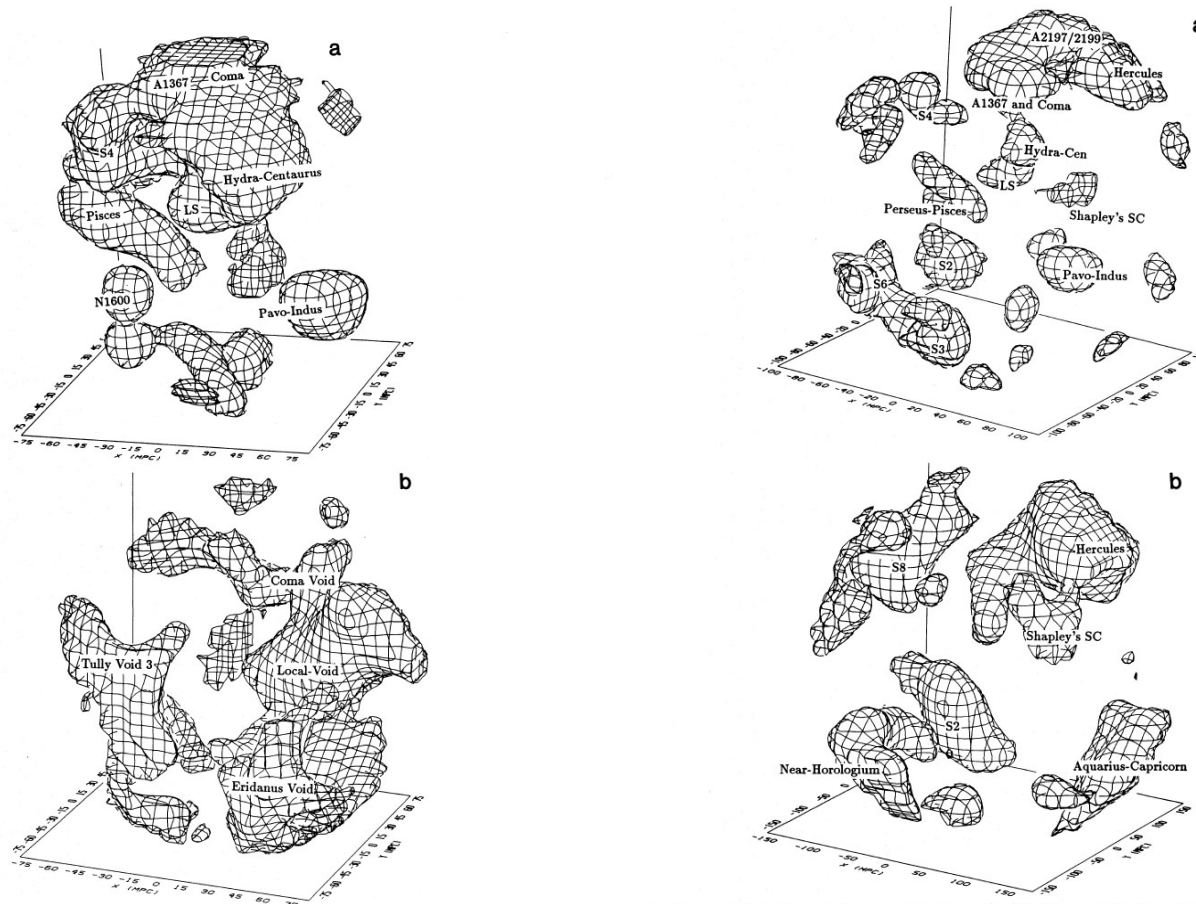


Figure 3. Isodensity contours in the QDOT survey enclosing roughly one third of the total volume. The Galactic Centre points towards the right-hand side of the plot, along the positive  $x$ -axis, with galactic longitude running anticlockwise around the sphere. (a) High-density regions within a sphere of radius  $75 h^{-1}$  Mpc smoothed with a Gaussian of width  $\lambda = 12 h^{-1}$  Mpc. (b) Low-density regions on the same scale and with the same smoothing as (a). (c) High-density regions to a depth of  $100 h^{-1}$  Mpc smoothed on scale  $\lambda = 15 h^{-1}$  Mpc. (d) Low-density regions on the same scale and with the same smoothing as (c).

Figure 4. High-density regions of the QDOT survey. The coordinates are as in Fig. 3. (a) The high-density field of Fig. 3(c) but at a higher threshold so that roughly only one tenth of the total volume is enclosed. (b) High-density regions enclosing the same volume as in (a), but in a sphere of radius  $150 h^{-1}$  Mpc smoothed with  $\lambda = 24 h^{-1}$  Mpc. (c) and (d) The density field of (a) but at the median density contour so that each plot shows one half of the total volume. The structures are interlocking and sponge-like, as expected in a Gaussian random field.

Vogeley et al. (94): Topology Analysis of the CfA Redshift Survey

Genus on  $R_G = 4.2 \sim 14 \text{ Mpc}/h$ . Statistics derived from the genus curve

Amplitude drop relative to the fields with the same PS due to phase correlation on scales  $< 10 \text{ Mpc}/h$

→ amplitude of the genus curve is not a good measure of  $n$ .

The amplitude of the genus curves on large scales is inconsistent with the predictions of a constant bias SCDM, but consistent with a LCDM with  $\Omega h = 0.24$  and  $\Omega_\Lambda = 0.6$  and an OCDM with  $\Omega h = 0.2$ .

\* CfA2:  $\sim 12000$  galaxies with  $m_B < 15.5$ .

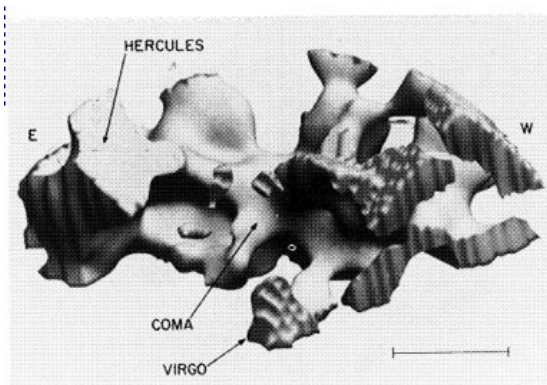


FIG. 3a

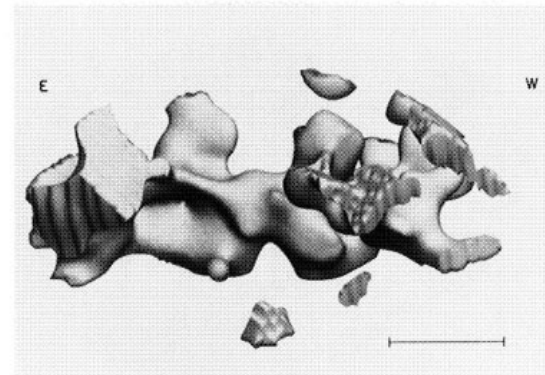


FIG. 3b

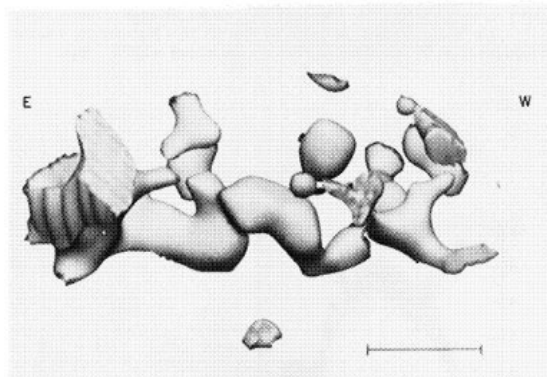


FIG. 3c

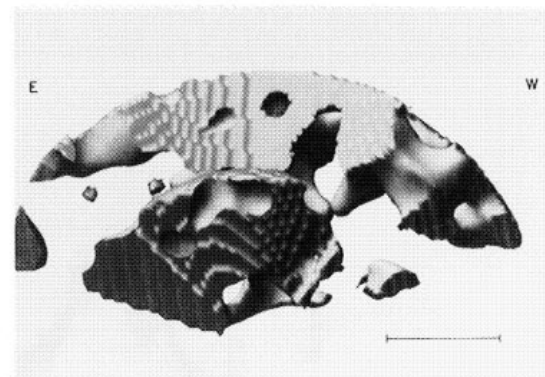


FIG. 3d

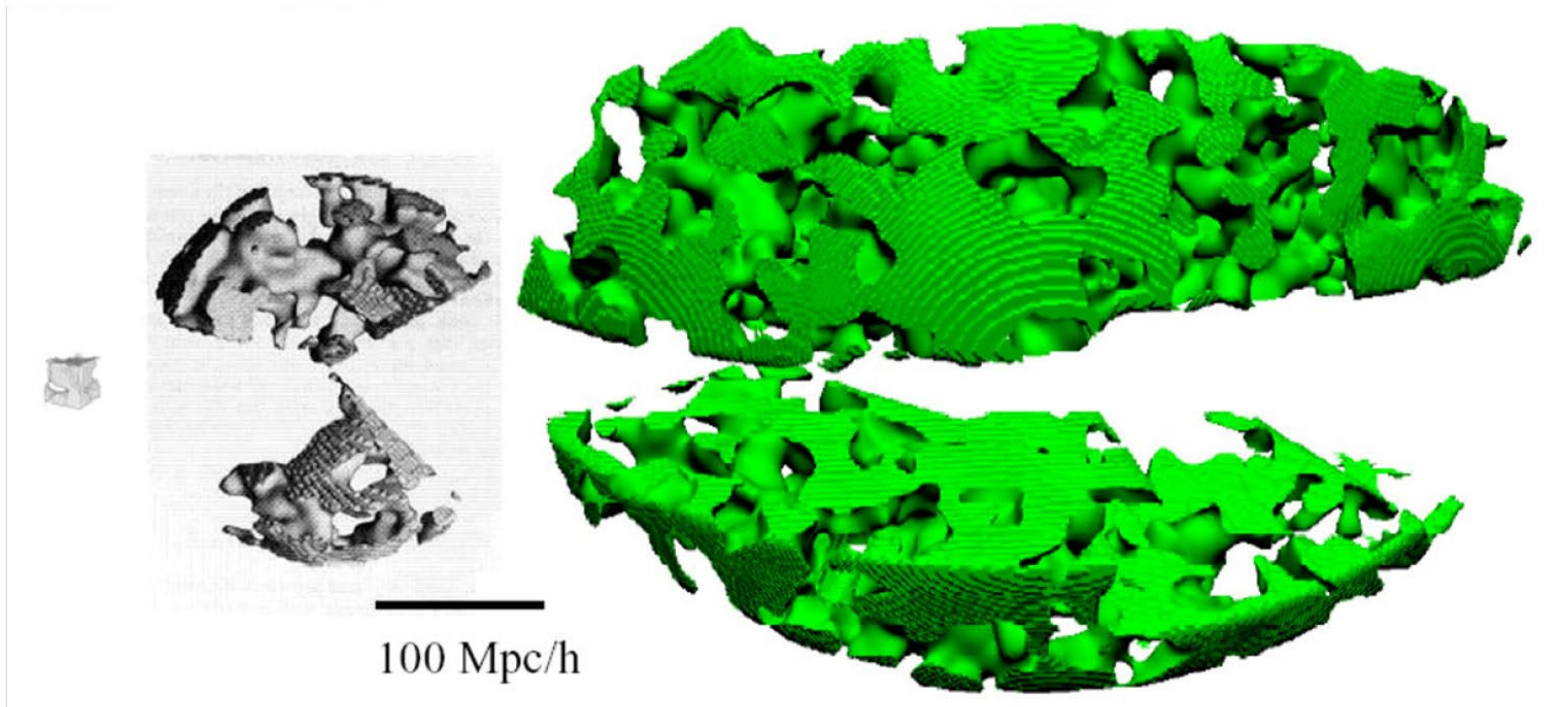


## Growth of observational samples

Gott et al.  
(1986):  
CfA1

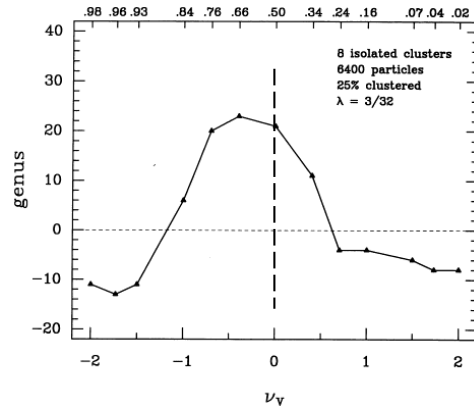
Vogeley et al.  
(1994): CfA2

Gott et al.  
(2006) : SDSS DR4plus

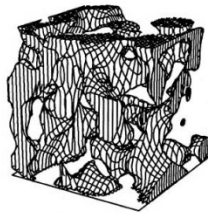


# Genus Non-Gaussian Fields

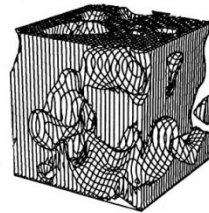
## Clusters



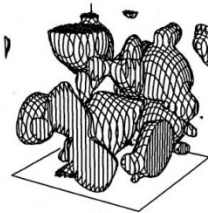
24% low



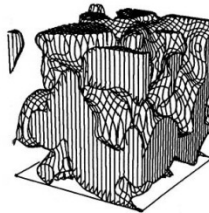
50% low



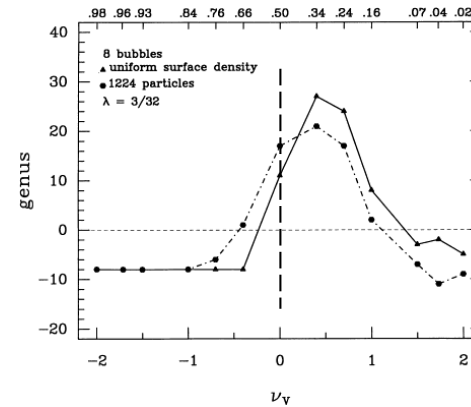
24% high



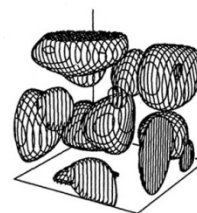
50% high



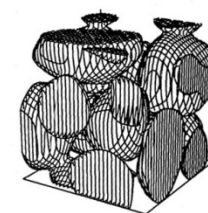
## Bubbles



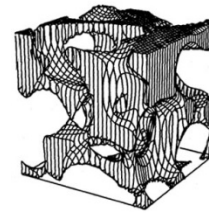
24% low



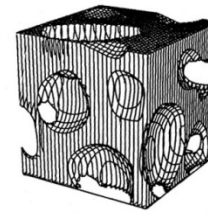
50% low



24% high



50% high



(Weinberg, Gott & Melott 1987)

# Minkowski Functionals

# Minkowski Functionals

- ❓ Complete quantitative characterization of local geometry and morphology of isodensity surfaces in terms of

## Minkowski Functionals

- ❓ Minkowski Functionals (defined by isodensity surface):

- Volume

$$V = \int dV$$

- Surface area

$$S = \oint dS$$

- Integrated mean curvature

$$C = \frac{1}{2} \oint \left( \frac{1}{R_1} + \frac{1}{R_2} \right) dS$$

- Integrated Intrinsic curvature  
Euler Characteristic

$$\chi = \frac{1}{2\pi} \oint \left( \frac{1}{R_1 R_2} \right) dS$$

# Minkowski Functionals: Non-Gaussianity Measure

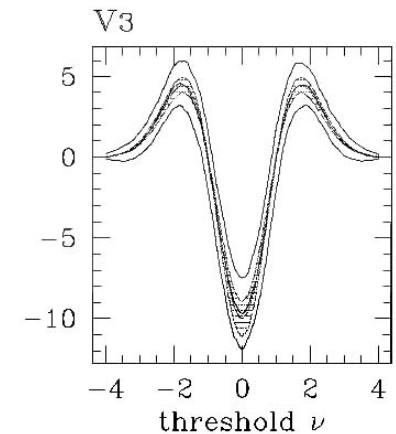
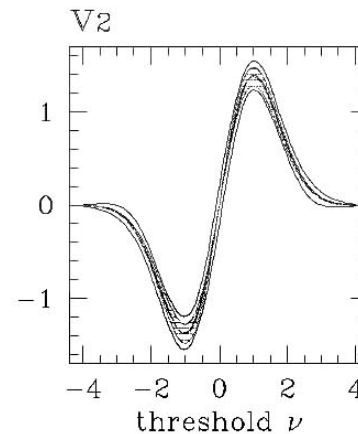
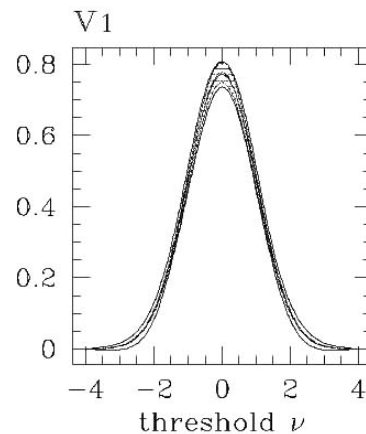
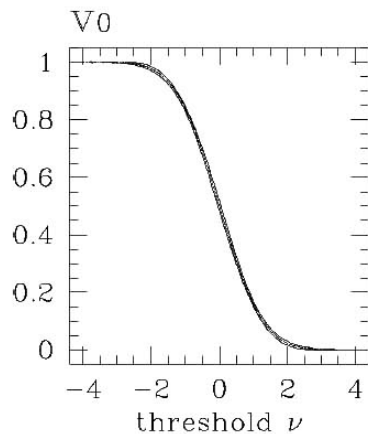
$$V_0(\nu) = \frac{1}{2} - \frac{1}{\sqrt{2\pi}} \int_0^\nu \exp(-x^2/2) dx$$

$$V_1(\nu) = \frac{2}{3} \frac{\lambda}{\sqrt{2\pi}} \exp(-x^2/2)$$

$$V_2(\nu) = \frac{2}{3} \frac{\lambda^2}{\sqrt{2\pi}} \nu \exp(-x^2/2)$$

$$V_3(\nu) = \frac{\lambda^3}{\sqrt{2\pi}} (\nu^2 - 1) \exp(-x^2/2)$$

Theoretical predictions for Gaussian fields are known.



$$\lambda^3 / \sqrt{2\pi} = \frac{1}{4\pi^2} \left( \frac{\langle k^2 \rangle}{3} \right)^{3/2}$$

(Schmalzing & Buchert 1997)

# Minkowski functionals

In  $R^3$  four functionals:

volume  $V$

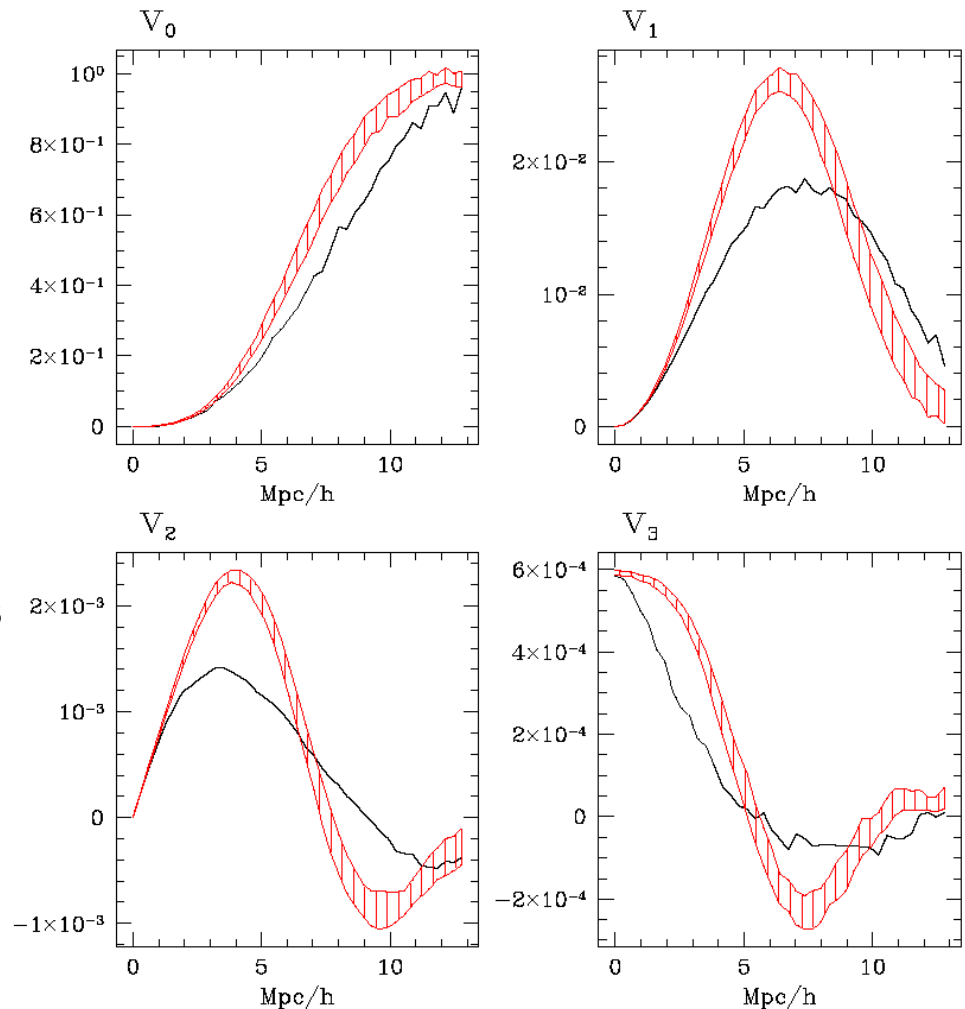
surface area  $A$

integral mean curvature  $H$

Euler-Poincare characteristic  $\chi$

These are the Minkowski Functionals

Kerscher & Martínez (1998),  
Bull. Int. Statist. Inst. 57-2, 363



# **Homology Analysis of the Cosmic Web**

# Cosmic Structure Topology

□ Complete quantitative characterization of homology in terms of

## Betti Numbers

□ Betti number  $\beta_k$ :  
- rank of homology groups  $H_p$  of manifold  
- number of  $k$ -dimensional holes of an object or shape

• 3-D object, e.g. density superlevel set:

$\beta_0$ : -  $\beta$  independent components  
 $\beta_1$ : -  $\beta$  independent tunnels  
 $\beta_2$ : -  $\beta$  independent enclosed voids



# Geometry & Topology

□ Complete quantitative characterization of homology in terms of

## Betti Numbers

□ Complete quantitative characterization of local geometry in terms of

## Minkowski Functionals

□ Minkowski Functionals:

- Volume
- Surface area
- Integrated mean curvature
- Genus/Euler Characteristic

# Genus, Euler & Betti

☐ Euler – Poincare formula

Relationship between Betti Numbers & Euler Characteristic ☐:

$$\chi = \sum_{k=0}^d (-1)^k \beta_k$$

# Genus, Euler & Betti

□ Euler – Poincare formula

Relationship between Betti Numbers & Euler Characteristic □.

3-D manifold □:

$$\begin{aligned}\chi(M) &= \beta_0 - \beta_1 + \beta_2 + \beta_3 \\ &\approx \beta_0 - \beta_1 + \beta_2\end{aligned}$$

2-D boundary manifold □□:

$$\chi(\partial M) = \beta_{0b} - \beta_{1b} + \beta_{2b}$$

# Genus, Euler & Betti

æ For a surface with  $c$  components, the genus  $G$  specifies  $2G$  handles on surface, and is related to the Euler characteristic  $\chi(\partial M)$  via:

$$G = c - \frac{1}{2} \chi(\partial M)$$

where, according to the Gauss-Bonnet theorem

$$\chi(\partial M) = \frac{1}{2\pi} \oint \left( \frac{1}{R_1 R_2} \right) dS$$

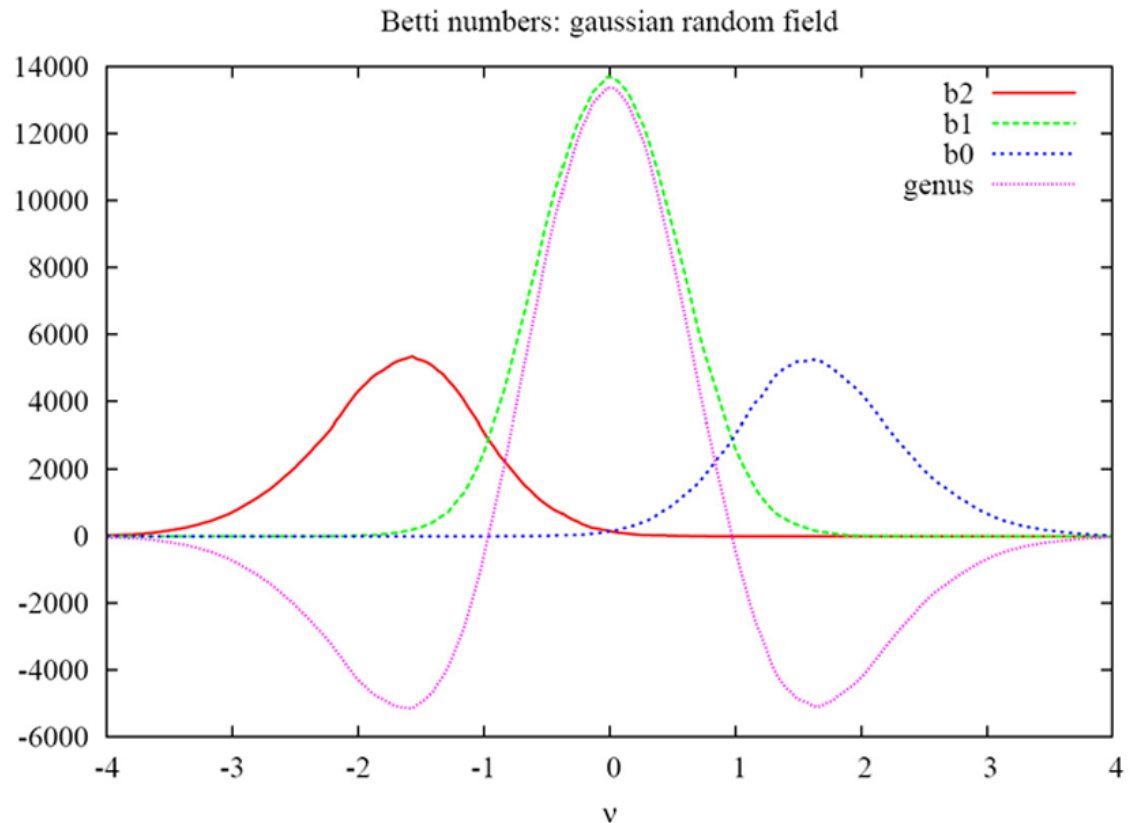
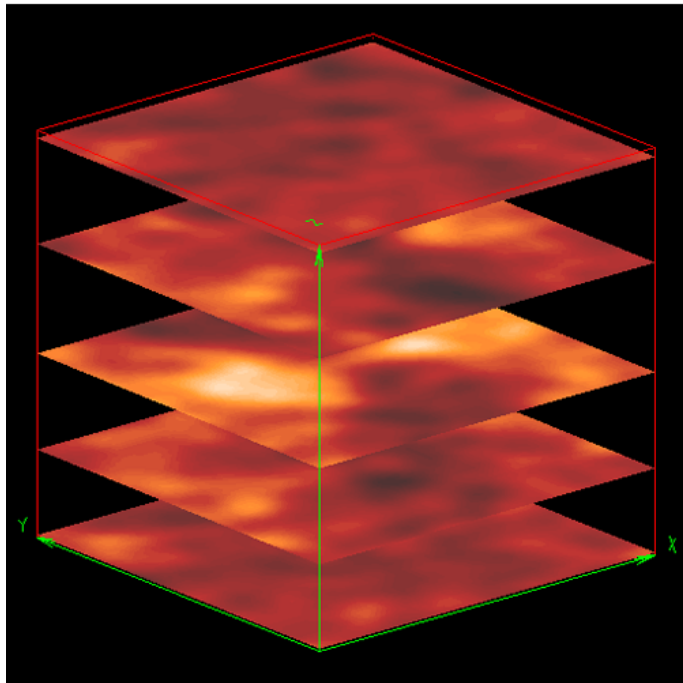
⊛ Euler characteristic 3-D manifold  $M$  & 2-D boundary manifold  $\partial M$ :

$$\chi(M) = \frac{1}{2} \chi(\partial M)$$



$$\chi(\partial M) = 2(\beta_0 - \beta_1 + \beta_2)$$

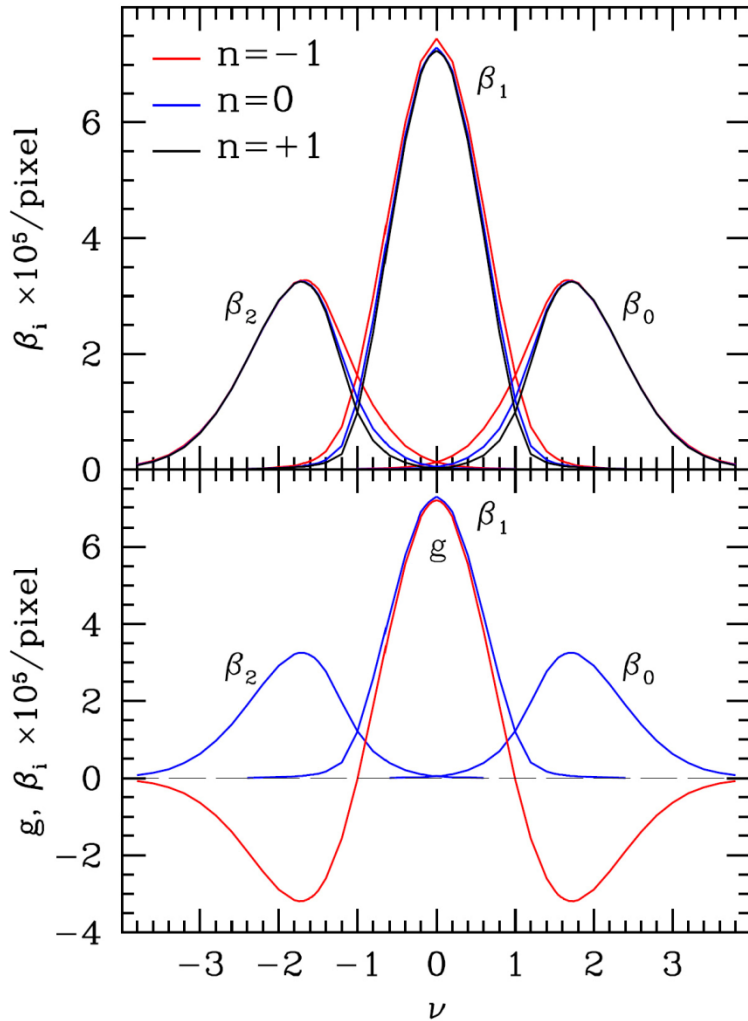
# Gaussian Random Fields: Betti Numbers



In a Gaussian field:

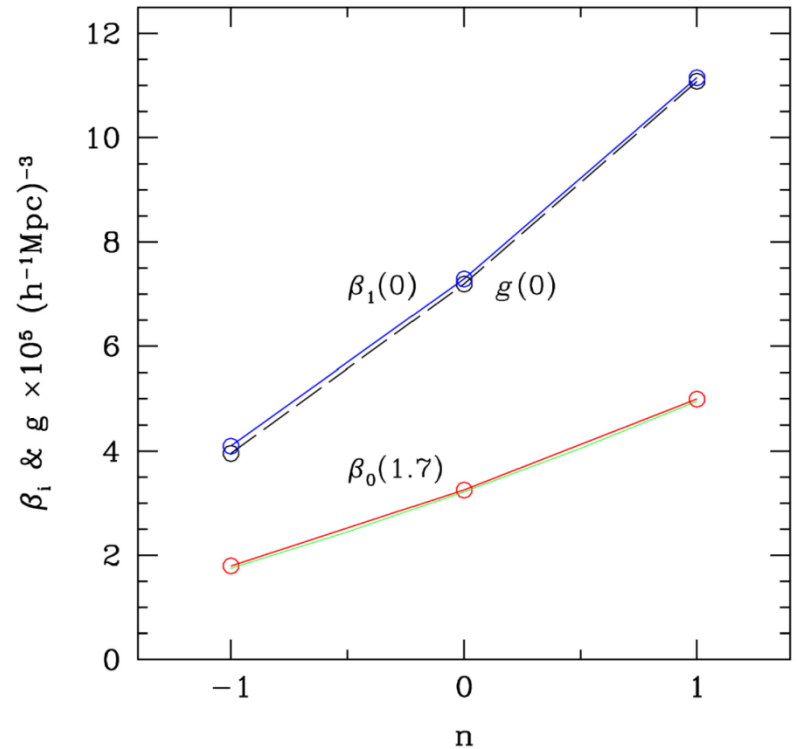
- # tunnels dominant at intermediate density levels, when superlevel domain spongelike
- overlap between  $\mathbb{R}_0$  and  $\mathbb{R}_2$  at  $\mathbb{R}=0$ , domain punctured by clumps with cavities
- # clumps/islands reaches maximum at  $\nu = \sqrt{3}$ , # cavities/voids at  $\nu = -\sqrt{3}$

# Gaussian Random Fields: Betti Numbers

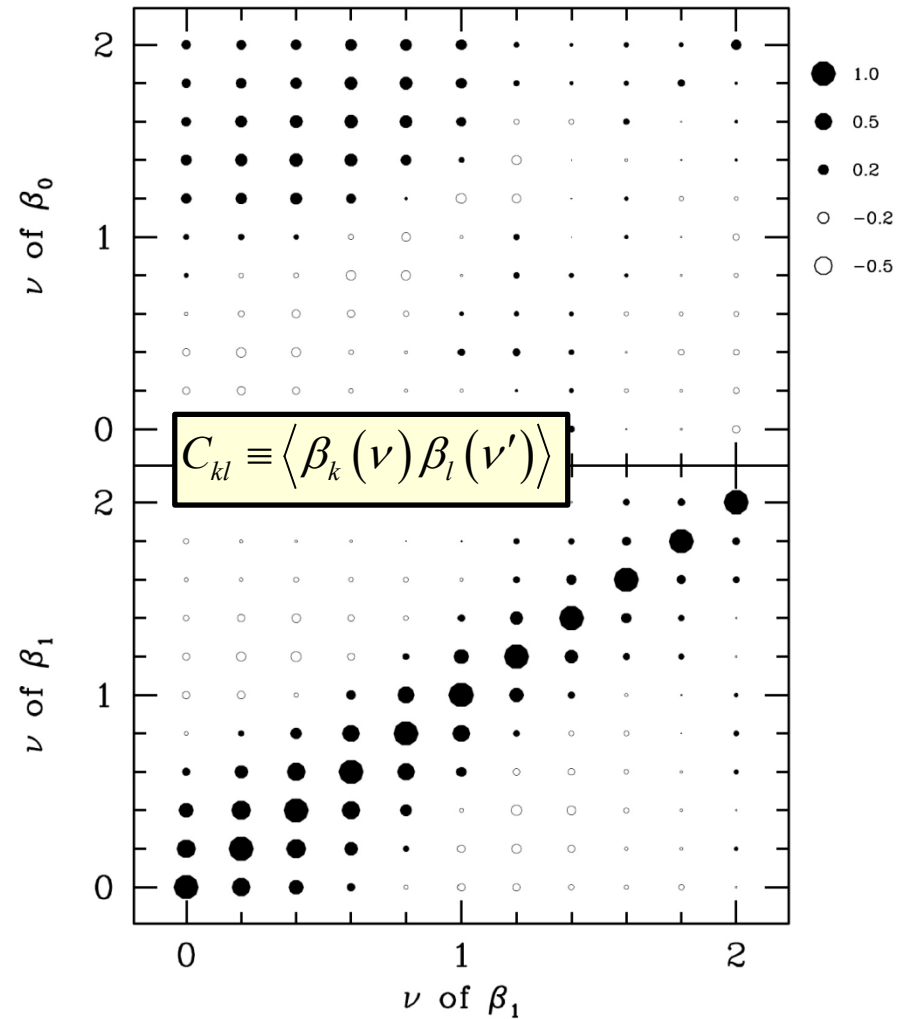
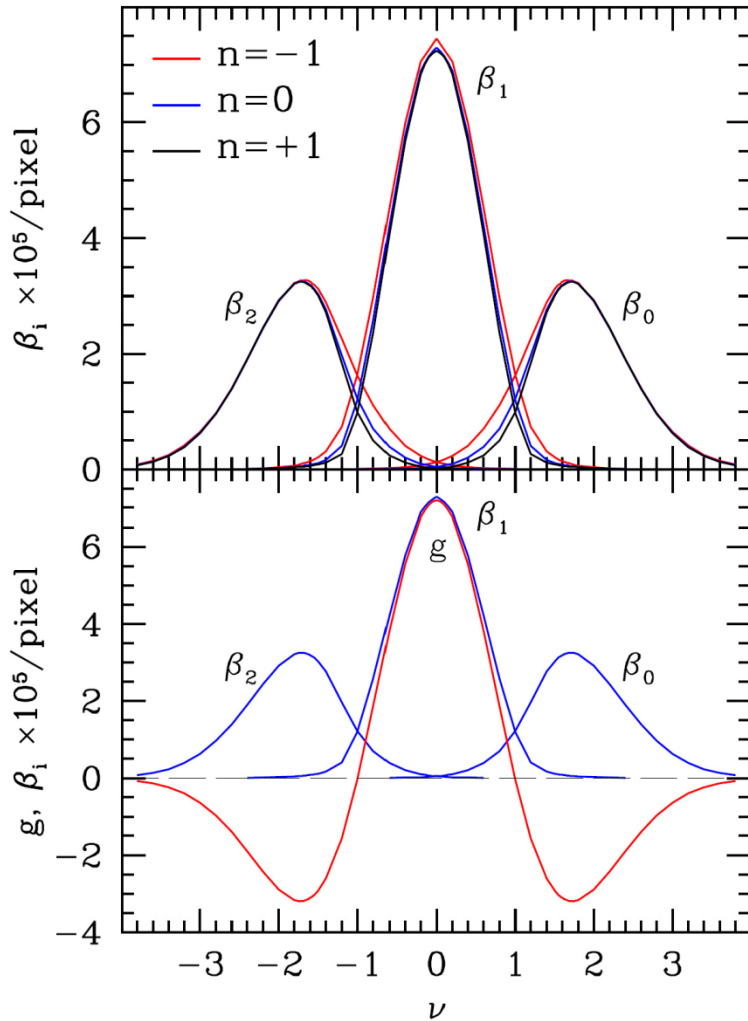


Distinct sensitivity of Betti curves on  
power spectrum  $P(k)$ :

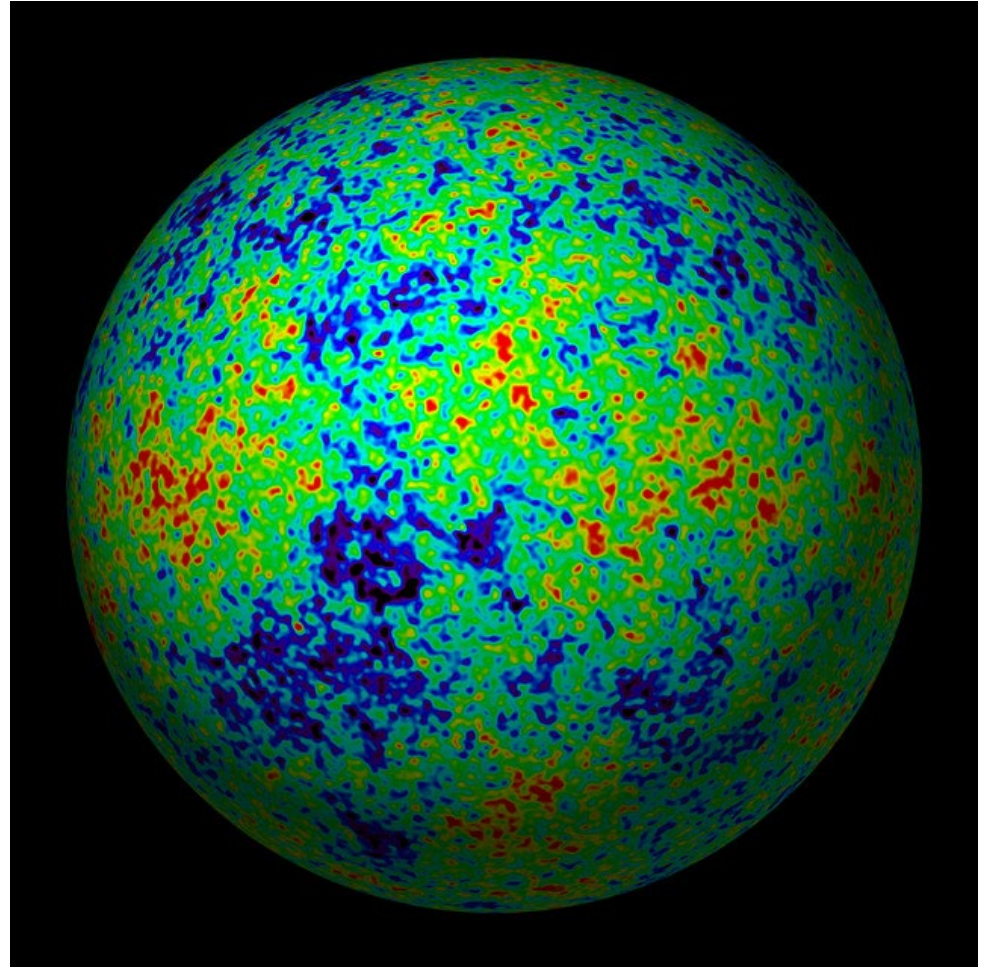
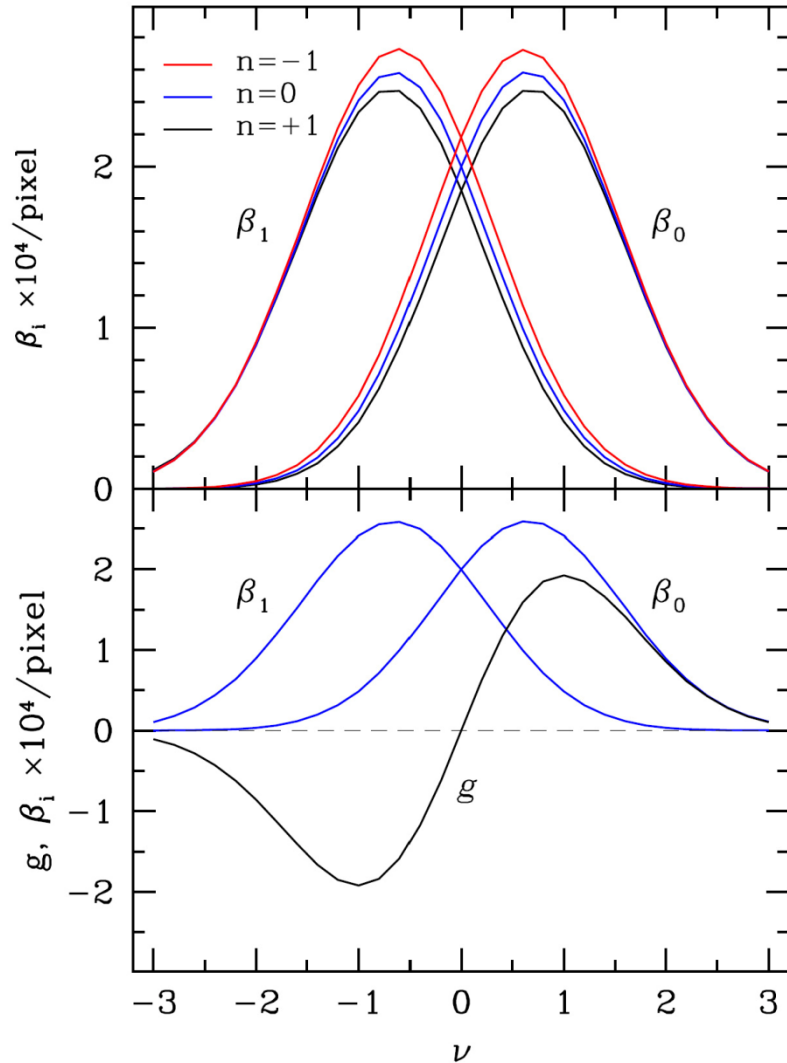
unlike genus (only amplitude  $P(k)$  sensitive)



# Gaussian Random Fields: Correlation Betti Numbers



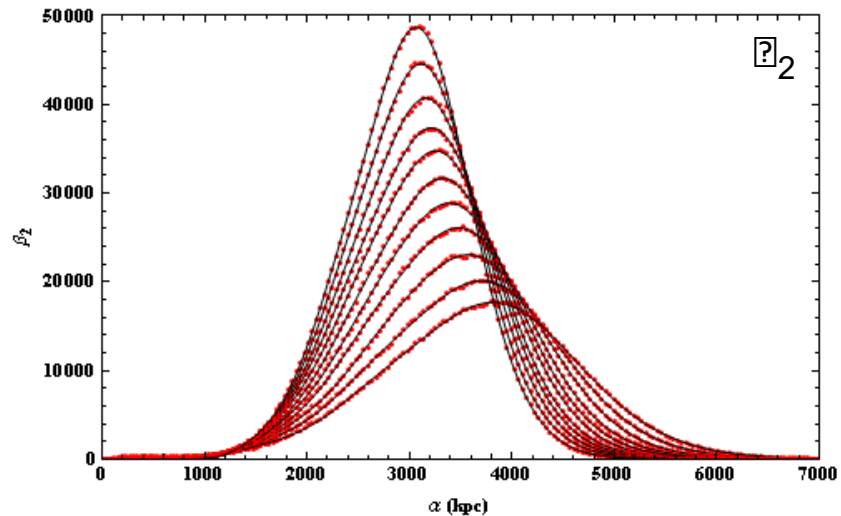
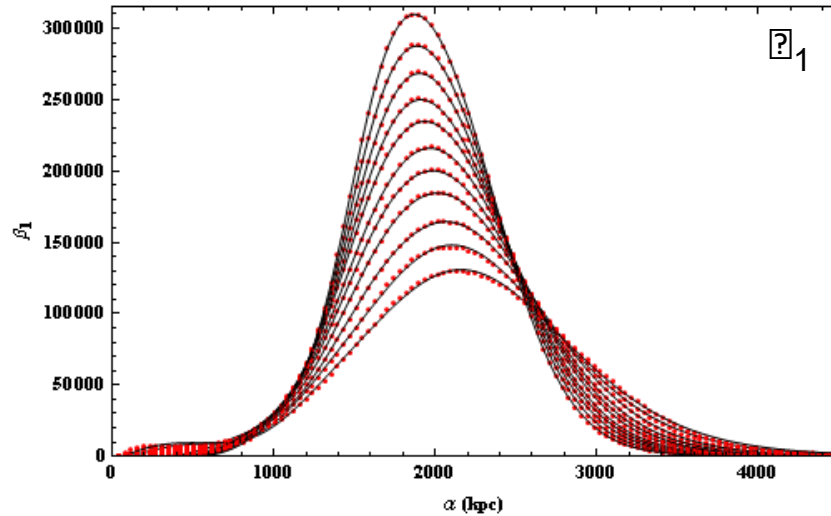
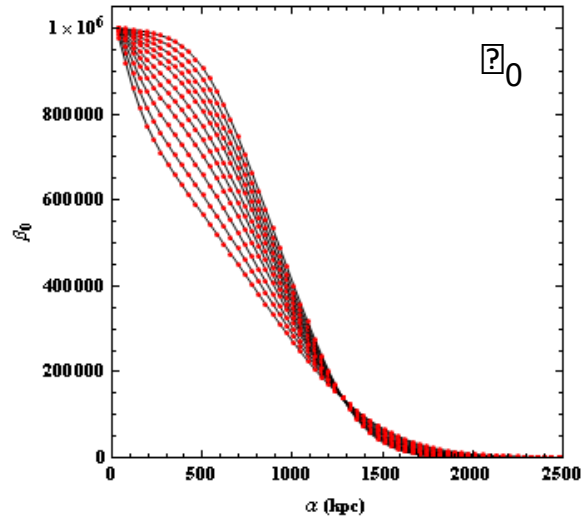
# Gaussian Random Fields: Betti Numbers



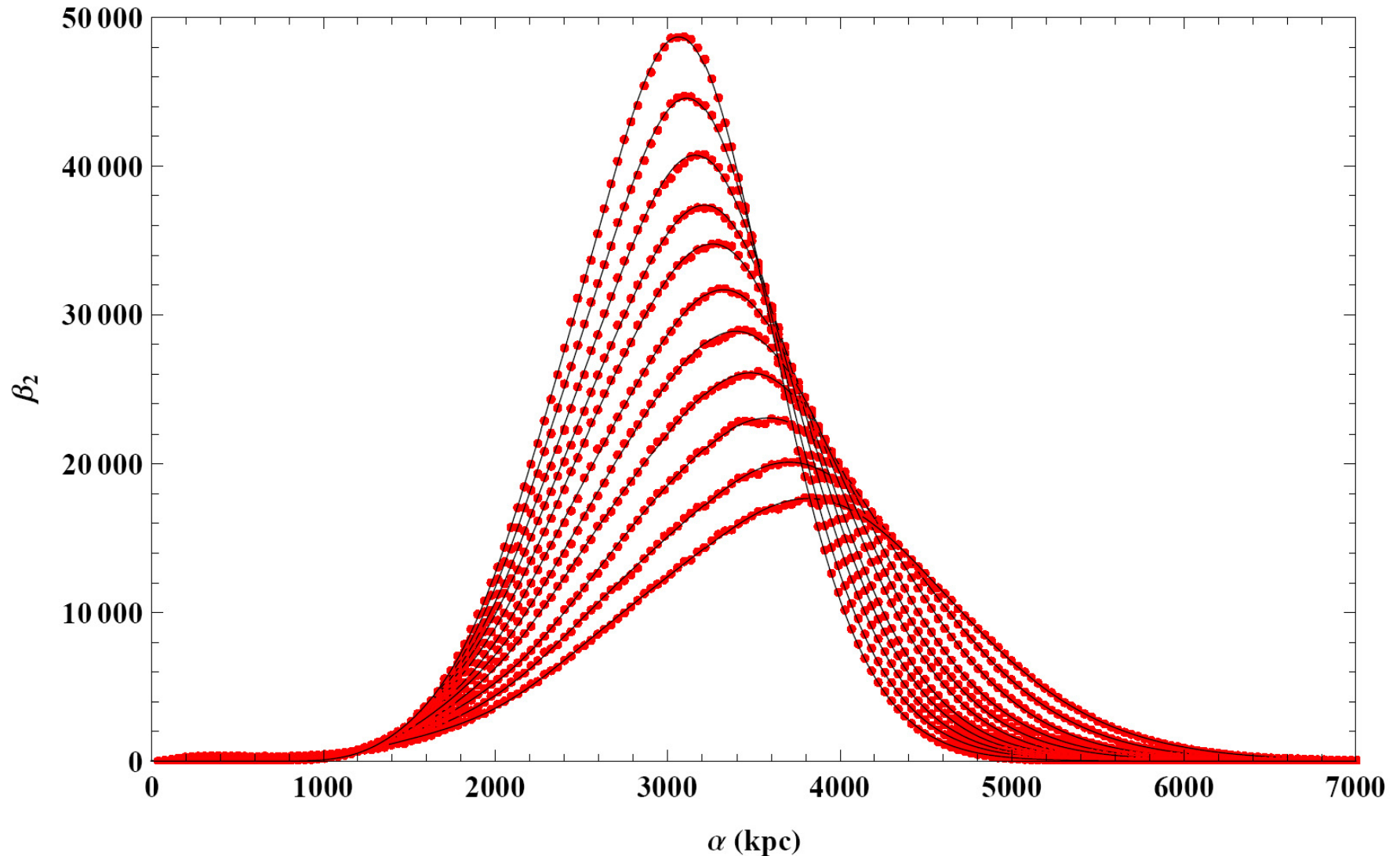


# **Homology of the Cosmic Web**

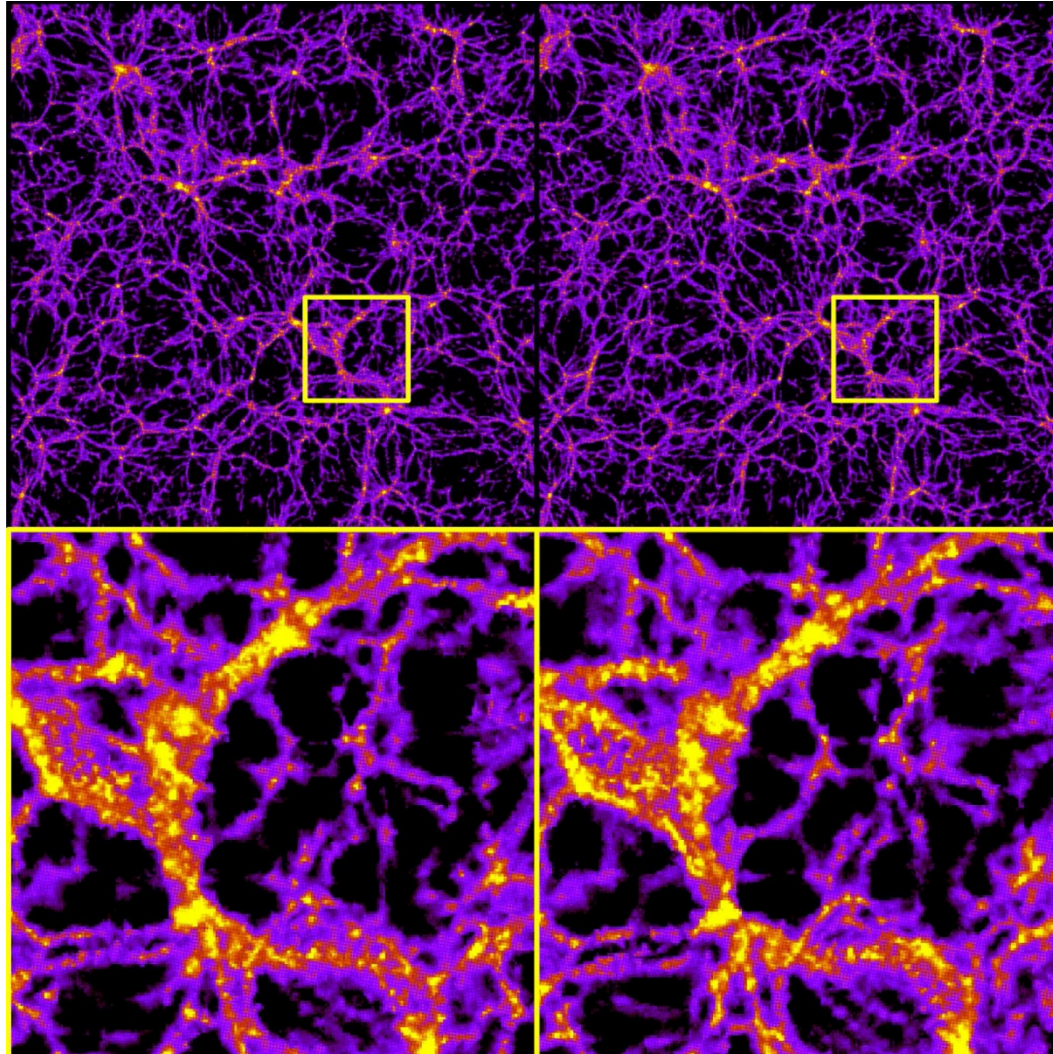
# Homology of evolving LCDM cosmology



# Betti<sub>2</sub>: evolving void populations

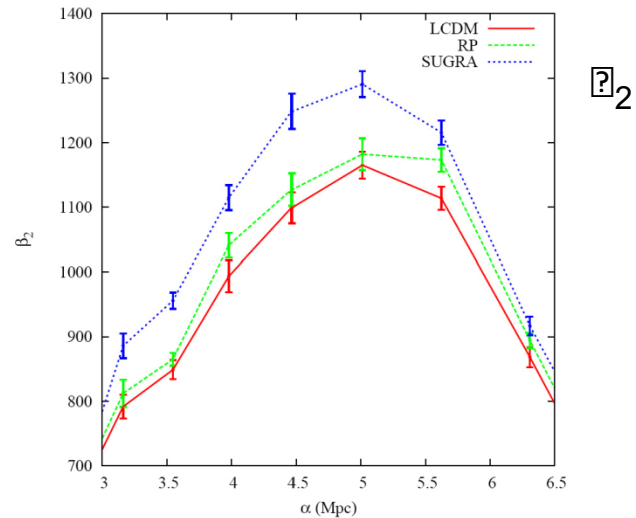
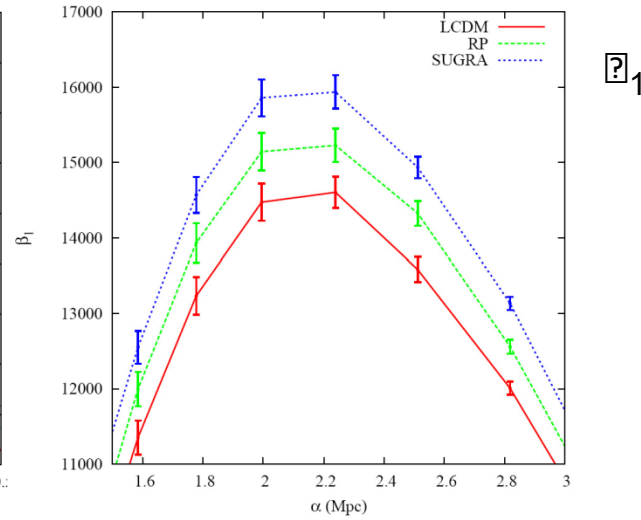
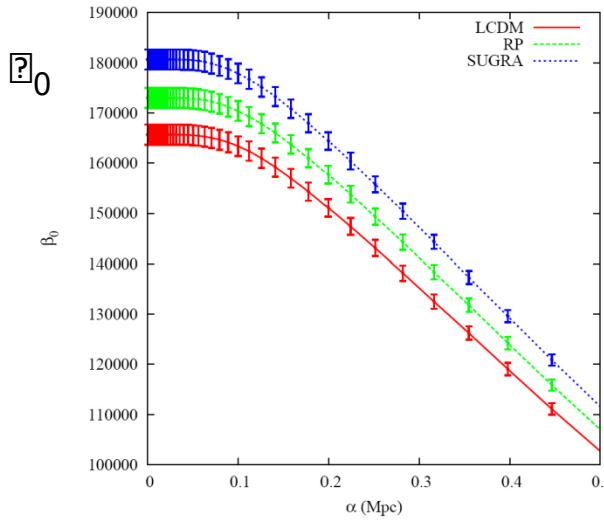


# LCDM vs. SUGRA



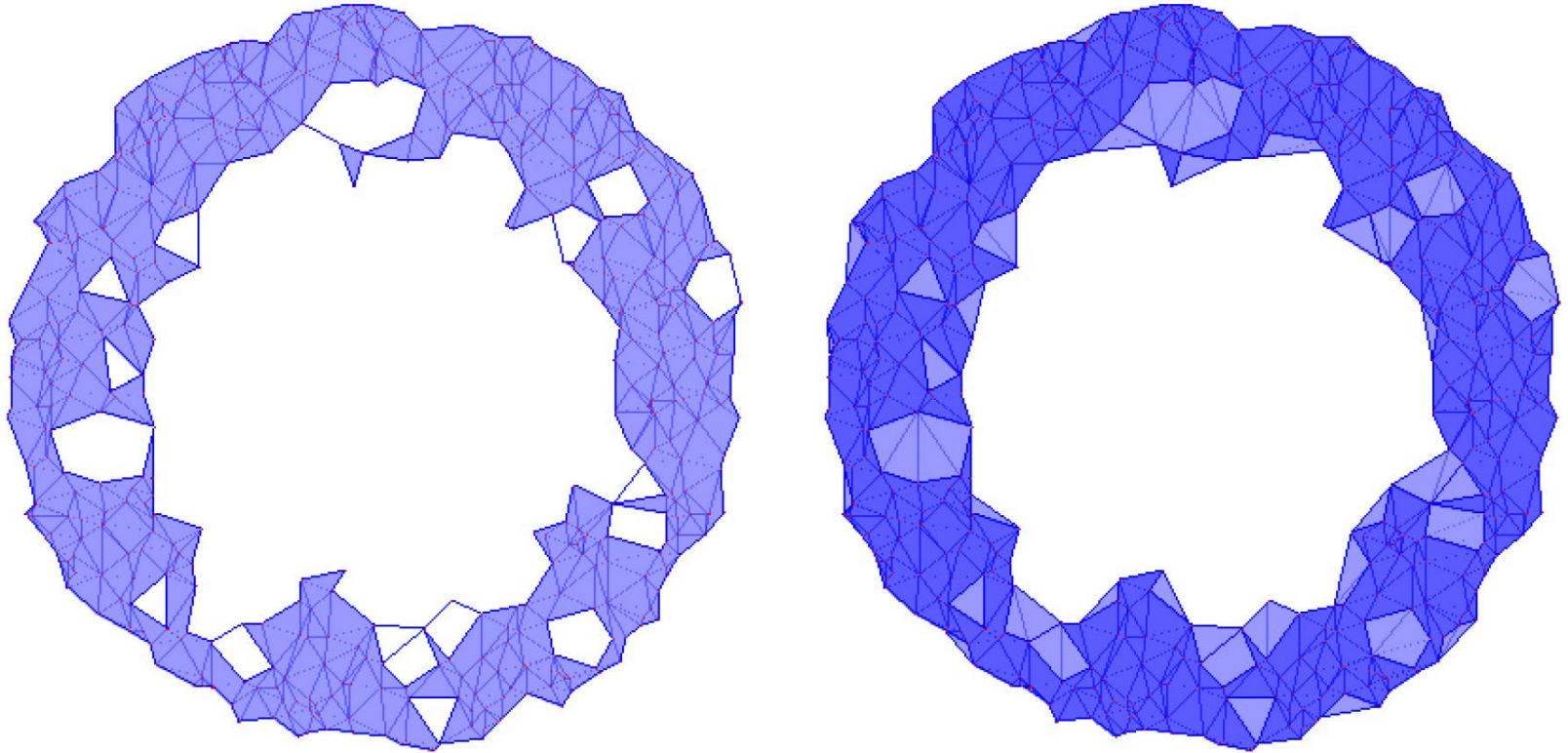
# Homology

## sensitivity LCDM vs. Quintessence



**Persistence**

# Persistence: search for topological reality

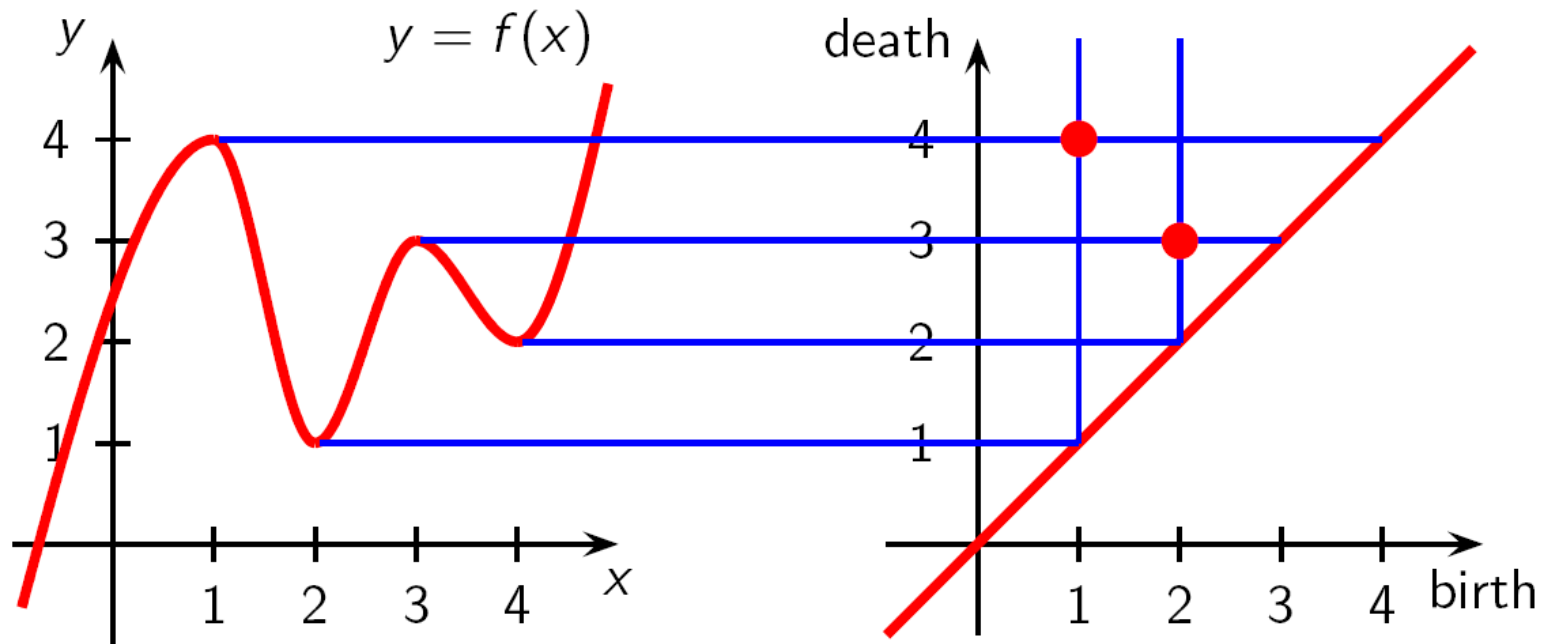


Concept introduced by Edelsbrunner:

Reality of features (eg. voids) determined on the basis of  $\mathbb{R}$ -interval between “birth” and “death” of features

# Persistent Homology

Persistent Homology describes the homological features which persist as a single parameter changes

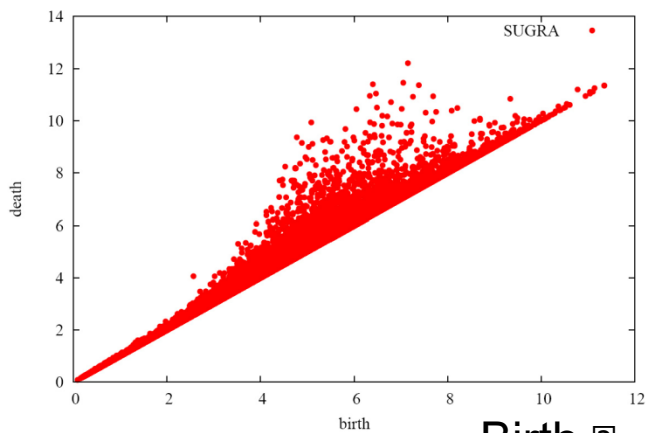
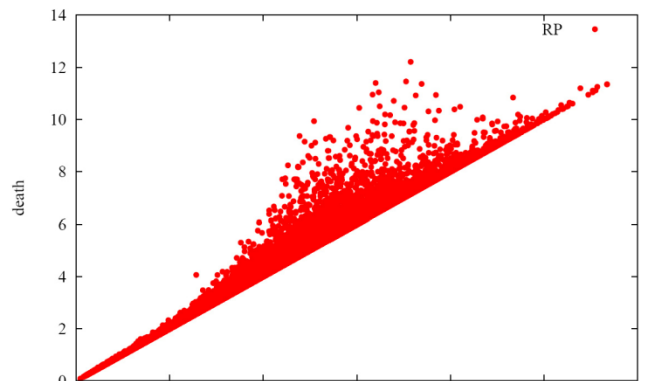
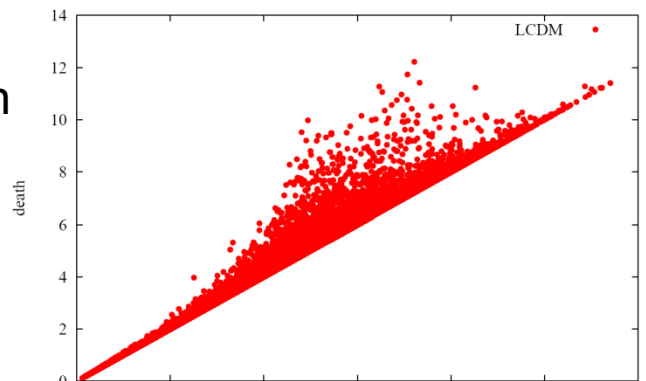




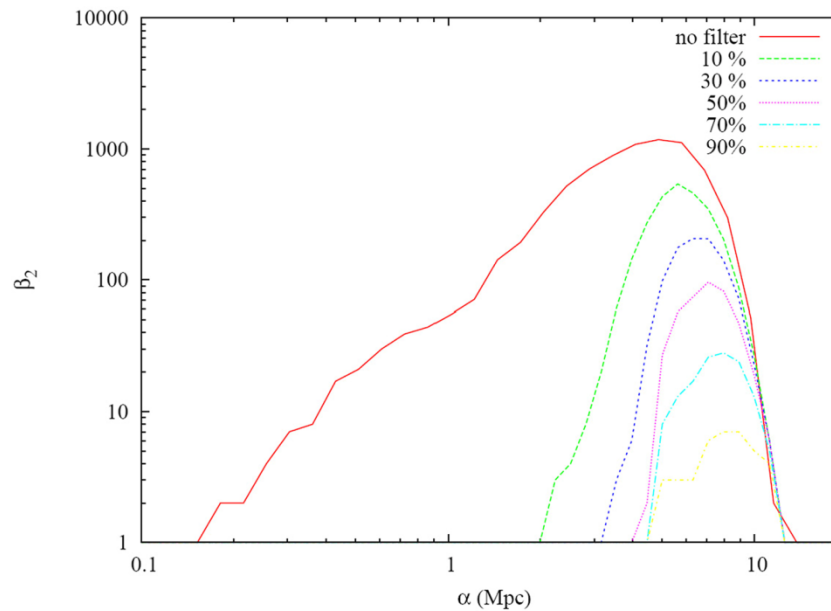
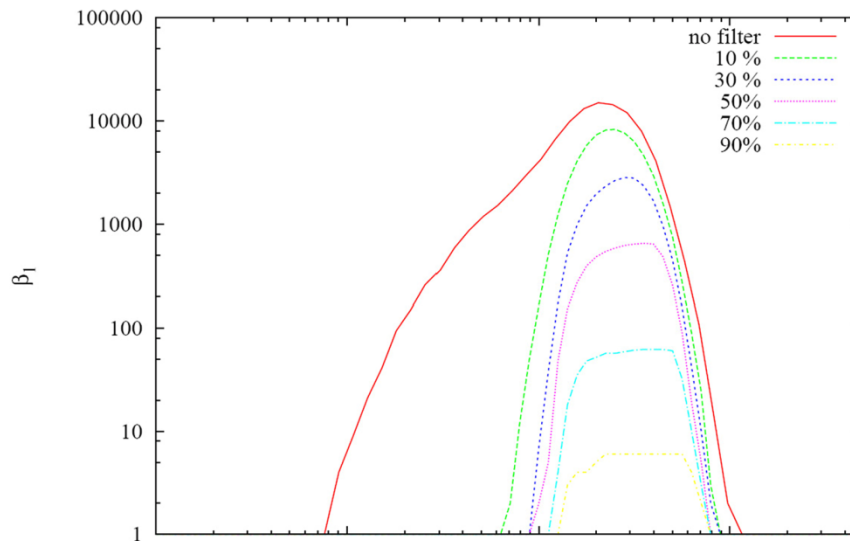
# Persistent LCDM Cosmic Web

Death

?



Birth ?



# Minimal Spanning Tree

